

**SSC-322**

**ANALYSIS AND ASSESSMENT OF MAJOR UNCERTAINTIES  
ASSOCIATED WITH SHIP HULL ULTIMATE FAILURE**



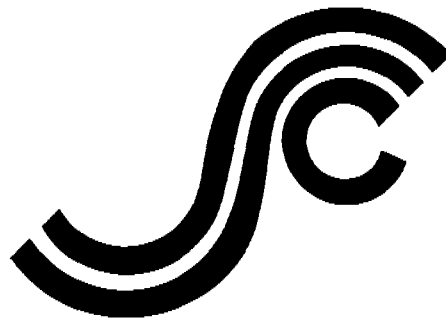
This document has been approved  
for public release and sale; its  
distribution is unlimited

**SHIP STRUCTURE COMMITTEE  
1984**

128-329 (1)

**SSC-322**

**ANALYSIS AND ASSESSMENT OF MAJOR UNCERTAINTIES  
ASSOCIATED WITH SHIP HULL ULTIMATE FAILURE**



This document has been approved  
for public release and sale; its  
distribution is unlimited

**SHIP STRUCTURE COMMITTEE**

**1984**

12/10P  
SHIP STRUCTURE COMMITTEE

THE SHIP STRUCTURE COMMITTEE is constituted to prosecute a research program to improve the hull structures of ships and other marine structures by an extension of knowledge pertaining to design, materials and methods of construction.

RADM C. T. Lusk, Jr., USCG (Chairman)  
Chief, Office of Merchant Marine  
Safety  
U. S. Coast Guard Headquarters

Mr. T. W. Pross  
Associate Administrator for  
Shipbuilding, Operations &  
Research  
Maritime Administration

Mr. P. M. Palermo  
Executive Director  
Ship Design & Integration  
Directorate  
Naval Sea Systems Command

Mr. J. B. Gregory  
Chief, Technology Assessment  
& Research Branch  
Minerals Management Service

Mr. W. M. Hannan  
Vice President  
American Bureau of Shipping

Mr. T. W. Allen  
Engineering Officer  
Military Sealift Command

CDR D. B. Anderson, U. S. Coast Guard (Secretary)

SHIP STRUCTURE SUBCOMMITTEE

The SHIP STRUCTURE SUBCOMMITTEE acts for the Ship Structure Committee on technical matters by providing technical coordination for the determination of goals and objectives of the program, and by evaluating and interpreting the results in terms of structural design, construction and operation.

U. S. COAST GUARD

CAPT A. E. HENN  
CAPT J. R. WALLACE  
MR. J. S. SPENCER  
MR. R. E. WILLIAMS

MILITARY SEALIFT COMMAND

MR. D. STEIN  
MR. T. W. CHAPMAN  
MR. A. ATTERMAYER  
MR. A. B. STAVOVY

NAVAL SEA SYSTEMS COMMAND

MR. J. B. O'BRIEN (CHAIRMAN)  
CDR R. BUBECK  
MR. J. E. GAGORIK  
MR. A. H. ENGLE  
MR. S. G. ARNTSON (COTR)  
MR. G. WOODS (COTR)

AMERICAN BUREAU OF SHIPPING

DR. D. LIU  
MR. I. L. STERN  
MR. B. NADALIN

MARITIME ADMINISTRATION

MR. F. SEIBOLD  
MR. N. O. HAMMER  
DR. W. M. MACLEAN  
MR. M. W. TOUMA

MINERALS MANAGEMENT SERVICE

MR. R. GIANGERELLI  
MR. R. C. E. SMITH

NATIONAL ACADEMY OF SCIENCES  
COMMITTEE ON MARINE STRUCTURES

MR. A. DUDLEY HAFF - LIAISON  
MR. R. W. RUMKE - LIAISON

INTERNATIONAL SHIP STRUCTURES CONGRESS

MR. S. G. STIANSEN - LIAISON

SOCIETY OF NAVAL ARCHITECTS &  
MARINE ENGINEERS

MR. N. O. HAMMER - LIAISON  
MR. F. SELLARS - LIAISON

AMERICAN IRON & STEEL INSTITUTE

MR. J. J. SCHMIDT - LIAISON

WELDING RESEARCH COUNCIL

DR. G. W. OYLER - LIAISON

STATE UNIVERSITY OF NY MARITIME COLLEGE

DR. W. R. PORTER - LIAISON

U.S. COAST GUARD ACADEMY

LT J. TUTTLE - LIAISON

U.S. NAVAL ACADEMY

DR. R. BHATTACHARYYA - LIAISON

U.S. MERCHANT MARINE ACADEMY

DR. C. B. KIM - LIAISON

10/14 Piers outside

Member Agencies:

*United States Coast Guard  
Naval Sea Systems Command  
Maritime Administration  
American Bureau of Shipping  
Military Sealift Command  
Minerals Management Service*



**Ship  
Structure  
Committee**

An Interagency Advisory Committee  
Dedicated to the Improvement of Marine Structures SR-1280

Address Correspondence to:

Secretary, Ship Structure Committee  
U.S. Coast Guard Headquarters, (G-M/TP 13)  
Washington, D.C. 20593  
(202) 426-2197

The reliability approach of analyzing the adequacy of ship structures is being pursued with increased interest in the maritime community.

This report considers the uncertainties of the primary hull longitudinal compression failure mode using coefficients of variation in order to obtain safety indices. Loading used includes still water bending, thermal, wave spectra, slamming, whipping, springing and combined loadings.

A handwritten signature in black ink, appearing to read 'Clyde T. Lue, Jr.', written in a cursive style.

CLYDE T. LUE, Jr.  
Rear Admiral, U.S. Coast Guard  
Chairman, Ship Structure Committee

1. Report No. SSC-322		2. Government Accession No.		3. Recipient's Catalog No.	
4. Title and Subtitle ANALYSIS AND ASSESSMENT OF MAJOR UNCERTAINTIES ASSOCIATED WITH SHIP HULL ULTIMATE FAILURE				5. Report Date June 1983	
				6. Performing Organization Code	
7. Author(s) P. Kaplan, M. Benatar, J. Bentson and T. A. Achtarides				8. Performing Organization Report No. 82-49	
9. Performing Organization Name and Address Hydromechanics, Inc. 182 Fairchild Ave. Plainview, N.Y. 11803				10. Work Unit No. (TRAVIS)	
				11. Contract or Grant No. DTCG-23-81-C-20006	
12. Sponsoring Agency Name and Address U. S. Coast Guard Washington, D.C. 20593				13. Type of Report and Period Covered Final Report	
				14. Sponsoring Agency Code	
15. Supplementary Notes SHIP STRUCTURE COMMITTEE Project 1280					
16. Abstract <p>The different uncertainties associated with ship longitudinal strength and external loading are reviewed when considering probabilistic analysis and design. The uncertainties are represented in the form of coefficients of variation, where that information can then be used in evaluation of the safety index and/or related quantities used for determination of structural failure probability. The emphasis is directed toward longitudinal strength, with the failure mode due to ultimate compression failure as the major consideration.</p> <p>Numerical values for coefficients of variation are found by data analysis and computation for different types of loads (wave-induced, springing, slamming, etc.) together with suggested means of determining the uncertainty for the combined loads acting on a ship. Methods for determining ship strength uncertainties are examined, with application to modern commercial ships illustrating the important prospective failure mechanisms and the limits of present mathematical models in predicting such failures. Proposed procedures for determining uncertainties for such ship structures by use of computationally efficient numerical computer programs are described.</p>					
17. Key Words Probabilistic design Ship longitudinal strength Coefficients of variation Load variability Hull girder failure			18. Distribution Statement Document is available to the U.S. public through the National Technical Information Service, Springfield, VA, 22161		
19. Security Classif. (of this report) Unclassified		20. Security Classif. (of this page) Unclassified		21. No. of Pages	22. Price

## METRIC CONVERSION FACTORS

### Approximate Conversions to Metric Measures

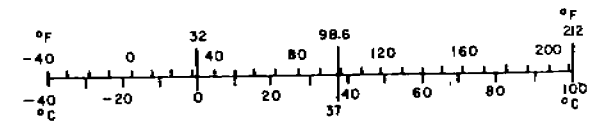
Symbol	When You Know	Multiply by	To Find	Symbol
<b>LENGTH</b>				
in	inches	2.5	centimeters	cm
ft	feet	30	centimeters	cm
yd	yards	0.9	meters	m
mi	miles	1.6	kilometers	km
<b>AREA</b>				
in <sup>2</sup>	square inches	6.5	square centimeters	cm <sup>2</sup>
ft <sup>2</sup>	square feet	0.09	square meters	m <sup>2</sup>
yd <sup>2</sup>	square yards	0.8	square meters	m <sup>2</sup>
mi <sup>2</sup>	square miles	2.6	square kilometers	km <sup>2</sup>
	acres	0.4	hectares	ha
<b>MASS (weight)</b>				
oz	ounces	28	grams	g
lb	pounds	0.45	kilograms	kg
	short tons (2000 lb)	0.9	tonnes	t
<b>VOLUME</b>				
tsp	teaspoons	5	milliliters	ml
Tbsp	tablespoons	15	milliliters	ml
fl oz	fluid ounces	30	milliliters	ml
c	cups	0.24	liters	l
pt	pints	0.47	liters	l
qt	quarts	0.95	liters	l
gal	gallons	3.8	liters	l
ft <sup>3</sup>	cubic feet	0.03	cubic meters	m <sup>3</sup>
yd <sup>3</sup>	cubic yards	0.76	cubic meters	m <sup>3</sup>
<b>TEMPERATURE (exact)</b>				
°F	Fahrenheit temperature	5/9 (after subtracting 32)	Celsius temperature	°C

\* 1 in = 2.54 (exactly). For other exact conversions and more detailed tables, see NBS Misc. Publ. 286, Units of Weights and Measures, Price \$2.25, SD Catalog No. C13.10.286.



### Approximate Conversions from Metric Measures

Symbol	When You Know	Multiply by	To Find	Symbol
<b>LENGTH</b>				
mm	millimeters	0.04	inches	in
cm	centimeters	0.4	inches	in
m	meters	3.3	feet	ft
m	meters	1.1	yards	yd
km	kilometers	0.6	miles	mi
<b>AREA</b>				
cm <sup>2</sup>	square centimeters	0.16	square inches	in <sup>2</sup>
m <sup>2</sup>	square meters	1.2	square yards	yd <sup>2</sup>
km <sup>2</sup>	square kilometers	0.4	square miles	mi <sup>2</sup>
ha	hectares (10,000 m <sup>2</sup> )	2.5	acres	
<b>MASS (weight)</b>				
g	grams	0.035	ounces	oz
kg	kilograms	2.2	pounds	lb
t	tonnes (1000 kg)	1.1	short tons	
<b>VOLUME</b>				
ml	milliliters	0.03	fluid ounces	fl oz
l	liters	2.1	pints	pt
l	liters	1.06	quarts	qt
l	liters	0.26	gallons	gal
m <sup>3</sup>	cubic meters	35	cubic feet	ft <sup>3</sup>
m <sup>3</sup>	cubic meters	1.3	cubic yards	yd <sup>3</sup>
<b>TEMPERATURE (exact)</b>				
°C	Celsius temperature	9/5 (then add 32)	Fahrenheit temperature	°F



486-329

IV

*(4 Pica Head)*

CONTENTS

	<u>Page</u>
1.0 INTRODUCTION . . . . .	1
2.0 PROBABILISTIC ANALYSIS OF STRUCTURES . . . . .	3
3.0 NATURE OF UNCERTAINTIES IN SHIP LONGITUDINAL STRENGTH: DEMAND AND CAPABILITY. . . . .	7
3.1 Uncertainties in Demand . . . . .	7
3.2 Uncertainties in Capability . . . . .	10
4.0 DATA ON UNCERTAINTIES OF VARIOUS SHIP HULL LOADS .	13
4.1 Still Water Loads . . . . .	13
4.2 Thermal Effects . . . . .	14
4.3 Wave Loads. . . . .	16
4.3.1 Effects of Sea State . . . . .	17
4.3.2 Effects of Theoretical Response Operators. . . . .	22
4.3.3 Effect of Extrapolation Method for Lifetime Maxima. . . . .	28
4.3.4 Combined Variability for Wave Loads. .	30
4.4 Springing Vibratory Loads . . . . .	30
4.5 Slamming and Whipping . . . . .	33
5.0 COMBINATION OF LOADS . . . . .	38
5.1 Still-Water, Thermal and Wave Loads . . . . .	38
5.2 Combined Vertical and Lateral Wave Loads. . .	40
5.3 Combined Wave and Springing Loads . . . . .	41
5.4 Combined Wave and Whipping Loads. . . . .	43
6.0 SHIP HULL STRENGTH ANALYSIS. . . . .	49
6.1 Application to Representative Ships . . . . .	55
7.0 ANALYSIS OF UNCERTAINTY OF SHIP STRENGTH . . . . .	59
7.1 Suggested Procedure for Calculating Objective Uncertainties . . . . .	63
7.2 Data for Determining Objective Uncertainties.	66
8.0 SUBJECTIVE UNCERTAINTIES IN SHIP STRENGTH. . . . .	69
9.0 SPECIAL CASES - LOADS AND STRENGTH . . . . .	75
10.0 APPLICATION TO RELIABILITY EVALUATION. . . . .	78
11.0 DESIGN LOAD ESTIMATION . . . . .	81
12.0 CONCLUSIONS AND RECOMMENDATIONS. . . . .	85
12.1 Conclusions. . . . .	85
12.2 Recommendations . . . . .	87
13.0 ACKNOWLEDGMENTS. . . . .	90
14.0 REFERENCES . . . . .	91

*8 1/2 Pica Bond*

(5 PicA Head)

LIST OF FIGURES

	<u>Page</u>
1. Probability density functions of load and strength. . . . .	4
2. 27-34 ft. significant wave height family-8 spectra . . . . .	18
3. Example of 10 sample wave spectra having a significant height of 30 ft. . . . .	18
4. Response operator and box spectrum bandwidth. . . . .	23
5. Calculated and measured nondimensional vertical bending moment amplitudes of the container ship (Fn=0.245). . . . .	24
6. Midship wave moments on SERIES 60, BLOCK.80 hull, Fn=0.15 . . . . .	25
7a. Midship vertical wave bending moments, 210° heading . . . . .	26
7b. Midship vertical wave bending moments, 180° heading . . . . .	26
8. COV of extreme value as function of number of cycles (for Rayleigh distribution). . . . .	31
9. Comparison between measured and predicted springing responses . . . . .	32
10. Teledyne measured stress spectrum for FOTINI-L, voyage 7FLI-3, interval 22. . . . .	42
11. Load combination; $X(t) + Y(t)$ . . . . .	45
12. Domain of integration . . . . .	46
13. Effective breadth of plates . . . . .	51
14. Effect of buckling on ultimate longitudinal strength-single deck ship-sagging condition . . . . .	54
15. Flat bar stiffener section, UNIVERSE IRELAND. . . . .	55
16. Load-shortening curves for square plates under uniaxial compression. . . . .	64
17. Reduction of section modulus due to corrosion . . . . .	68

1/2 PicA Outside

(5 Pic. Heel)

LIST OF TABLES

	<u>Page</u>
1. Still-Water Bending Stress in Container Ships . . .	14
2. Still-Water Bending Stress in Tankers . . . . .	14
3. Thermal Stresses - S.S. WOLVERINE STATE (Calculated). . . . .	15
4. Thermal Stresses - ESSO MALAYSIA (Measured) . . .	15
5. Measured Wave Spectral Family Groups. . . . .	17
6. Vertical Bending Moment Statistical Responses (Calculated) in Different Sea Conditions - UNIVERSE IRELAND. . . . .	20
7. Vertical Bending Moment Statistical Responses (Calculated) in Different Sea Conditions - FOTINI-L . . . . .	20
8. Vertical Bending Moment Statistical Responses (Calculated) in Different Sea Conditions -SL-7. . .	21
9. Vertical Midship Whipping Bending Moment Values, $10^{-5}$ Probability. . . . .	36
10. Vertical Midship Whipping Bending Moment Values, $10^{-8}$ Probability. . . . .	36

(8 1/2 Pic. Bend)

(The Hand)

NOMENCLATURE

a	wave amplitude
A	section area
b	plate width
COV	coefficient of variation
B	ship beam
D	ship depth
E	modulus of elasticity
$E_t$	tangent modulus
$f(x)$	probability density
$F(x)$	cumulative probability
g	acceleration of gravity; also used for distance from center of deck area to neutral axis
$g(y)$	probability density of extreme value
$H_{1/3}$	significant height of waves
L	external load; also used for ship length
M	bending moment
n	number of oscillation cycles
P	probability of occurrence
$P_f$	failure probability
s	stress
S	ship strength
$S_n(\omega)$	wave power spectral density
t	plate thickness; also used for time variable
$ T(\omega) $	response amplitude operator
Z	section modulus; also used as sum of wave and slam-induced bending loads
$\alpha$	mean value of slam load; also used for general parameters in ship strength representation
$\beta = \frac{b}{t} \sqrt{\frac{s_{yc}}{E}}$	plate slenderness ratio
$\beta_f$	safety index
$\gamma_o$	overall partial safety factor (ratio of characteristic strength and load)
$\delta$	objective coefficient of variation
$\Delta$	subjective coefficient of variation
$\epsilon$	broadness factor of spectrum
$\theta$	central safety factor (ratio of mean strength and load)
$\mu$	mean value
$\rho$	fluid density; also used for correlation coefficient
$\sigma$	standard deviation
$\phi$	stress ratio factor
$\Phi(x)$	normal distribution cumulative distribution function
$\omega$	circular frequency, rad./sec.
$\Omega$	total uncertainty coefficient of variation

(2/3 Page Outside)

## 1.0 INTRODUCTION

The design of any structure by rational means involves consideration of the uncertainties that arise in regard to the external actions imposed on the structure as well as the strength and response properties of the structural elements. These different uncertainties can be taken into account by introducing probability concepts into the structural design procedure.

In the case of ships, these concepts were introduced by St. Denis and Pierson [1] when determining the ship motions, structural loads, etc. due to operating in a realistic random seaway. At about the same time, other work was being carried out in the area of probabilistic design of structures. A basic application of the probabilistic approach to the safe design of engineering structures was given by A. M. Freudenthal [2], and later he dealt specifically with marine structures [3]. Others have considered the ship problem including Abrahamsen et al [4], Lewis [5], Nordenstrøm [6], Mansour [7], [8], Mansour and Faulkner [9], Stiansen et al [10], where the theory of structural reliability was applied to ships. The basic theory tells us that if we can clearly and completely define a probability distribution for loads (demand) and for strength (capability) it is possible to calculate the probability of failure or collapse. A design strength standard can then be established on the basis of an acceptable failure probability without resorting to a factor of safety, an allowable stress or a load factor.

When considering structural failure, separate analyses are necessary for all possible failure modes such as

1. Ultimate tension failure
2. Ultimate compression failure or collapse
3. Brittle fracture
4. Fatigue

Of the first two modes, the second (ultimate compression failure) is of first importance, for the compression flange of the hull girder is more likely to fail by buckling than is the tension flange by extensive yielding. Brittle fracture is very difficult to deal with because of the large uncertainties associated with the material quality (notch-toughness in relation to temperature). Fortunately, this mode of failure has been brought under control on the basis of improved design details and workmanship and use of notch-tough strakes as crack stoppers to provide "fail-safe" design.

Fatigue failure is an important consideration even though fatigue cracks do not normally in themselves threaten the complete failure of the hull girder [11]. The problem appears to be to control the growth of microscopic cracks to a critical size requiring the trouble and expense of frequent repairs. However, the problems are distinctly different from ultimate strength and are not as much a basic consideration in ship longitudinal strength as is ultimate strength in bending. Consequently attention is primarily focused on ultimate failure, usually involving collapse of the compression flange.

Ship structural design for longitudinal strength has been based mainly on elastic beam theory with emphasis on the maximum expected load (bending moment) and an allowable stress that provides a factor of safety against unspecified failure. Some consideration is given to avoiding local buckling but the main emphasis- enhanced by the development of computer-aided finite element methods of stress analysis - has been on detailed calculation of stresses. The probabilistic approach to design requires renewed attention to the ultimate strength of the ship girder (as described by Caldwell [12] or to the "load-carrying ability" of the structure as discussed by Vasta [13]. Although ultimate failure invariably involves buckling, the problem is complicated by the fact that buckling may occur progressively in different segments of the structure and the first occurrence of a buckle does not usually constitute failure. Recent work by Smith [14] and by Billingsley [15] attempts to account for the successive transfers of load from buckled areas to those that are still effective. But these theories have not explicitly allowed for the variability of ultimate strength, and other approaches must be considered.

The biggest problem then in applying the probabilistic approach to the practical design of ships is the identification and evaluation of the uncertainties in loads (demand) and strength (capability). The objective of the present study is to identify these uncertainties, and to evaluate them as fully as possible from available published data. Indications of areas in particular need of further research can then be identified also. A description of the work carried out in this study in order to satisfy these objectives is given in the following sections of this report.

## 2.0 PROBABILISTIC ANALYSIS OF STRUCTURES

Since the present study is concerned with uncertainties associated with the design of ship structures, this information is to be used within the context of a probabilistic design and analysis approach. That approach is distinctly different from deterministic methods whereby the strength of the structure is selected at such a value that it would survive the greatest expected imposed external load by some pre-established margin. That particular margin, which is the ratio of the structural strength to the design load, is called the factor of safety, which is assumed to account for all of the unknown in both loads and structural strength.

The procedure involved in the probabilistic approach accepts the fact that there is no absolute assurance of safety for any structure, with structural performance described only in terms of probabilities. The structural strength and also the applied load can be described as being random variables, each of which have respective probability density functions. The occurrence of failure for any structure implies that the load (represented by the variable  $L$ ) exceeds the strength (represented by the variable  $S$ ), which in probability form is given by the equation for the probability of failure,  $P_f$ , as shown by the relation

$$P_f = P(L > S) \quad (1)$$

Assuming that the probability density functions of the load and the strength are represented by  $f_L(l)$  and  $f_S(s)$  respectively, together with their cumulative distribution functions defined by the respective integrals of the density functions, as illustrated by

$$F_L(l) = \int_0^l f_L(l) dl, \quad F_S(s) = \int_0^s f_S(s) ds \quad (2)$$

the failure probability can then be expressed in terms of those quantities. The probability of failure is then given by

$$P_f = \int_0^{\infty} F_S(x) f_L(x) dx \quad (3)$$

or

$$P_f = \int_0^{\infty} [1 - F_L(x)] f_S(x) dx = 1 - \int_0^{\infty} F_L(x) f_S(x) dx \quad (4)$$

These expressions for failure probability represent the convolution between probability densities of load and strength, as shown below in Figure 1.

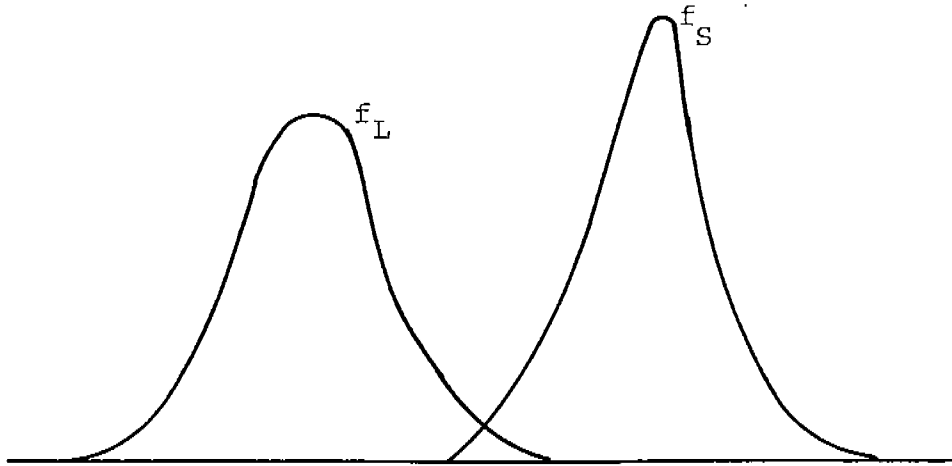


Fig. 1 Probability density functions of load and strength

The magnitude of the failure probability depends on the relative positions of these distributions with respect to each other and the degree of dispersion of each density function relative to their peak values, i.e. the "spread" of the density functions.

The determination of the failure probability, as shown above, depends upon knowledge of the density and distribution functions of both load and strength. If these quantities are known precisely, then the evaluation is relatively simple and the failure probability can be directly calculated. However that is the major problem in the use of these simple formulas, since the information is not directly available. The form of the probability density functions must be developed or established from available data and/or experience with the particular phenomena, together with the determination of the magnitude of parameters associated with the density functions.

With the present state of the art, various assumptions are made with regard to the form of the probability density functions, together with estimates of parameters determined from a limited set of measurements. In most engineering applications, approximate methods are the most useful procedure for obtaining results. The most important elements to be determined are then seen to be the central values (i.e. mean values) and the measures of dispersion, regardless of the precise nature of the actual probability density functions. For many practical applications, the calculated failure probability is not very sensitive to the exact form of the density functions  $f_L$  and  $f_S$ , i.e. in the range  $P_f \geq 10^{-3}$ , while in the range  $P_f < 10^{-5}$  the failure probability would generally be sensitive to the actual form of the probability densities [16].

As a result of the difficulties in determining the actual probability functions, etc. used for a precise analysis in accordance with Eqs. (3) and (4), as well as the prime importance of the central value and dispersion measures, simpler methods have been applied to the structural design. These methods are semi-probabilistic and are based on the capability of determining statistical properties of the load and strength up to their second moments, i.e. the evaluation of mean values and standard deviations.

One particular "second moment" method makes use of the "safety index" which is defined in terms of the means and standard deviations of the load and strength variables. Defining the margin of safety  $M = S - L$ , with mean value  $\mu_M$  and standard deviation  $\sigma_M$ , the inverse of the coefficient of variation (COV) of  $M$  is defined by

$$\beta_f = \frac{\mu_M}{\sigma_M} = \frac{\mu_S - \mu_L}{\sqrt{\sigma_S^2 + \sigma_L^2}} \quad (5)$$

where  $\beta_f$  is called the safety index.

For the conditions where  $L$  and  $S$  are statistically independent random variables, characterized by normal distributions with mean values  $\mu_L$  and  $\mu_S$  and standard deviations  $\sigma_L$  and  $\sigma_S$ , the probability of failure is then

$$P_f = 1 - \Phi(\beta_f) \quad (6)$$

where  $\Phi(x)$  is the cumulative distribution function corresponding to the normal distribution. The failure probability is also defined as

$$P_f = P[M < 0] \quad (7)$$

which can be shown to reduce to the result in Eqn. (6) for a normally distributed  $M$ .

The safety index  $\beta_f$  should be as large as possible in order to result in a low value of failure probability, thereby illustrating its utility as a measure of safety for a structural design (assuming normal distributions apply). However the basic concept of a sufficiently large safety index is still useful as a measure of design safety independent of the exact nature of the probability functions, and it is used accordingly.

Another semi-probabilistic approximate method based on second moment concepts is the "partial safety factor" method, which also makes use of information on the mean

values and standard deviations of the load and strength. This method makes use of special factors that represent the effect of strength reduction and load magnification in terms of minimum strength allowance and maximum load relative to average conditions. A safe design requires the minimum strength to exceed or equal the maximum load. The choice of values of these factors depends upon the various uncertainties of the load and strength variables. This method has been applied to ships in [17] and [10].

The analysis of uncertainties in the case of ship structures which is carried out in this study will be applied toward use in the above methods, with primary emphasis on the safety index methods (since it directly uses information in the form of COV values) and some consideration of partial safety factors. Developments that provide information on basic probability distributions will also have applicability toward the full probabilistic approach that uses information in terms of such probability distributions.

### 3.0 NATURE OF UNCERTAINTIES IN SHIP LONGITUDINAL STRENGTH: DEMAND AND CAPABILITY

When considering ship longitudinal strength and the requirements for adequate structural design, the loads acting on the ship represent the "demand" and the ship structural strength represents the "capability" of the structure. A separate discussion is given below of the basic sources of uncertainty that are present in both of these elements that contribute to ship structural design.

#### 3.1 Uncertainties in Demand

The principal loads acting on a ship's hull may be summarized as follows, with particular reference to longitudinal hull bending:

- Static bending moments resulting from uneven distribution of weights and buoyancy in still water.
- Essentially static bending moment caused by the waves generated by the ship's forward motion in calm water.
- Quasi-static or low frequency bending moments caused by relatively long encountered waves.
- Dynamic (vibratory) bending moments caused by wave-hull impacts or high-frequency wave forces.
- Thermal loads, resulting from uneven temperature gradients.

Other loads not considered here are internal loads caused by liquid cargoes, machinery or propellers; collision, grounding and docking loads; aerodynamic and ice loads.

Of all of the above loads, the one receiving the greatest attention through the years has been the quasi-static wave bending moment. Recent work has followed the probabilistic approach, since it was clearly established by St. Denis and Pierson [1] that the waves causing such bending moments could only be understood and described by statistics and probability theory. A specific sea condition can be fully described by its directional spectrum, defining the component wave frequencies and directions present. Uncertainties arise from:

- Variability in the directional properties of wave spectra, with only limited data available.
- Combined effects of two storms, or sea and swell.

- Variability of spectral shapes for a given significant height. Considerable data are available for limited ocean areas, but more data are needed.
- Possibility of "freak" waves, usually as a result of effects of shoaling water nearby coasts, currents, etc.

Short-term responses, including bending moments, can be calculated statistically by means of the principle of linear superposition [1] combining calculated responses to regular waves (RAO's) and assumed ocean wave spectra. The RAO (response amplitude operator) is the amplitude of the ship response at a particular frequency to a unit sinusoidal wave at that frequency. Uncertainties involved in the calculation of RAO's using the usual "strip-theory" approach are:

- Assumed linearity of response in relation to wave height.
- Inaccuracy of strip theory.
- Effect of variation in weight distribution on motions and on inertia loads (usually ignored).

After calculating response spectra by means of superposition, there are uncertainties regarding the statistics of response. Various studies, e.g. [18] have shown that these uncertainties can be reduced if a spectral width parameter is included in deriving the distribution of response (bending moment) maxima and minima. Otherwise, the use of a simple Rayleigh distribution can result in a bias toward values that are too high in severe seas [19].

Other uncertainties are associated with the operation of the ship, including:

- Cargo distribution and resulting drafts
- Ship headings to the sea
- Ship speed

Still-water bending moments are comparatively easy to calculate if the distribution of cargo and other weights is known, as shown in [20]. Unfortunately calculations are not always made before every voyage, and in any case they are seldom recorded. Hence, very little statistical data are available. Estimates can be made on the basis of calculations customarily made for every new ship design

covering representative conditions of loading expected in service.

The bending moment caused by the ship's own generated wave system can be determined experimentally or from a calculation of the ship's wave profile at different speeds. Uncertainties are small and can be estimated.

Theoretical methods of calculating wave-induced dynamic or vibratory bending moments must consider both steady-state high-frequency loads and impulsive loading. The former, known as springing, involves unresolved uncertainties in the excitation, structural damping, nonlinear effects, etc. The latter, known as slamming and whipping, involves unresolved uncertainties in the prediction of the occurrence of slamming; in the calculation of slamming loads as a function of ship form, relative vertical velocities and ship heading; and in the structural damping of the whipping response. Hence, at the present time, it would appear that the most suitable approach to evaluating the uncertainties in dynamic loadings is by analyzing available statistics on measured hull stresses.

Reliable methods are available [21] for calculating thermal stresses when temperature gradients in the hull are known. Uncertainties consist of:

- Ambient conditions - air and water temperatures, winds, sunlight and local shading. Meteorological and oceanographic data are available but have not been analyzed.
- Methods of calculating temperature gradients from known ambient conditions are unreliable.

Estimates are required pending further research and full-scale measurements on ships at sea.

Perhaps the most difficult problem in defining loads or demand in probability terms is that of combining the disparate loads discussed above.

- Static loads usually vary only from one voyage to the next (although they can also vary within one voyage).
- Thermal effects are generally diurnal.
- Low-frequency wave loads are evidenced in the frequency of wave encounter bandwidth range.
- Dynamic loads occur at the natural hull frequency (usually vertical, fundamental mode).

If all of these loads can be considered to be statistically independent, the principles of probability theory can be utilized to determine the necessary combined distributions. However, as noted by St. Denis (in Report of Committee I.3 to ISSC, 1979), "the essential problem that arises when seeking to combine loads is not so much that of their formal treatment by theory of probability but rather the derivation from an analysis of observations of the correlation existing between loads." For example, high dynamic loads may often occur in rough seas when large low-frequency loads also occur, but high thermal effects may generally coincide with calm, sunny days when wave-induced loads are relatively mild.

It appears that the most difficult problem of combined loads is that of low- and high-frequency wave-induced loads. Not only is there a question of statistical correlation in the long term, but there is the question of short-term phasing - does a maximum vibratory load ever coincide with an extreme low-frequency load? Hence, instead of collecting separate statistics on uncertainties of dynamic loads (as previously mentioned) and in correlation with low-frequency loads, it may be simpler to collect overall data on how much the vibratory loads add to or modify the distribution of low-frequency loads for different ship types in various services, as described in [20] and [22].

### 3.2 Uncertainties in Capability

These uncertainties are usually classified as objective - those that are measurable or quantifiable - and subjective - those for which there is no factual information available and for which subjective judgment is therefore required. As noted by Daidola and Basar [23], "Future efforts ..... should be directed toward identifying and quantifying more uncertainties. Most subjective uncertainties are really 'as yet - unquantified' objective uncertainties." The uncertainties arise from methods of calculating structural responses, including the effect of boundary conditions, and variability in physical behavior of materials and structures.

The objective uncertainties that have been discussed in the literature and from which some data are available will first be summarized (e.g. see [9] and [23]):

- Main dimensions of hull, which is a minor factor for which data are available.
- Material properties - including yield strength, ultimate strength and Young's modulus - where data are available as in [23] and [25].
- Variations in material thickness and shape dimensions.

- Manufacturing imperfections, including variations in fabrication tolerances, weld quality, alignment, and residual stresses in weldments.
- Corrosion and wear, which must be dealt with separately, since they involve "time-dependent strength" [23].

It will be noted that all of the above involve physical uncertainties in the materials used or in the methods of ship construction.

There is less agreement in the literature regarding subjective uncertainties, but the following are listed by Mansour and Faulkner [9]:

- Shear lag and other shear effects (considered negligible).
- Major discontinuities; openings, superstructures.
- Torsional and distortional warping.
- "Poisson's ratio" effects, especially at transverse bulkheads and diaphragms.
- Stress redistribution arising from changes in stiffness due to deformations, inelasticity, or both.
- Gross-panel compression nonlinearities; effective width, inelasticity, residual stresses and shake-out effects (considered negligible).

It will be noted that the above subjective uncertainty items involve inaccuracies or simplifications of theories of stress analysis and structural response. The authors believe that none of them is serious except for the effect of superstructures, and neglect of all except the first would lead to systematic errors on the safe side, i.e. a bias. However, it is obvious that further knowledge is needed to reduce these subjective uncertainties to the objective category. A seventh item of subjective uncertainty mentioned in [9] is "'residuary strength' after gross panel failure", which is a special important item that affects the entire question of the theory of ultimate strength and its variability. As noted by Lewis [25], "available data on probabilistic aspects of capability in general seem to apply to local panel failure rather than complete failure of the entire girder flange in compression or tension. For example, for a tanker such as that under consideration here, the local compression buckling of a deck panel in the center

tank would shift the load to the top of the side tank structure - deck, side shell and longitudinal bulkheads. This structure would probably carry considerably higher load before there would be further buckling, such that complete failure or collapse could be said to have occurred." Smith[14] and Billingsley [15] have considered these effects (as previously noted), but a thorough study of experimental data on panel buckling such as that by Smith [26] will be required in order to estimate the degree of uncertainty involved in these approaches.

The modes of failure to which the above uncertainties are considered and applied include:

- Tension yield
- Compression failure of stiffened panels between transverses (strut-panel or stiffener tripping)
- Compression failure by overall grillage buckling, including transverses. This type of failure considers grillage instability or beam-column type collapse.

The contribution to overall uncertainty in predicting ultimate strength of ship hull girders composed of different types of panels has to consider these different possible failure modes.

#### 4.0 DATA ON UNCERTAINTIES OF VARIOUS SHIP HULL LOADS

When considering the type of external environmental loads that act upon a ship, it is necessary to separately determine the uncertainties of each of these individual loads. The present section discusses the individual type loads and also procedures for determining the uncertainties associated with such loads, as well as providing numerical values that can be used for future calculations. The discussion below considers each load separately, with treatment of the problem of the combination of loads given in a later section of the report.

##### 4.1 Still-Water Loads

The still-water loads are bending moments that act on the ship due to the difference between the distributed weight of the vessel and the buoyancy due to the hydrostatic support effect of water. As such these still-water bending moments will vary with the degree of loading and ballast of the ship, which can change during its voyages. In general any ship will have a probability distribution of still-water bending moment corresponding to the loaded condition and another distribution corresponding to the ballast condition, where the validity of this concept is supported by the work in [27] and [28].

These different operating conditions of the ship can be established so that estimates can be made via calculations that cover representative conditions of cargo and other weights that are expected to vary in particular service for any vessel. However, poor logbook records for different ships that have been studied as part of full-scale investigations, e.g. [22] and [29], have not been adequate to provide this information in such a way that the still-water bending moments could be calculated. While the loading booklets for any vessel do provide some range of representative operating conditions, these conditions do not correlate well with the actual experienced operating conditions of ships in their commercial services.

A research project is being carried out for the Ship Structure Committee (Project SR-1282) in order to develop a plan to obtain data that would provide information on such still water bending moments which is an indication of the necessity for additional data in this area. However, some recent data have become available as a result of work carried out in Japan [30], with the data corresponding to the still-water bending stresses of different ships being summarized in [31]. This information was presented separately for a group of 10 containerships as well as for a group of 8 tankers. The containerships represent the class of ships that have small variation of their cargo loading conditions, which is also representative of general cargo ships. Tankers and ore carriers represent a group of ships having variable loading conditions, with different results corresponding to the full load condition and the ballast

condition.

A listing of this Japanese data for the still-water bending stress in the form of information useful for probabilistic design studies, viz. the mean value, standard deviation, and COV, is given below for these two types of ships.

Table 1

Still-Water Bending Stress In Container Ships

Mean Value	Standard Deviation	COV
6.04 kg/mm <sup>2</sup> (8.63 kpsi)	1.76 kg/mm <sup>2</sup> (2.51 kpsi)	0.291

Table 2

Still-Water Bending Stress in Tankers

Loading	Mean Value	Standard Deviation	COV
Ballast Cond.	4.38 kg/mm <sup>2</sup> (6.26 kpsi)	4.33 kg/mm <sup>2</sup> (6.19 kpsi)	0.989
Full Load Cond.	-3.64 kg/mm <sup>2</sup> (-5.20 kpsi)	1.90 kg/mm <sup>2</sup> (2.71 kpsi)	0.522

In these tables, positive stress values correspond to the hogging condition and negative to sagging. The bending moment for any ship of similar type is then estimated by multiplying by the appropriate section modulus for that ship. For use in either deterministic or semi-probabilistic design and analysis when considering ultimate strength, it is usual to select representative extreme values of either hogging or sagging still-water bending moments.

#### 4.2 Thermal Effects

Thermal stress values were indicated to have fairly significant magnitudes (3-5 kpsi) in some cases, as shown by the measurements on five bulk carriers in [29]. The records there show a consistent diurnal variation in that range. The thermal stress values are not necessarily loads on the ship, but are considered to be loads because they have similar effects. Thermal stresses develop from temperature gradients in the ship structure which arise from the different air-water temperature differences as well as the temperature effects due to insolation, which is the absorption of radiant heat. Any temperature change due to insolation depends upon cloud cover as well as the color of the deck. The degree of cloud cover varies in different areas of the

world as a function of the season, with different relative frequencies of occurrence of these different degrees of cloud cover.

A discussion and illustration of representative data that could be used for calculation of thermal stresses are given in [20], where calculations were made for a representative cargo ship (S.S.WOLVERINE STATE). Using the data for the temperature differences corresponding to different cloud conditions, as well as their frequency of occurrence, allowed determination of calculated estimates of thermal stresses in that vessel. Using the information on the weighted average, as well as establishing a standard deviation from those calculated values, allowed determination of the COV for the WOLVERINE STATE vessel, as shown below in Table 3:

Table 3

Thermal Stresses - S.S. WOLVERINE STATE (Calculated)

Mean Value	Standard Deviation	COV
1040 psi	557 psi	0.536

At the same time, the information available in [29] allowed determination of this same type of information from measured thermal stresses on the tanker ESSO MALAYSIA. Using the data for the 11 day-night or night-day stress variations for the period 9/18/68 through 9/28/68 allowed determination of the statistical information given below in Table 4 (this is only an example which is given for the available data).

Table 4

Thermal Stresses - ESSO MALAYSIA (Measured)

Mean Value	Standard Deviation	COV
1.8 kpsi	0.261 kpsi	0.145

It can be seen that there is a smaller value of the COV of thermal stresses as determined from actual ship measurement as compared to that from theoretical calculations, although the calculated thermal stresses due to the assumed temperature changes which is shown in [20] do provide the correct order of magnitude for these stresses. Since the thermal stresses are generally low compared to other environmental effects, and greater reliability is generally given to measured data results, the values in Table 4 may be considered to be more useful for the present study of uncertainties.

The calculation of thermal stresses is seldom required in ship design except when considering special vessels that carry low or high-temperature cargoes such as LNG and asphalt. Since these thermal stresses vary diurnally, which corresponds to a larger time scale as compared to other larger environmental disturbances (such as waves), the selected value for any design or analysis studies can be considered as a fixed constant value for such purposes (although there is still a statistical uncertainty associated with such stresses).

#### 4.3 Wave Loads

The low-frequency bending moments due to waves have received the greatest attention in published literature, with extensive theoretical treatments available for estimation of such loads. Similarly there is a fair amount of test data available for models as well as some limited information for full scale also. These bending moments are also generally the largest loads acting on a ship at sea, with the main emphasis in prior studies of probabilistic design approaches being concerned with that type of load.

The ship response operators in the frequency domain (RAO's) are determined by means of either computation based upon a theoretical technique such as the one of linear strip theory (e.g. [32], [33]) or by use of model test results determined in regular wave tests. When considering using the probabilistic approach, the loads are usually determined by the linear superposition technique evolved by St. Denis and Pierson [1] whereby the spectral representation of responses is established in terms of ship response operators (in the frequency domain) and the wave spectra. There are possible limitations of the hydrodynamic theory in regard to linearity and inaccuracies in certain frequency and speed ranges (also dependent upon the heading angle, e.g. in stern quartering seas). Other possible limits when determining the wave loads are present in the representation of different sea conditions in terms of spectral variability in both the frequency domain as well as in regard to directional properties.

All of these features contribute to uncertainties in determining the load response of a ship subjected to waves, primarily in establishing statistical measures such as the rms value and other response statistics. The spectral bandwidth parameter described in [18] affects the various response statistics, and the nature of the probability densities characterizing the response determines the properties of extreme values. In addition, there may be certain nonlinear effects present that will also influence these load characteristics, which provides another source of uncertainty.

A description of the different approaches used in order to obtain some quantitative measures of the uncertainties in wave loads is given below, with different approaches used to apply to the different sources of uncertainty discussed above. It is intended that the treatment described in the following analyses will provide a more firm basis for establishing values for the uncertainties associated with this important load component, since the past literature in this field of probabilistic analysis for ship structures has only used rough orders of magnitude without providing sufficient basis for the values used and the range of applicability of such values.

#### 4.3.1 Effects of Sea State

One of the important influences on the wave load (i.e. bending moment) variability is the effect of the variation of the wave spectra that correspond to a given "sea state." A number of different methods have been used to assess the effect of this variability, including the work of Lewis [34] as well as an investigation by Ochi [35]. In [34], the variability of the wave spectra was based upon the use of actual measured wave data from which a "family" of spectra were established corresponding to a particular range of significant height.

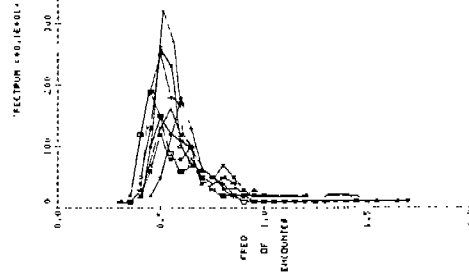
A set of useful data for this purpose is that presented in [36], which was obtained from the analysis of wave records from weather ships located at Station "India" in the North Atlantic Ocean. The data presented in [36] cover 323 wave records and resultant spectra, from which selected groups were established. These groupings are described in [37], and are denoted as Group 3, Group 4, Group 6, Group 8 and Group 10. The number of representative spectra chosen in Groups 3, 4, 6 and 8 comprise eight spectra for each group. The number of spectra in Group 10 were only 2. The significant wave height range for each of these groups was as follows:

Table 5

#### Measured Wave Spectral Family Groups

<u>Group</u>	<u>Range of <math>H_{1/3}</math>, ft.</u>
3	6-9
4	9-12
6	16-21
8	27-34
10	37-45

The data plots and tabulations of the wave spectra used for these real wave conditions are provided in [36], and representative samples are given in Figures 2 and 3.



Record No.	Symbol	$H_{1/3}$	$T_1$
172	+	27.10	8.36
295	◆	27.16	10.44
176	*	26.58	8.91
267	□	26.64	11.89
184	[ ]	30.28	10.62
199	×	26.89	9.81
187	■	32.97	10.03
190	\$	33.08	9.88

Fig.2 27-34 ft. significant wave height family-8 spectra

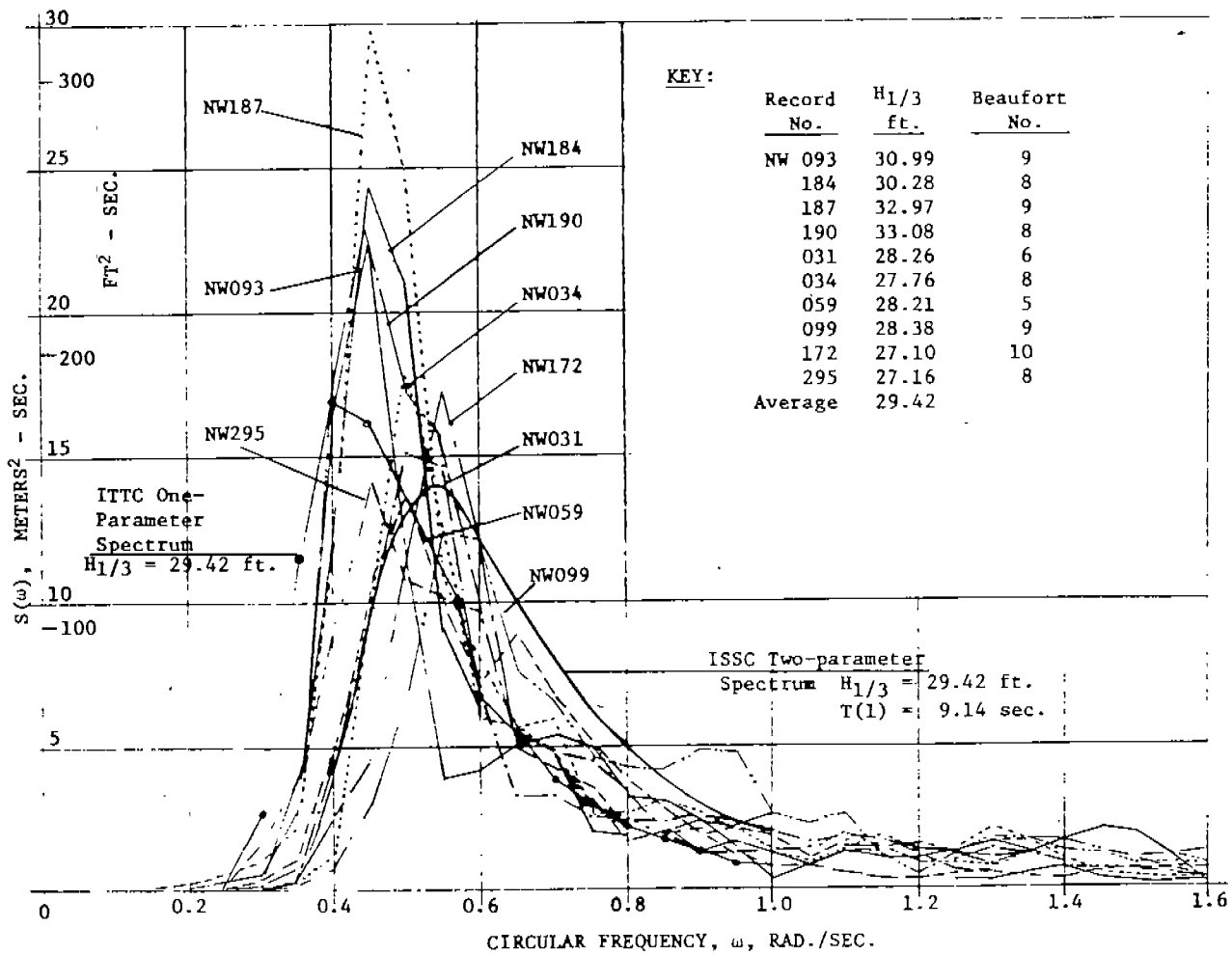


Fig. 3 Example of 10 sample wave spectra having a significant height of 30 ft.

The earlier bending moment variability calculations carried out in [34] made use of some measurements where a different grouping wave spectra was used. It was these data that led to the estimate of a value of COV equal to 0.149, which has been quoted in many publications without any close investigation of the source of that value. An illustration of calculated results was given in [34] for the WOLVERINE STATE ship which demonstrated the analysis used to find the COV value due to wave spectrum variability. The resulting value was determined there to lie in the range of 0.22-0.30 when considering the effects of different spectral families, different significant height, different headings, and short-crested sea conditions. The statistically averaged values were calculated on the assumption that all headings are equally probable. The range of COV values was not affected by the ship forward speed, although there were some small differences (on the order of 10% at most) for the relative magnitudes of the mean values for each particular speed.

The analysis provided in [35] considered different representative mathematical formulations for wave spectra, from which an analysis of maximum force was calculated on a ship with these different wave spectral representations. The parameters of the wave spectral formulations, for a particular significant wave height, were varied in accordance with different confidence values so that a family of spectra was established for each significant wave height condition. There were 9 members of the family corresponding to the Bretschneider 2-parameter spectrum and 11 members of the family for the 6-parameter spectrum of Ochi and Hubble [38]. The results in [35] indicated a COV for the Bretschneider spectrum results of about 0.20, and a COV value of about 0.10 when using the 6-parameter spectra. Thus, it would appear that the choice of the spectral model representation being used has a definite influence on the uncertainty values (COV) of loads due to the manner of specification and/or definition of the wave spectrum, for these theoretical spectral models.

In order to illustrate the influence of actual sea conditions, the family of measured spectra obtained from [36], and which have been described above in Table 5, have been applied to 3 representative ships that will be considered for many of the illustrations throughout this report. These ships are a tanker (UNIVERSE IRELAND); a bulk carrier (FOTINI-L); and a containership of the SL-7 type. Calculations to illustrate the nature of the vertical bending moment values obtained for these 3 different vessels were carried out for different headings and operating speeds of the vessels, using the tabulated response operators given in [22] together with the spectra in [36]. Results were found for the rms response for each particular member of each spectral family, from which a mean value, standard deviation and resulting COV were then found. A tabulation of the different values found from this computational procedure is given in Tables 6-8.

Table 6

Vertical Bending Moment Statistical Responses  
(Calculated) in Different Sea Conditions

UNIVERSE IRELAND

(All values in ft.-tons, multiplied by  $10^5$ )

Wave Group	Group 3			Group 4		
	$\mu_V$	$\sigma_V$	COV	$\mu_V$	$\sigma_V$	COV
Heading Angle						
120°	0.692	0.188	0.272	0.977	0.283	0.290
150°	0.769	0.278	0.362	1.162	0.423	0.364
180°	0.770	0.311	0.404	1.176	0.461	0.392

Wave Group	Group 6			Group 8		
	$\mu_V$	$\sigma_V$	COV	$\mu_V$	$\sigma_V$	COV
120°	1.76	0.420	0.239	3.4	0.411	0.121
150°	2.07	0.705	0.340	4.31	0.608	0.141
180°	2.096	0.808	0.385	4.69	0.772	0.165

Table 7

Vertical Bending Moment Statistical Responses  
(Calculated) in Different Sea Conditions

FOFINI-L

(All values in ft.-tons, multiplied by  $10^5$ )

Wave Group	Group 3			Group 4		
	$\mu_V$	$\sigma_V$	COV	$\mu_V$	$\sigma_V$	COV
Heading Angle						
120°	0.541	0.128	0.237	0.685	0.161	0.234
150°	0.541	0.163	0.302	0.793	0.264	0.332
180°	0.502	0.181	0.360	0.767	0.280	0.364

Wave Group	Group 6			Group 8		
	$\mu_V$	$\sigma_V$	COV	$\mu_V$	$\sigma_V$	COV
120°	1.248	0.154	0.123	1.810	0.128	0.071
150°	1.389	0.390	0.281	2.540	0.289	0.114
180°	1.330	0.445	0.335	2.632	0.350	0.133

Table 8  
Vertical Bending Moment Statistical Responses  
(Calculated) in Different Sea Conditions

SL-7

(All Values in ft.-tons, multiplied by  $10^5$ )

Wave Group	Group 3			Group 4		
Heading Angle	$\mu_V$	$\sigma_V$	COV	$\mu_V$	$\sigma_V$	COV
120°	0.380	0.091	0.237	0.498	0.117	0.234
150°	0.505	0.144	0.302	0.711	0.230	0.324
180°	0.465	0.164	0.360	0.692	0.255	0.368

Wave Group	Group 6			Group 8		
	$\mu_V$	$\sigma_V$	COV	$\mu_V$	$\sigma_V$	COV
120°	0.884	0.105	0.119	1.266	0.098	0.077
150°	1.274	0.302	0.237	2.293	0.260	0.113
180°	1.219	0.397	0.326	2.418	0.315	0.130

The results in Tables 6-8 illustrate the influence of the level of the sea state, i.e. the significant height range, and the heading angle on the COV values for these vessels. In general, it can be seen that the larger sea states exhibited the lowest COV values, with similar results for the largest waves (Group 10) which were not shown since there were not enough wave spectra (i.e. only 2) in that grouping to provide reliable statistics. Since the basic interest for design purposes is the extreme values of bending moment, which generally occur in the larger sea states, the information in that range would be the most useful for the present study. Considering the condition for head and bow seas also provides the larger values of vertical bending moment as well. On that basis, the range of COV values due to wave spectral shape variability as obtained using theoretical response operators from strip theory would lie between 0.11-0.17 with the value 0.14 as representative.

This value is quite close to the value 0.149 that has been quoted in previous references. However it is also appropriate to large ships, with lengths in the range 800-1100 ft. The COV values for the WOLVERINE STATE in [34] applied to a cargo vessel of 500 ft. length, with the calculations carried out using model test data for the bending moment response operators. Since the COV values for the extreme force on the particular illustrative case of a semi-

submersible ship in [35] ranged from 0.10 to 0.20, depending upon the particular wave spectral representation used, for a vessel that was about 280 ft. long, the possible reason for differences in the case of the WOLVERINE STATE [34] may be the use of model test experiment response operators. On the basis of the above considerations, it may be assumed that the possible range for bending moment COV due to wave spectral variability will extend from 0.10 to 0.20, with an average value of 0.15 (almost exactly the estimate given in [34] and used in the published literature!).

#### 4.3.2 Effects of Theoretical Response Operators

A possible influence on the variability of wave loads is due to the degree of validity of the theoretical response operators that are usually calculated by means of strip theory. Some differences are known to exist between bending moment response operators determined by theory and those from experiment, and a method of evaluating the effect on load variability has been applied in this study. The procedure for establishing a measure of the "correct" response operator involves comparing theoretical responses with model test data values, with the assumption that the model test data are the proper values, i.e. data should be used from tests at a reputable laboratory with high standards and accurate measurement and data analysis equipment and procedures.

Since the frequency response data represent the variation of an amplitude ratio as a function of frequency, any deviation between theory and experiment at particular frequencies alone should not be used as the measure of an error. A representative measure of the use of response operators is the value of rms response to a wave spectrum, but any possible measure of difference between theory and experiment would then be dependent upon the shape of both the response operator and the input wave spectrum when obtaining rms response outputs. In order to overcome this difficulty, a suggested approach is to choose a representative spectral input in the form of a rectangular (i.e. constant) unit amplitude "box" spectrum extending over the entire bandwidth of the response operator, as shown in Figure 4.

The mean square response is then found from the relation

$$\begin{aligned}\sigma^2 &= \int_0^{\infty} |T_V(\omega)|^2 S_{\eta}(\omega) d\omega \\ &= \int_{\omega_1}^{\omega_2} |T_V(\omega)|^2 d\omega\end{aligned}\tag{8}$$

where  $S(\omega)$  is the unit amplitude rectangular spectrum input, and  $\omega_1$  and  $\omega_2$  are the bounds of the response operator  $|T_V(\omega)|$  bandwidth in the frequency domain. This procedure is applied to both the theoretical and experimental response operators, using the same unit amplitude spectral input, and the ratio of the rms values found by this procedure for both the theoretical and experimental response operators is

used as a measure of the uncertainty associated with present strip theory methods.

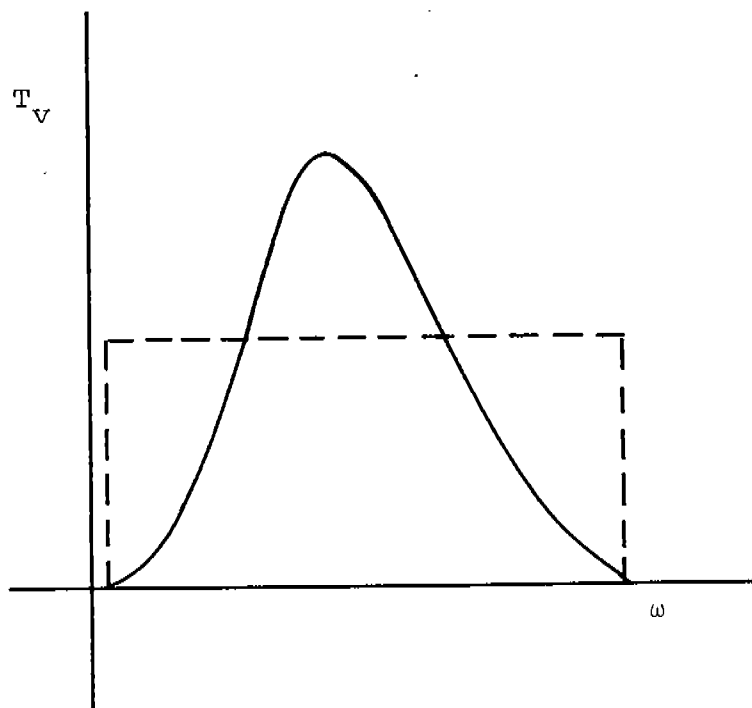


Fig. 4 Response operator and box spectrum bandwidth

This method was applied to a large set of available model test data for which associated theoretical calculations have also been made. The primary source of data was [32], for which data were available for two Series 60 ships (.70 and .80 block coefficients) and also for the WOLVERINE STATE. These data covered different speeds and headings for these models in regular waves. The theoretical calculations used for comparison with the test results in [32] was the original SCORES theory, with the mathematical derivation given in [32] and the computer program given in [39]. Another source of data, together with theoretical calculations shown in comparison with the test data, was obtained from [40] which contained test data for a container ship model and a Series 60 model, where the model test data were obtained at NSMB. The theory used for comparison with the test data was a different form of strip theory, whose development was described in [40]. Model test data and calculated results were obtained also for the SL-7 from [41], where the theory used was a modification of the original SCORES theory that had been used in [42]. The modification of the theory involved incorporating the effects of additional speed-dependent terms in the equations of motion, which resulted in an improvement in the degree of correlation between theory and experiment for the SL-7 model as compared to the earlier work in [42]. Representative sets of data that were used in this comparison are illustrated in Figures 5-7.

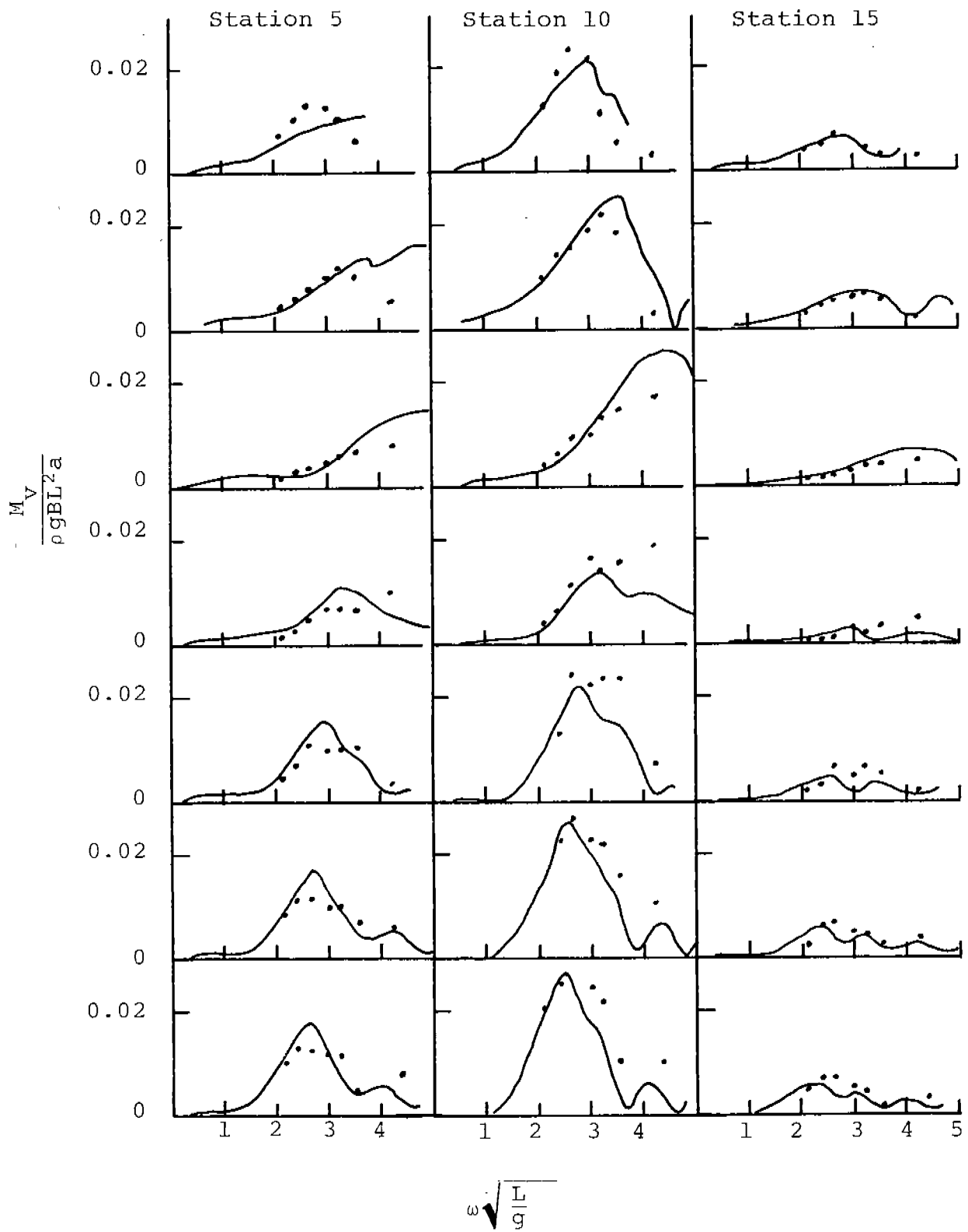


Fig. 5 Calculated and measured nondimensional vertical bending moment amplitudes of the container ship ( $F_n=0.245$ ).

Sheet A-959 486-329

-25-

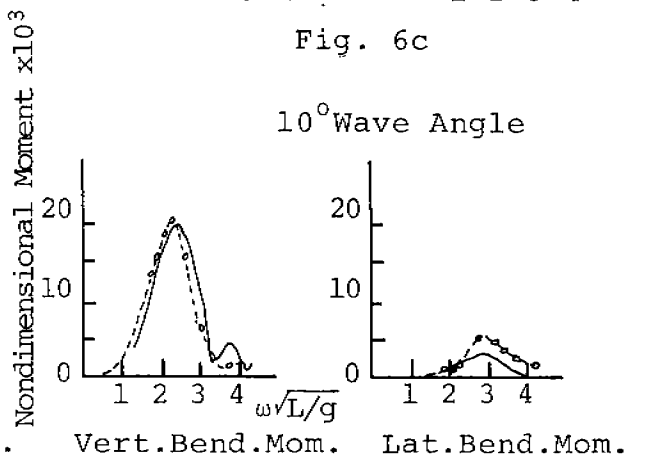
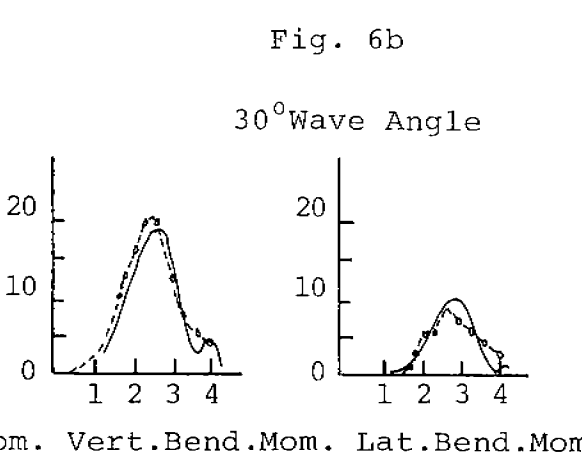
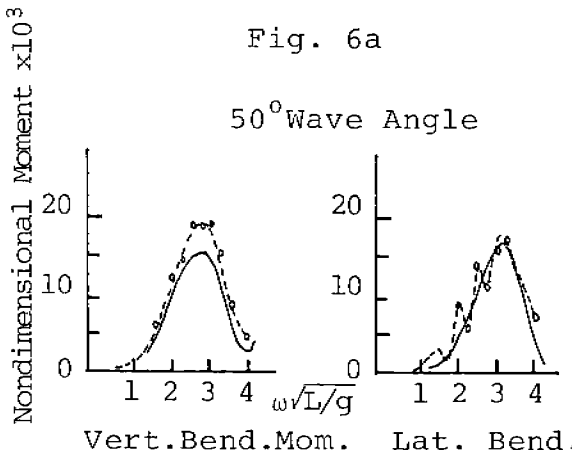
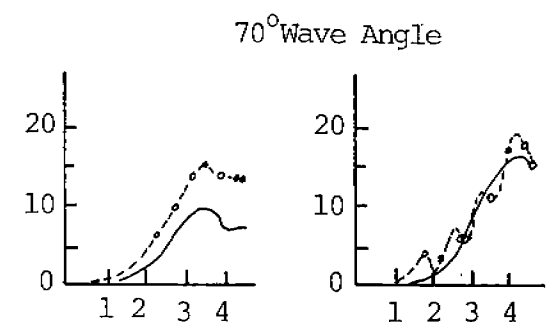
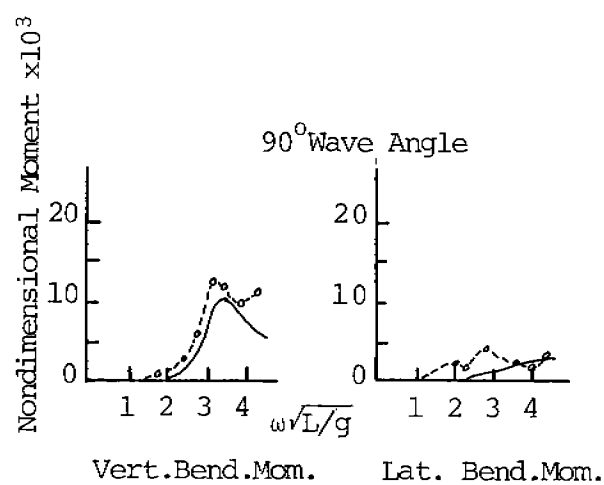
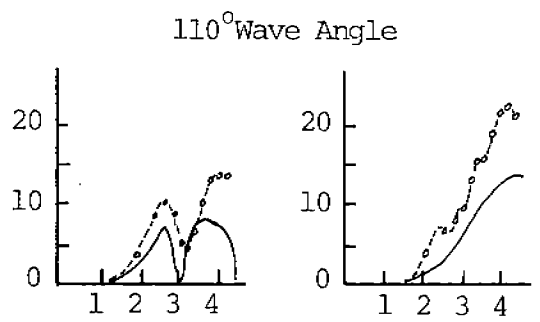
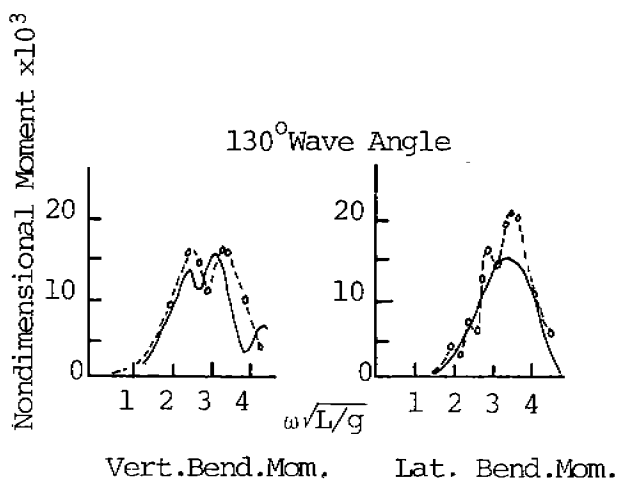
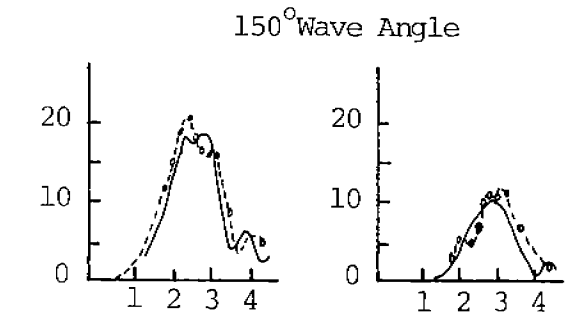
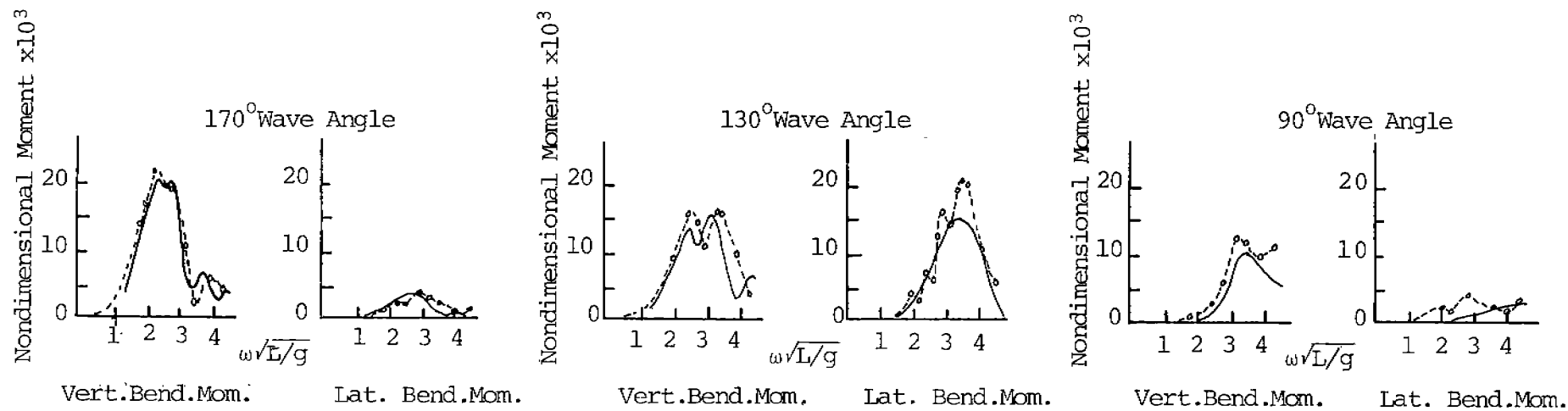


Fig. 6a

Fig. 6b

Fig. 6c

Fig. 6d

Fig. 6e

Fig. 6 Midship wave moments on SERIES 60, BLOCK.80 hull, Fn=0.15

-o- experiment  
 \_\_\_\_\_ calculation

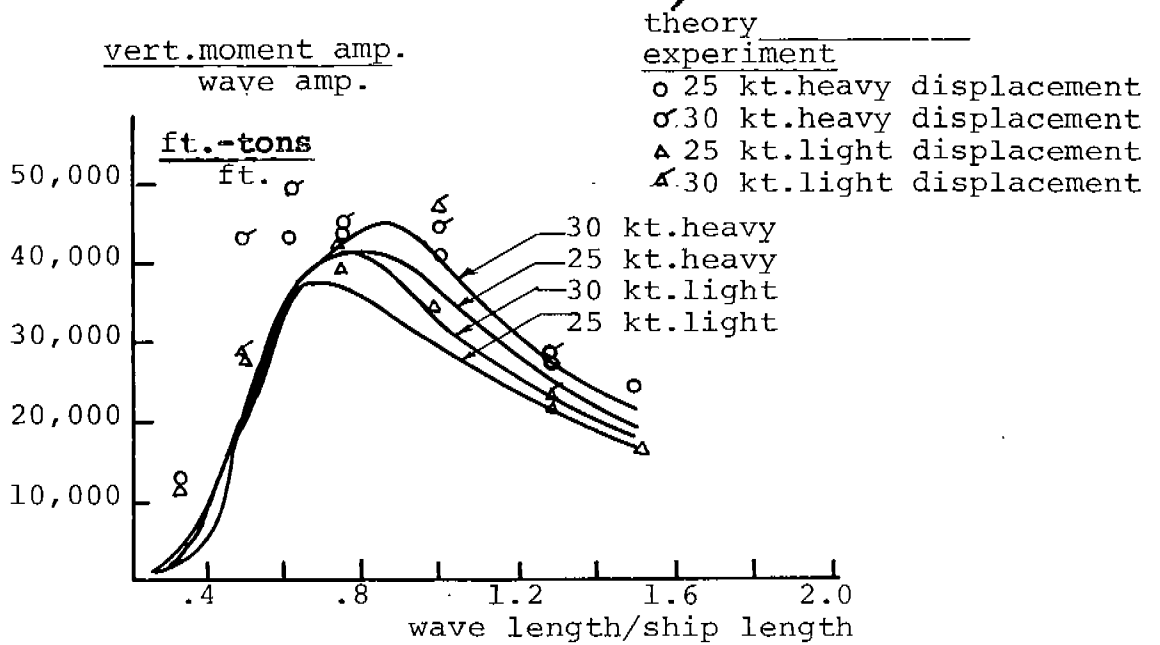


Fig. 7a Midship vertical wave bending moments,  $210^\circ$  heading

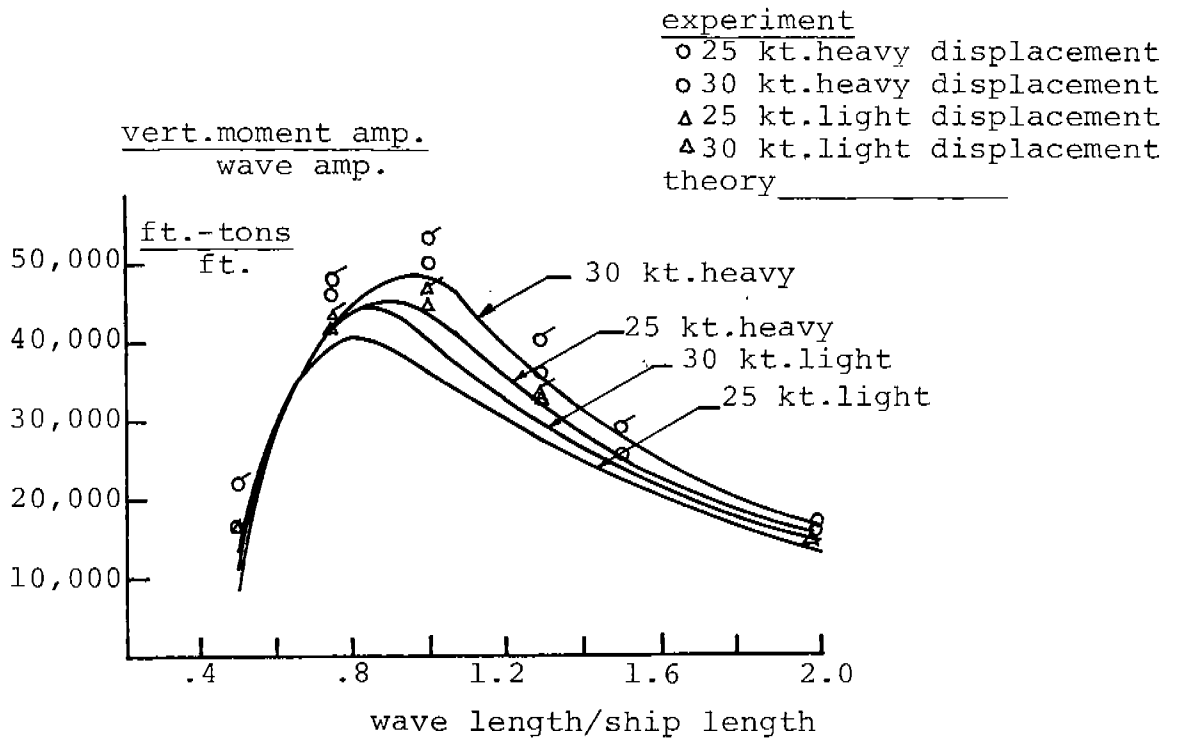


Fig. 7b Midship vertical wave bending moments,  $180^\circ$  heading

The particular data used for the different models were a selected set that contained a sufficient amount of model test data that could be considered to extend out near the ends of the bandwidth of the response operators (where the operator values approached zero). This requirement of a fairly "full" set of data thereby limited the number of conditions that were analyzed by the method described above. A total of 40 different cases was analyzed in this manner for all of the above vessels, with the largest number (16 cases) for the WOLVERINE STATE and the smallest number (2 cases) for the SL-7. The resulting ratios of the rms values obtained from theory with respect to representative values determined using experimental data were found to generally group around the value 1.0, with the extremes ranging from 0.65 to 1.31.

All of these ratios were then averaged in order to find a mean value and standard deviation, with those values found to be 0.959 and 0.061, respectively. These values only correspond to the particular data analyzed (40 cases), while other sources of data are also generally available, such as the information given in ISSC reports, other published research reports, etc. This additional information considers data from both model tests and full-scale tests as a means of indicating the general utility of theory to calculate vertical bending moments. According to all of these available data, it does not appear that there is any systematic bias in any of the currently used calculation methods and theories. The average value of the ratio of theoretical load to the load value determined using model test data, which was given as 0.959 in the present analysis, was biased toward a lower value than 1.0 because of the large number of cases (16) for the WOLVERINE STATE, which has a ratio less than 1.0, viz. 0.927.

When examining the results of theory compared with experiment, especially in the case of full-scale data, the predictions from theory were generally higher than the measurements (which provides a conservative error for use in design). However, a large part of that difference may be due to the lack of complete information about the local ambient wave spectrum properties (e.g. see [43] and the associated paper discussions). Other effects may be the application of incomplete theory to cases such as fast ships in following quartering seas, etc. as illustrated by the problems highlighted in [41] and [42]. On the basis of the limited analysis described above, it can be assumed that the total uncertainty for most ships, in their more common modes of operation, is due to (statistical) dispersion effects and that such a dispersive error for the theoretical calculation methods (linear hydrodynamic strip theory) can be accounted for with a COV that can extend up to 0.10.

There is a particular manifestation of nonlinearity in wave-induced vertical bending moments which exhibits itself in unsymmetrical sagging and hogging values. This

effect is due to nonlinear variation of buoyancy and hydrodynamic effects (added mass and damping) for ships that have significant degrees of flare and which have non-vertical sections at their waterlines. Such vessels include container-ships and naval combatant ships (destroyers, frigates, etc.). In those cases the sagging loads exceed hogging, when examining the extreme loads for design purposes, with a ratio of 1.2:1, i.e. 20% larger. This type of result has been observed in analysis of full-scale data (see [22]) as well as indicated by theory and correlation between theory and experiment (see [44] and [45]). Since this difference has been observed in many cases, it can be considered as a measure of bias for the mean value of vertical bending moments used in design (i.e. when considering sagging moments as the dominant design load) by use of probabilistic or semi-probabilistic methods. However, it is only appropriate for a particular class of vessels (containerships, etc.) and not others such as tankers and bulk carriers ("full" ships), as shown in [22] and [45].

#### 4.3.3 Effect of Extrapolation Method for Lifetime Maxima

When considering design loads for ships, the procedures for determining such values for wave loads use two different approaches, viz. the long term distribution method [34] and the extreme value method [35]. The results found by use of both approaches are generally quite close to each other in practical cases, as shown in [46], although the calculation requirements are lesser for the extreme value approach. In both methods, long-term distribution and extreme value, the procedure depends upon knowledge of the short-term probability densities which are established by analysis of measured responses for short time periods of the order of 20 minutes under statistically stationary conditions.

Most cases of ship bending moment response have been assumed to follow the Rayleigh distribution for the amplitudes of the response maxima, and this has been the basis for most analyses for design loads. Although the data analysis in [22] indicated some departures of the measured data from the assumed Rayleigh characteristics for one of the ships studies there, viz. the SL-7 containerships at higher speeds, that assumption of Rayleigh distribution can still be applied to most ships of interest with conservative safety. Calculations were carried out using theoretical RAO values combined with realistic wave spectra from spectral families for the 3 ships studies in [22], with the results found for the spectral bandwidth factor  $\epsilon$  (as defined in [18]) showing that the Rayleigh assumption was appropriate for these ships. The  $\epsilon$  values ranged from 0.16 to 0.53 with the majority lying in the range 0.30 - 0.36.

The methods used for determining the long-term probability or extreme value design wave load will also involve some degree of uncertainty. A detailed analysis of the basis and

interpretation of the long-term distribution method was provided by Karst [47] who considered the problem of the probability of exceeding a particular bending moment at least once during its operating lifetime, rather than the probability of exceeding a specified value during any one cycle at any time in a ship's lifetime. The cumulative probability distribution ordinarily found for bending moments by the method of [34] provides the modal value at the specified number of cycles in its lifetime. For such a large number of cycles, the distribution of the highest wave bending moment that would ever be experienced in the ship's life is approximated by a discrete Poisson distribution in histogram form superimposed on that long-term distribution. The parameters of the Poisson distribution and the modal value of the bending moment are used to determine the mean value and standard deviation of the largest demand wave load in the ship lifetime, from which the COV due to the statistical variability of the maximum lifetime is determined. A particular case where this method of analysis was applied was described in [17] for a naval frigate, with the value of the COV found to be 0.075.

Another approach which is the extreme value method, proceeds in a different manner to obtain the maximum value that will be experienced in a ship's life. In that approach, the probability density and the cumulative short-term probability are used to determine the probability density of the maximum of the bending moment, from which the most probable extreme value and other related statistics are found. For a random variable having the probability density  $f(x)$  and cumulative probability distribution function  $F(x)$ , for  $n$  cycles of encounter, the probability density function of the extreme value (denoted as  $y_n$ ) is given by

$$g(y_n) = nf(x) \left[ F(x) \right]^{n-1} \Big|_{x=y_n} = \frac{d}{dy_n} \left\{ \left[ F(y_n) \right]^n \right\} \quad (9)$$

With the short-term probability density given by the Rayleigh law, which is expressed in normalized form by

$$f(\xi) = \xi e^{-\xi^2/2} \quad (10)$$

where  $\xi$  is the ratio of the response amplitude to the rms level of the response, the cumulative probability distribution is then given by

$$F(\xi) = 1 - e^{-\xi^2/2} \quad (11)$$

For this case, the mean value and standard deviation of the extreme value are then found from the basic definitions

$$\mu_{y_n} = \int_0^{\infty} y_n g(y_n) dy_n \quad (12)$$

$$\sigma_{Y_n}^2 = \int_0^{\infty} (Y_n - \mu_{Y_n})^2 g(Y_n) dy_n \quad (13)$$

The appropriate values are found from these expressions by integration by parts, etc., leading to a determination of the COV as a function of the number of cycles  $n$ . That result is shown in Figure 8 for the COV of the extreme value, based upon the statistical variability of that quantity.

The results in Figure 8 allow determination of the COV of the extreme value in terms of the number of cycles for the specified condition for determining an extreme, such as operation in a particular large sea state. Thus, the quantity  $n$  corresponds to such a situation and not the entire ship lifetime (see [46] for a description of the application of extreme value statistics in practical cases). The derivation of the COV value in this case is assumed to be applicable to any extreme value determined from the probability representation given by the general definition in Eq. (9). Since the determination of an extreme value by the method of Ochi [35] is simpler and involves less computational effort than the long-term distribution technique of [34], and also provides the same final result, the use of COV values from Figure 8 is also adequate for probabilistic design studies.

#### 4.3.4 Combined Variability for Wave Loads

On the basis of the above analysis, it is seen that the variability of wave loads which has been quantified arises due to the wave spectral variability, the limits of linear hydrodynamic strip theory, and the statistical variability of extreme values. The COV value for all of these effects together, since they are uncorrelated, is given by the square root of the sum of the squares of each contribution. Assuming that the extreme value is found for a condition corresponding to 10,000 cycles, for which the COV value is 0.065, the total COV for wave loads is then

$$\text{COV}_{\text{wave loads}} = \sqrt{(.15)^2 + (.10)^2 + (.065)^2} = 0.192 \quad (14)$$

which is close to the overall value of 20% that is often quoted in published literature.

#### 4.4 Springing Vibratory Loads

The phenomenon of springing is a steady-state oscillatory bending moment that arises due to exciting the natural structural vibratory frequencies of the ship due to encountering short waves. The high encounter frequencies are close to the ship natural frequencies, primarily the first vertical mode, which then results in such a continuous high-frequency response for generally long flexible ships. Significant

6 Pict Bwd

486-329

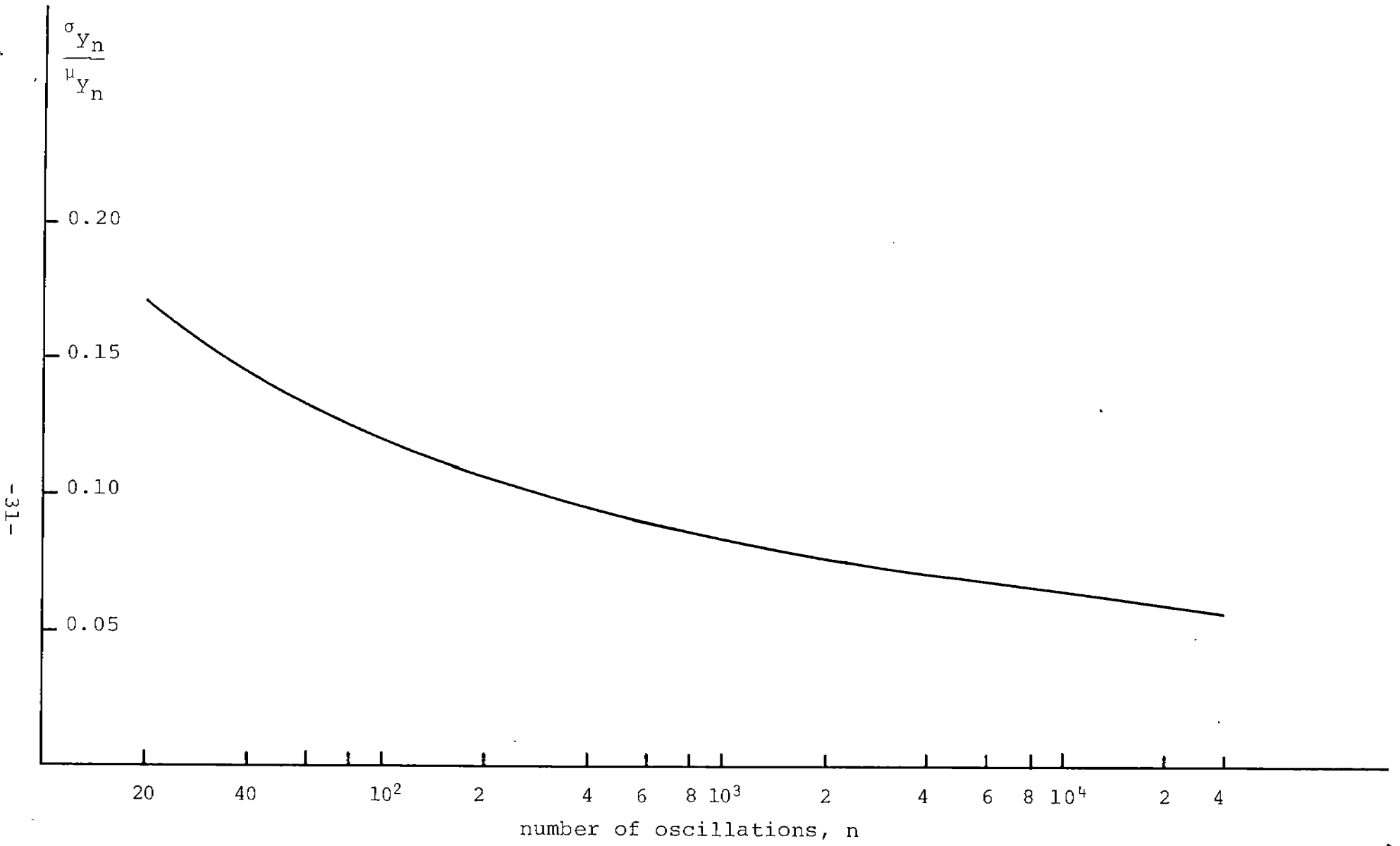
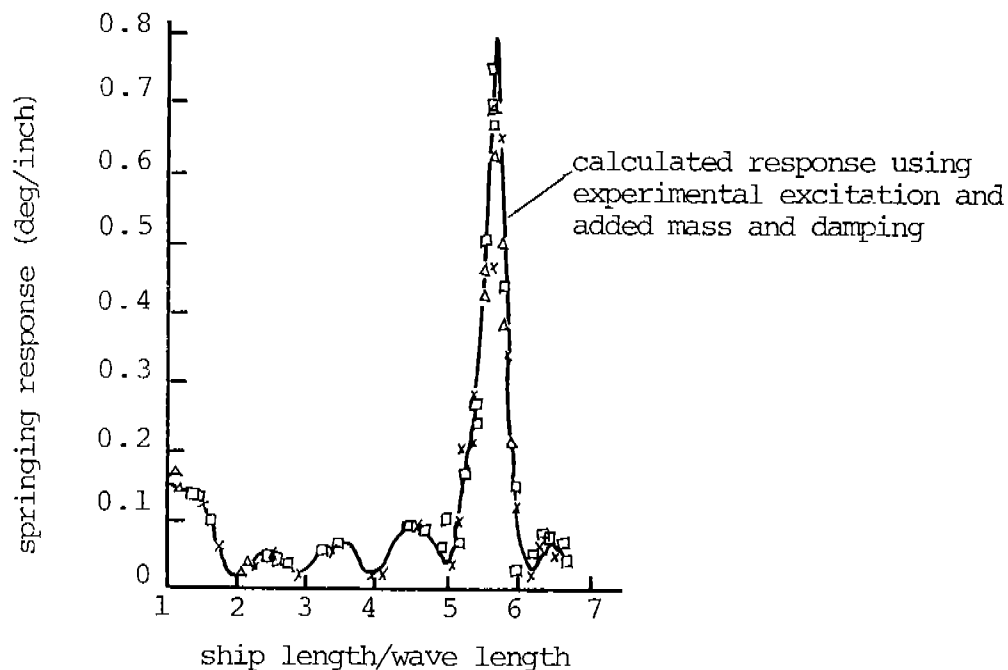


Fig. 8 COV of extreme value as function of number of cycles (for Rayleigh distribution)

springing stresses have been measured and theoretically predicted for such vessels as Great Lakes ore carriers, fast containerships and large tankers. However the importance of springing has not been fully settled since no structural failures of ships have been attributed to this type of load.

A number of theoretical analyses have been carried out for the purpose of predicting springing loads, both in the frequency domain and the time domain (see [48]-[50]), with some model test validation studies in [51] and [52]. These analyses include consideration of the flexibility of the ship structure in determining the magnitude of the response as well as the various component terms entering into the equations. More recent studies ([53], [54]) have acted to focus attention to some of the major problems associated with theory, which include the calculations of the wave excitation forces for short waves and high Froude numbers, the evaluation of damping (including structural damping), and the influence of nonlinearity in calculating the wave excitation forces. According to the model experiment results in [52] and [53], the springing response can be accurately predicted from oscillator theory when using measured values of excitation, added mass and damping, as shown in Figure 9.



then an important factor. Other influences determined from both theory and experiment indicate a nonlinear effect in the excitation forces which requires further examination, which is ongoing at this time. A large amount of work has been carried out in full-scale measurements on Great Lakes bulk carriers together with the subsequent data analysis (e.g. [55]). While the analytical models used in the work of [55] have not considered the more fundamental problems associated with the hydrodynamic effects considered in [53] and [54], they are used in an effort to essentially "calibrate" the theory by means of such measurements and data analysis. Other important considerations associated with that work include the analysis of combined wave and springing loads, which is a topic considered in a later section.

When considering the problem of the uncertainties associated with springing loads per se, only estimates can be made based on the present state of the art. The effects of wave spectral variability will certainly involve a COV as large as that for conventional ship wave loads, and probably larger due to the problems associated with accurate measurement of the high-frequency tail of the wave spectrum. Thus, the COV value for that aspect will be of the order of 0.20. As a result of the problems in obtaining an accurate hydrodynamic representation of wave excitation and damping, the basic theoretical RAO values are subject to error. That particular uncertainty can be approximately estimated to be of the order of 0.20, in comparison to the COV level for conventional wave loads.

The variability due to the extreme value probability effects is expected to be less than in the case of conventional wave loads, since the number of oscillations will be much higher for springing due to the occurrence of springing oscillations at the first structural natural frequency of the ship. On the basis of the results in Figure 8, that effect can be represented by a COV of about 0.05. The resulting COV estimate for springing is then estimated to be

$$\text{COV}_{\text{springing}} = \sqrt{(.20)^2 + (.20)^2 + (.05)^2} = 0.287 \quad (15)$$

While this value is fairly large, the overall contribution to the uncertainty of the ship total extreme load may not be as significant since the combination of springing with other loads must be considered; it is only important for certain types of ships, under special operating conditions; etc.

#### 4.5 Slamming and Whipping

The dynamic vibratory loads on a ship that are of a transient nature are generally described by the terms slamming and whipping, where slamming refers to the initial effect of a wave-ship impulsive force and whipping refers to the subsequent vibratory hull response in one or more natural

modes of ship structure. These loads occur at relatively high frequency, corresponding to the two-node mode of the natural vertical structural frequency of the ship as well as higher modes that also may be excited due to the impulsive slam load. These transient slamming type responses are associated with the effects of bottom impact on the waves or as a result of bow flare immersion.

While extensive work has been carried out to predict the frequency of occurrence of slamming, e.g. [56], a more important requirement is the ability to determine the magnitude of the slam load as well as other related statistical characteristics. Theoretical studies have been carried out by means of computer simulation in the time domain in order to provide time histories of slam loads such as bending moments, etc. as described in the work of [50] and [57-59]. These analyses include both bottom impact and bow flare slamming, with the responses reflecting the influence of the ship flexibility in exhibiting transient time histories at the natural frequencies of the hull.

The important aspect of any of these theoretical analyses is the method of representing the impact force itself which acts as the source of excitation, with that quantity reflecting significant nonlinear effects for both types of slamming. The methods that have been used in the theoretical studies have been based upon a combination of the forces due to the variation of fluid momentum, buoyancy and impulsive pressure variation, where these quantities are determined as a function of time due to the time-varying immersion of different ship sections with respect to the local wave elevation. The subsequent response to such an impulsive load, i.e. the whipping response, then follows in the form of a decaying oscillation due to the inherent structural damping in the ship. This type of slamming-whipping response repeats after another impact occurs, with the repetition not being regular or related directly to any of the wave properties, and as such the response is considered to be nonstationary. The transient response due to slamming from the theoretical studies appears to have the same qualitative characteristics as that measured in full scale at sea, but there is still insufficient available experimental data for a complete correlation between theory and experiment at this time. There have been limited model test studies of slamming, but such investigations are not carried out more extensively due to the technical problems (and associated expense) of model construction that would represent a properly built structurally scaled ship model.

The only way in which information on the effect of slamming and whipping can be satisfactorily obtained is in terms of the magnitudes of the stresses or bending moments that arise from these effects, as determined from analysis of measured data. Some information in this area has been obtained from the work in [20], [22], [60] and [61]. The

data obtained for slamming and whipping have primarily been found for container ships, naval frigates, and cargo ships, with both types of slamming (bottom and bow flare) represented in the bending moment records. The analysis of these full-scale measurements provides data that can be applied to obtain information useful to the present study, although extensive quantitative values (compared to the amount of information available for wave loads) cannot be obtained on the basis of these limited data.

The slam loads do not occur at random during a cycle of ship motion in waves, but within a definite narrow range of phase angles with respect to the wave load. However, the particular phase angles found for a cargo ship in [20], for the container ship in [22], and the frigate in [61] were somewhat different. In the case of the frigate, the whipping transient loads in the midship region significantly increased the conventional wave-induced sagging of the ship since the maximum whipping amplitude was nearly coincident with the maximum wave induced sagging. In general, it can be assumed that the phase difference between the occurrence of a slam and the peak of a local wave load maximum is generally relatively smaller than the average encounter period of the wave load.

As far as the magnitude of the whipping bending moment is concerned, that quantity varies relative to the wave load for each ship as shown in the various full-scale study reports. The data in [60] provide a numerical value for the whipping bending moment (peak to peak range) as determined from analysis of measurements on 4 different ships ranging in length from 420 ft. to 750 ft. covering cargo ships, an ore carrier and a container ship. The value of the whipping bending moment magnitude expected to occur in a ship's lifetime (probability of  $10^{-8}$ ) is given by  $0.00075 \rho g L^3 B$  for each ship. This value is the mean value for the whipping load (peak to peak range) as specified for the 4 vessels in [60] from full scale data analysis at this particular probability level. At the higher probability level of  $10^{-5}$ , it was given as  $0.0004 \rho g L^3 B$ . Substituting the dimensions of a particular ship of this class will result in numerical values of this dynamic bending moment which can then be used for design purposes.

Although the values of the whipping bending moments are only presented for 4 ships in [60], that information can be used to assess the variability since the actual values for the vessels are given there. A listing of the values is given below in Tables 9 and 10 for the two cited probability levels, from which the mean values and standard deviations can be determined, leading to COV values for whipping bending moments.

Table 9

Vertical Midship Whipping Bending  
Moment Values,  $10^{-5}$  Probability

Ship type	Moment coefficient $10^3 M / \rho g L^3 B$
Cargo	0.332
Cargo	0.424
Ore Carrier	0.456
Container	0.365

Table 10

Vertical Midship Whipping Bending  
Moment Values,  $10^{-8}$  Probability

Ship type	Moment coefficient $10^3 M / \rho g L^3 B$
Cargo	0.733
Cargo	0.694
Ore Carrier	0.876
Container	0.696

From the data in Table 9 for  $10^{-5}$  probability, the mean value is  $0.394 \rho g L^3 B \times 10^{-3}$ , and the standard deviation of the numerical factor (multiplying  $\rho g L^3 B \times 10^{-3}$ ) is 0.097, leading to a COV of 0.246. The data in Table 10 for  $10^{-8}$  probability result in a mean value of the numerical factor as 0.75 and a standard deviation of 0.149, which produces a COV of 0.199. On the basis of these values, when considering the extreme value of whipping bending moment, the COV value of 0.21 would be a good estimate to reflect the variability in whipping loads for the different ships.

The analysis of the whipping bending moment amplitudes also provides information on the short-term probability characteristics of that load. In the case of the frigates [61], the probability density of the whipping load was found to be exponential. The data in [22] showed a possible tendency toward an exponential distribution also, as was the case for the WOLVERINE STATE cargo ship analysis [20]. The results in [20] and [22] did not fit that type distribution in a full statistically verified sense, but there was a sufficient tendency toward that form of representation. Considering the fact that whipping loads are the result of transient response of a (primarily) linear oscillator to an impulsive nonlinear force that has quadratic behavior (with respect to relative vertical velocities) as shown in [50] and [57-59], there is a plausible basis for considering an exponential probability density as representing the short term characteristics. This probability density is expressed in the form

$$f(x) = \frac{1}{\alpha} e^{-x/\alpha} \quad (16)$$

with the cumulative distribution given by

$$F(x) = 1 - e^{-x/\alpha} \quad (17)$$

where  $\alpha$  is the mean value of the load experienced in that short term period to which the probability representation applies.

With this short-term probability representation, it is then possible to establish the extreme value properties, similar to the treatment of wave loads. Since the value of  $\alpha$  has to be found for each case from data analysis of records, it would be best to use the information in Table 10 as the basis for estimating the actual extreme whipping load per se. Although no detailed evaluation of the extreme value distribution and its properties was made since the short-term probabilities are of exponential type, it can be expected that the COV value due to the variability of the extreme will lie in the range of 0.05 to 0.10, depending on the number of oscillation cycles as the determining factor.

The above information considers only the properties of the whipping bending moment itself. However, the influence of the whipping load in determining the total design load on the ship as well as the load properties is the important information required for the present study. That topic is considered in the next section which treats the combination of loads.

## 5.0 COMBINATION OF LOADS

The next item to be considered, which is associated with defining the demand (i.e. the loads on the vessel) in probabilistic terms involves combining the disparate loads that have been discussed above. In particular, problems arise in static loads which vary between voyages, and the thermal effects are diurnal in nature. With regard to the different oscillatory effects produced by interaction with the waves, it is known that the low-frequency wave loads cover frequencies in the bandwidth associated with the wave encounter due to forward speed relative to the wave spectral frequency extent, while the dynamic vibratory loads occur at the natural hull frequencies, primarily in the fundamental vertical mode. The means of combining these different loads must be established so that there is a calculation method that can be used in design studies. In addition, procedures that would allow establishing some measure of the uncertainties in the total combined load also have to be established.

### 5.1 Still Water, Thermal and Wave Loads

The combination of still-water loads and wave loads has been considered in a number of investigations applied toward probabilistic structural design of ships. Since some information is available that indicates the nature of the probability density of still water loads, some efforts have been applied to establish the probability density of the sum of still-water and wave bending loads (e.g. [20]). This has been done with the assumption that these two types of loads are statistically independent variables. However, that may not be the case since the different cargo distribution weight loadings which establish the still-water bending moment will also affect the value of the wave loads. This is due to the contribution of inertial forces that are important elements in the total wave bending moment (see [32] for a description of the various component forces contributing to ship wave loads). Thus, a variation in the weight distribution can lead to variation in wave loads as well.

On the basis of the above, the problem of combining still-water and wave loads can be treated by selecting a large representative still-water load as a constant value that is added to the value of the wave load. This still-water load will correspond to the operating loading conditions, i.e. whether the vessel is fully loaded or in ballast condition, with the wave loads also determined for the same operating condition. Since the still-water loads vary over a long period (the extent of a voyage) as compared to the wave load time scale, this would appear to be an acceptable procedure.

In view of the same aspect of thermal effect load as relatively steady in contrast to the wave loads, the thermal effect load can be combined with the still-water load as a constant load reference about which the wave loads and vibratory dynamic loads will vary. The thermal effect load to be used for design purposes is either the average value found by calculation similar to those in [20] or a value found for a predominant temperature-weather condition. The general magnitude of the thermal effect load is usually small relative to the wave and vibratory loads so that the variability aspect can be considered as absorbed within the uncertainties for the predominant loads. In most cases, large thermal effect loads due to significant sun exposure are unlikely to occur at the same time as large wave loads due to ocean storms, although the effects of swells producing large wave loads can still be present during good weather. On the basis of all of the reasoning discussed above, the thermal effect loads should be treated together with the still-water loads, where the sum of these loads is considered as a static reference level for the larger time-varying loads. This type of treatment has been applied in a similar manner for ships in [10] as well as for other structures with different static and dynamic load contributions (e.g. [62]).

The preceding method for combining relatively static loads and wave loads is suggested initially since the information on statistical properties of the static loads (e.g. still-water loads) is not sufficiently complete at this time, although efforts are presently ongoing in order to obtain an appropriate data base useful for probability-type design. Some limited data of this nature, from Japanese results on containerhips and tankers, is given in Tables 1 and 2 which can be used as a measure of variability in the absence of more extensive data.

When considering the combination of static and wave loads, from the point of view of obtaining a measure of uncertainty in the form of a COV value when information on COV values is known for each element, a suggested procedure for determining the combined load COV is given by the following. If the total load is represented by the sum

$$L_t = L_s + L_w \quad (18)$$

where the t-subscript represents total, the s-subscript represents static, and the w-subscript represents wave, the mean value is

$$\mu_{L_t} = \mu_{L_s} + \mu_{L_w} \quad (19)$$

and the COV of the total load ( $COV_t$ ) is given by

$$COV_t = \left[ (COV_s)^2 \left( \frac{\mu_{L_s}}{\mu_{L_t}} \right)^2 + (COV_w)^2 \left( \frac{\mu_{L_w}}{\mu_{L_t}} \right)^2 \right]^{1/2} \quad (20)$$

This procedure has been used in a comparative study of off-shore structure codes [63], and can be further extended to include dynamic vibratory loads as well (to be discussed in a later section).

## 5.2 Combined Vertical and Lateral Wave Loads

In all of the prior treatment of wave loads in this report, the primary concern has been the vertical bending moment. However, a ship that travels obliquely into waves is subject to unsymmetrical bending about a neutral axis that constantly shifts its angular position. This can be accounted for by including the effect of the lateral wave bending moment that will be combined with the vertical bending moment. The lateral bending moment is primarily dynamic as it arises from the hydrodynamic forces due to the waves and the resulting ship motions. Response operators (RAO's) for determining lateral bending moments can be established either by theoretical computation, e.g. [32], [33], or from model test data, as illustrated in [32] and [40-42].

If one is concerned with extreme stresses, such as occur at the deck edge, an effective vertical bending moment due to the combined vertical and horizontal bending can be determined. This combined load depends on the ratio of the section moduli for both vertical and horizontal bending. While recent work in [15] has questioned the applicability of such a procedure when large loads and nonlinear and inelastic response of the structure can occur, the analysis of loads at this stage of technical development cannot consider the effects of such structural deformations. Thus, the procedure involving the combination of these loads in terms of the relative section moduli is considered as an acceptable approach. While each of these low-frequency wave loads has some degree of uncertainty, the combination of the two must also be assessed to determine the uncertainty of the total wave-induced load.

A number of different approaches have been applied in order to determine properties of the combined effective longitudinal bending moments, as described in [20], [64] and [65]. These methods include determining effective RAO values for the combined load in terms of the frequency-dependent phase angle between the 2 components, power spectra, cross-spectra, etc. The mean square value of the combined load is represented by the relation

$$\sigma_c^2 = \sigma_v^2 + \left(\frac{Z_v}{Z_h}\right)^2 \sigma_h^2 + 2\rho_{vh} \left(\frac{Z_v}{Z_h}\right) \sigma_v \sigma_h \quad (21)$$

where  $\sigma_v^2$  and  $\sigma_h^2$  are the mean square values of the vertical and lateral bending moments,  $Z_v$  and  $Z_h$  are the vertical and lateral section moduli and  $\rho_{vh}$  is a correlation coefficient

between vertical and lateral bending moments which reflects the phasing between them. However, the effect of the correlation coefficient value in the combined moment rms value is found to be small according to results shown in [65].

Similar type results are shown in [31] from analysis of measured data in 23 ships, including tankers, bulk carriers and containerships. There the effect of phasing between the different stresses when considering the resultant maximum gunwale stress was shown to be small, even when including the warping stress due to torsion. This result in [31] also illustrated a negligible effect of the warping stress on the total maximum gunwale stress, although the warping stress was much larger in value for "open" ships such as containerships. The average value of the wave loading maximum stress, which is found to be independent of the ship length and type of ship for this collection of measured data, is given as 14 Kg/mm<sup>2</sup> or 20 kpsi, which is a useful value for design comparison.

As for the variability of the combined effective bending moment, that can be found in a similar manner as for the pure vertical bending moment described in the last section. The only difference is in regard to the COV of theoretical calculation methods. Since the comparisons between theory and experiment in [32], [40] and [42] show that lateral bending moments are not predicted as well as vertical bending moments, the COV value for the effect of linear strip theory calculations for the combined moment would then be about 0.15. This would result in a COV for the combined wave load, assuming the effects of wave spectral variability and extreme value variability remain the same, to be

$$\text{COV}_{\text{combined wave load}} = \sqrt{(0.15)^2 + (0.15)^2 + (0.065)^2} = 0.222 \quad (22)$$

### 5.3 Combined Wave and Springing Loads

For the case of combined vertical wave-induced and springing bending moment loads, which applies to Great Lakes ore carriers and in some cases to other bulk carriers and possibly tankers (if sufficient flexibility is present), there is fairly extensive work available to provide guidance for design loads, e.g. [55]. Since the springing response is continuous and a stationary random process, with narrow band spectral properties, the rms value of the combined vertical bending moment is found as

$$\sigma_c = \sqrt{\sigma_w^2 + \sigma_{sp}^2 + 2\rho_{wsp}\sigma_w\sigma_{sp}} \quad (23)$$

where  $\sigma_c$  is the combined bending moment rms value,  $\sigma_w$  is the wave induced bending moment rms,  $\sigma_{sp}$  is the springing bending moment rms, and  $\rho_{wsp}$  is a correlation coefficient

between springing and wave-induced bending moments. Since the wave-induced bending moment and the springing bending moment responses occur primarily in frequency ranges that are generally well separated from each other, the correlation coefficient  $\rho_{wsp}$  is quite small and close to zero. Thus, for practical <sup>wsp</sup> purposes and simplification these two responses can be considered as essentially uncorrelated. Particular empirical data to allow calculations of the rms springing bending moment is available in [55], which also provides the basic support for the relationships described above.

When considering extreme values of the combined bending moment, there have been some questions concerning the manner of counting the number of maxima to which extreme value theory is applied because of the effects of the different frequencies that are present, i.e. due to the higher number of oscillations associated with springing occurring at the first mode of structural vibration of the ship (see [66] for some discussion of this point). A typical illustration of the stress spectrum of a Great Lakes ore carrier, showing the two distinct spectral energy peaks due to wave loads and springing, is given in Figure 10.

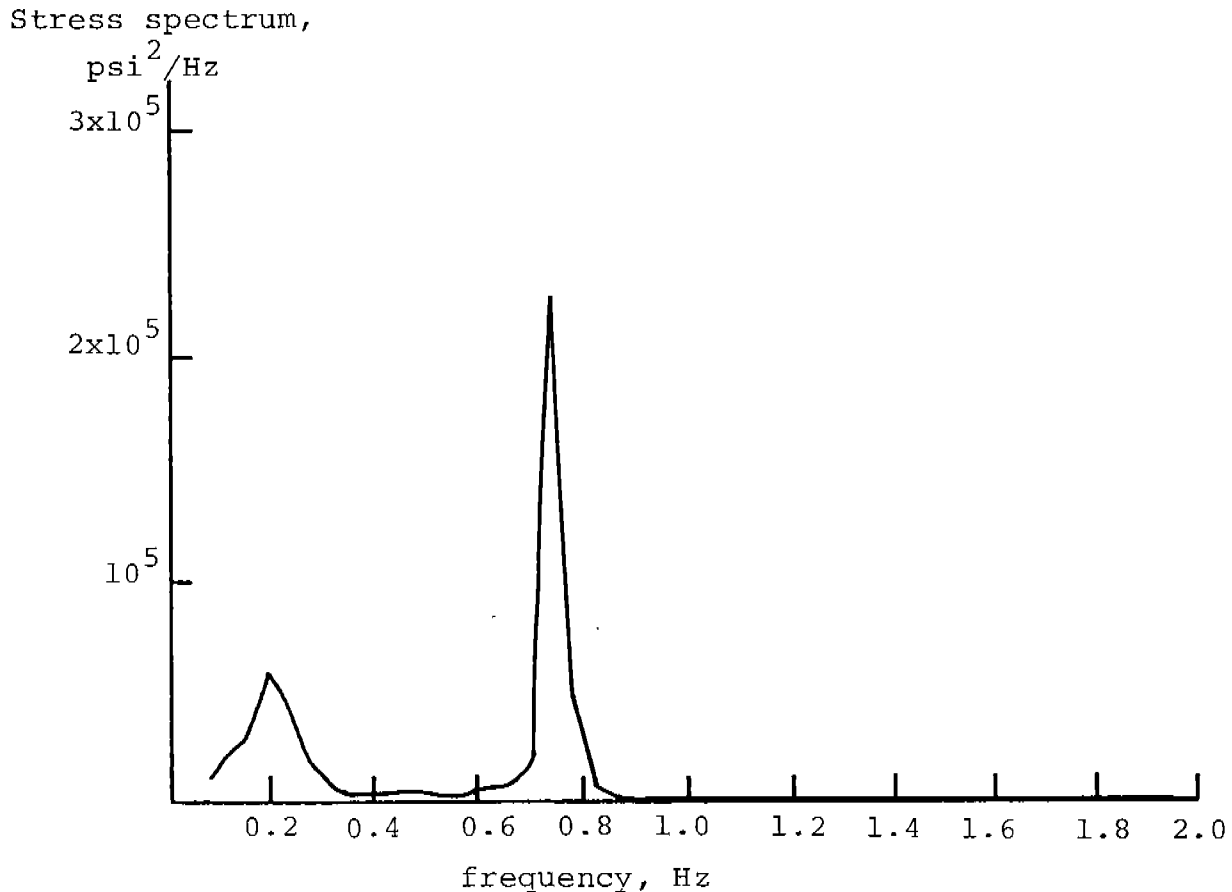


Fig. 10 Teledyne measured stress spectrum for FOTINI-L, voyage 7FLI-3, interval 22

An analysis of extreme values, following from the truncated probability density function for positive maxima (as is used by Ochi in [35]), provides the most probable extreme value in terms of the number of zero crossings for the combined signal (see [67]). The zero crossing concept provides a better picture of the number of oscillations to which the extreme value expressions apply. More exact relations for the extreme, which reflects the influence of the spectral width parameter  $\epsilon$  more completely together with the effect of the average period ratio and the relative degree of magnitude of rms of the 2 load components, are also provided in [67]. The factors for the extreme value determination (which multiply the rms value) are also expressed in [67] in terms of their uncertainties, which are shown to be small relative to the uncertainty in calculating the rms load value. Those uncertainties for the effect of the extreme value variability are generally similar to those shown in Figure 8 for conventional wave loads, with the COV value dependent on the number of oscillation cycles and lying in the range of 0.05 to 0.10.

The determination of the COV of combined wave and springing loads depends upon the relative contributions of each of those separate components to the total load. The mean value of the extreme load is found from the rms value in terms of the factor for extremes described above from [67], to which is added the still water bending moment. The COV of the combined wave and springing loads (assuming for simplicity that the still-water bending moment and other static load terms are considered as constants) is determined by an extension of the relation in Eq. (20)... Thus,

$$\text{COV}_{\text{combined wave and springing}} = \left[ (\text{COV}_w)^2 (\mu_{L_w} / \bar{\mu}_{L_t})^2 (\text{COV}_{sp})^2 (\mu_{sp} / \mu_{L_t})^2 \right]^{1/2} \quad (24)$$

where a separate determination is required to find the extreme loads for wave-induced effects and springing effects alone, as well as in combination (for the mean load only). Since the COV values for wave loads and springing loads separately have been given in the present section and the preceding section of this report, it can be seen that the COV value for combined wave and springing loads lies in the range banded by 0.222-0.287 (i.e. between the COV values for wave and springing loads above).

#### 5.4 Combined Wave and Whipping Loads

The combination of wave loads and whipping loads due to ship slamming can be considered from a particular viewpoint that reflects the present state of the art in applying analytical models and the parameters therein. Both of these elements are known to include a great deal of uncertainty arising from various sources. Therefore, an effort to use highly sophisticated models for load combination analysis does not appear to be warranted, but an approach using rel-

atively simple analytical representations for the essential physical phenomena is consistent with the current state of knowledge of the factors contributing to such load combinations. A description of the procedures for combining wave loads and those arising from slamming is given below in terms of estimating design loads, estimating the COV for such loads, and also determining the probability characteristics of such a combined load.

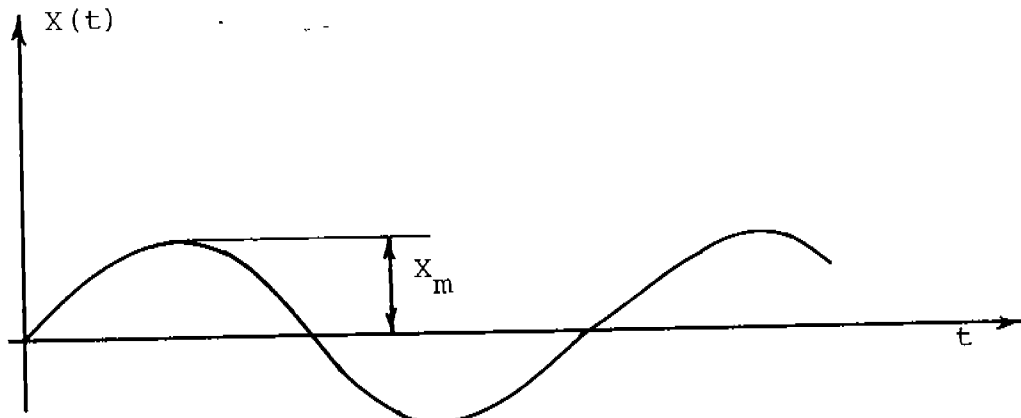
According to the results in [22], the vibratory loads arising from slamming, etc. are statistically independent of the ordinary wave-induced loads. The vibratory loads due to slamming and shipping are interpreted as dynamic increments to the wave-induced loads, with this increment related to half the double amplitude (peak-to-peak) of the vibratory load. These data in [22] provides support for establishing the extreme total load as the sum of the maximum wave-induced load amplitude (either hogging or sagging) and a fractional multiple of the dynamic vibratory increment described just above. This fraction is uniformly distributed between 0 and 1.1 in all of the records analyzed in [22].

A conservative estimate of the sum of the wave load and the slam load is obtained by direct summation of each load amplitude as found from the general time history form of each component, as shown in Figure 11. The wave bending moment is represented by  $X(t)$  with peak values  $X_m$ ; the slam bending moment time history is  $Y(t)$  with maximum value  $Y_m$ ; and the sum  $Z(t) = X(t) + Y(t)$  has a maximum value  $Z_m$ . In this figure, the time difference  $\tau$  between the time at which  $X(t)$  assumes a local maximum and the time at which a slam occurs may be considered as a random variable, which is generally much smaller than the encounter period  $T_0$ . The combination  $Z(t)$  of these two different loads is estimated conservatively by summing  $X_m$  and  $Y_m$ , i.e.

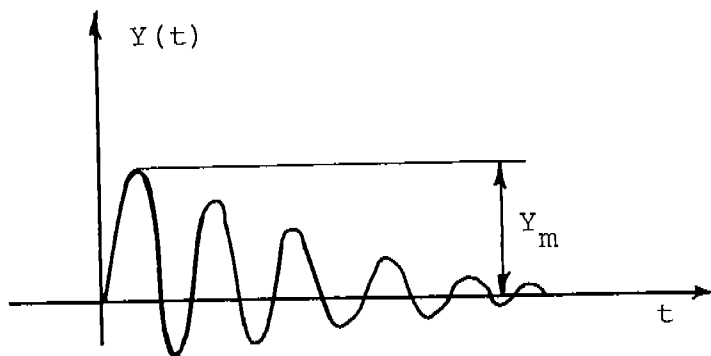
$$Z_m = X_m + Y_m \quad (25)$$

which assumes a negligible value of the time difference  $\tau$ . This approach is useful when establishing the probability distribution function for the combined load, which is treated below.

The distribution function  $F_{Z_m}(z)$  of  $Z_m$  defined in Eq. (25) is found by integrating the joint density function  $F_{X_m Y_m}(x, y)$  of  $X_m$  and  $Y_m$  over the domain  $D$  shown in Fig. 12 below.



Wave-induced bending moment



Slam-induced bending moment

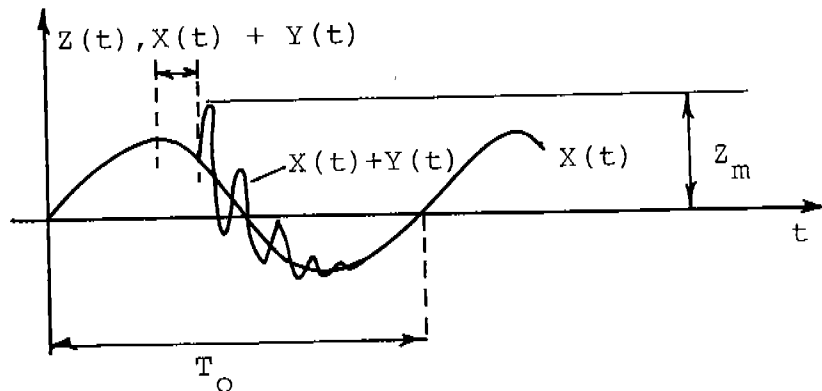


Fig. 11 Load combination;  $X(t) + Y(t)$

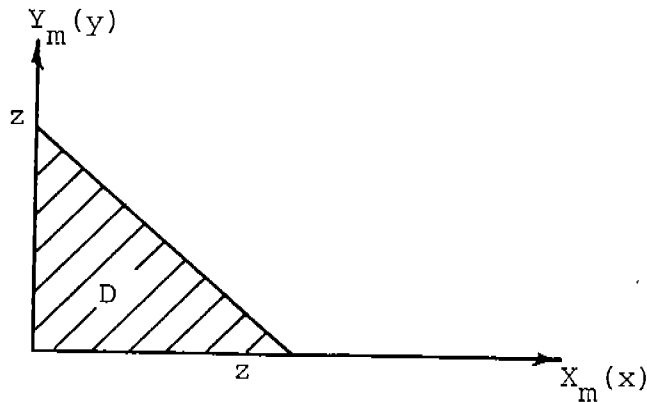


Fig. 12 Domain of integration

$$F_{Z_m}(z) = \iint_D f_{X_m Y_m}(x, y) dx dy = \int_0^z \left[ \int_0^{z-x} f_{X_m}(x) f_{Y_m}(y) dy \right] dx \quad (26)$$

where the statistical independence is assumed between  $X_m$  and  $Y_m$  and  $f_A(\cdot)$  indicates the density function of the random variable  $A$ . With the probability densities of the wave load amplitude given by the Rayleigh distribution

$$f_{X_m}(x) = \frac{x}{\sigma^2} e^{-x^2/2\sigma^2} \quad (27)$$

where  $\sigma$  is the rms parameter value, and the exponential distribution for the slam load amplitude given by

$$f_{Y_m}(y) = \frac{1}{\alpha} e^{-y/\alpha} \quad (28)$$

the value of the function  $F_{Z_m}(z)$  is found by integration to be

$$F_{Z_m}(z) = 1 - e^{-z^2/2\sigma^2} + e^{\sigma^2/2\sigma^2} e^{-z/\alpha} \left[ e^{-\frac{1}{2} \left( \frac{z}{\sigma} - \frac{\sigma}{\alpha} \right)^2} - e^{-\sigma^2/2\alpha^2} - \sqrt{2\pi} \frac{\sigma}{\alpha} \left\{ \Phi(z/\sigma - \sigma/\alpha) - \Phi(-\sigma/\alpha) \right\} \right] \quad (29)$$

where  $\Phi(\cdot)$  indicates the standardized Gaussian distribution function. This information on the probability of the combined load found by this procedure can be used to determine failure probability in a complete probabilistic structural analysis, which will be discussed in a later section of the report.

Since the two different loads are statistically independent, an estimate of the design maximum can be obtained by means of the relation

$$M_{\text{combined wave and slam}} = \sqrt{M_w^2 + M_{\text{slam}}^2} \quad (30)$$

where the extreme value of the separate components is given by  $M_w$  for the wave load and  $M_{\text{slam}}$  for the slam load. The slam load extreme value is found from the information in Table 10, using half the value of the bending moment value since the information in Table 10 is for the peak-to-peak range.

The COV value for slamming loads alone is discussed in the preceding section, and it can be estimated to be about 0.223 when considering the general variability of the slam loads as well as the effect of extreme value variability. Since the COV of wave loads is 0.222, the COV for the combined wave and slam loads can be determined in a manner similar to the combined wave and springing loads (another type of dynamic vibration load). The method for calculating the COV of combined wave and slam loads is based upon the relation

$$\text{COV}_{\text{combined wave and slamming}} = \left[ (\text{COV}_w)^2 \left( \frac{\mu_{L_w}}{\mu_{L_t}} \right)^2 + (\text{COV}_{\text{slam}})^2 \left( \frac{\mu_{L_{\text{slam}}}}{\mu_{L_t}} \right)^2 \right]^{1/2} \quad (32)$$

when the static loads are assumed here (for simplicity) to be constant. The mean value of the wave and slam loads separately are determined by use of the procedures described in the preceding section of the report, and the mean value of the combined wave and slam loads is found from Eq. (30). On the basis of the above method, the COV value for the combined wave and slam load will have a value about 0.223.

This conclusion is based upon using the COV value for slam and whipping loads found from the data presented in [60], which is only a limited set of values. In fact, the results obtained in the full-scale measurements in [43] showed the whipping bending moment of one of the frigates exceeded the value from Table 10 by about 25%. There may be other measurements that give values of whipping bending moments for estimating extreme loads that are also not consistent with that source (i.e. [60]), which will also increase the uncertainty in estimating loads associated with slamming. The development of theoretical methods of prediction of slamming loads by time domain computer simulation has not proceeded to the point where proper comparison with data can be made to provide an adequate validation of those methods. Thus, there are still some remaining issues related to the uncertainties about slam loads and their influence on combined loads for design use. The COV value for slamming per se should then be considered to be larger than the value of 0.223 mentioned above, possibly

tending to be closer to 0.30, with its influence on the combined load due to the sum of wave and slam loads leading to an estimated COV of about 0.25 for that combination.

The discussions in this section on combined loads have provided some estimate of COV values as well as description of methods for determining extreme loads for design use. However, there are still gaps in the present state of knowledge concerning various aspects of environmental loads. This lack of complete information will require more data to be recorded and analyzed in order to provide a larger data base than present data provides. In addition, there is further need for improvement in theoretical calculation capability for determining the dynamic vibratory loads due to springing and slamming, as well as the need for validation of the theories by comparison with test data (both model and full scale). In the absence of such complete information, the present results can still be used as more valid estimates than have been generally assumed in past studies.

## 6.0 SHIP HULL STRENGTH ANALYSIS

The structural failure of a ship hull can occur as a result of various possible mechanisms, and a discussion of possible failure modes has been given previously. In the present investigation the emphasis was placed on failure that could occur due to yielding, plastic collapse, and instability due to buckling of main elements such as grillages or their elements. A discussion is given below of these failure modes and some of the methods used in their evaluation.

One particular mode of failure is that resulting from yielding of the hull girder due to bending, when the entire deck or bottom has attained the yield state. In that case, the initial yield moment is determined in terms of the elastic section modulus. The expression for this initial yield bending moment is

$$M_i = Z_e s_y \quad (32)$$

where  $Z_e$  is the elastic section modulus and  $s_y$  is the material yield stress.

Another possible failure mode is that of fully plastic collapse which assumes that the entire hull cross section (including the sides) has reached the yield state. In this case, the material may be treated as elastic-perfectly plastic, and the loads gradually increase up to collapse. This ultimate collapse condition was analyzed by Caldwell [12] and is expressed by

$$M_p = Z_p s_y \quad (33)$$

in terms of the plastic section modulus  $Z_p$ . This plastic section modulus is given in [12] by

$$Z_p = A_D g + 2A_S \left( \frac{D}{2} - g + \frac{g^2}{D} \right) + A_B (D-g) \quad (34)$$

where

- $A_D$  = cross-section area of the deck (including stiffeners)
- $A_B$  = total effective area of bottom (including stiffeners)
- $A_S$  = effective area of one side (including stiffeners)
- $D$  = depth of midship section
- $g$  = distance from center of deck area to the plastic neutral axis, which is given by

$$\frac{g}{D} = \frac{A_B + 2A_S - A_D}{4A_S} \quad (35)$$

In the expressions given above, it is assumed that no buckling has occurred, only vertical bending is considered, and the effects of axial and shear forces are neglected.

When considering buckling instability, the major interest is concerned with grillage failure. The modes of grillage failure that are envisioned as possibly leading to ultimate collapse are panel buckling, including column flexural buckling and column tripping (coupled flexural and torsion buckling), as well as overall grillage failure. The local failure of plates between stiffeners is also considered since the plate buckling leads to a reduction of the plate-stiffener combination strength.

The analysis of plating failure between stiffeners is an element that is used in further analysis of grillages. The ultimate compressive load for a plate is based on the von Kármán concept of a limit to the load carrying capacity when the edge stress approaches the yield point. The ultimate moment due to plate failure, denoted as  $M_{bp}$ , is expressed as

$$M_{bp} = Z_e s_{yc} \phi \quad (36)$$

where

$s_{yc}$  = compressive yield stress of material

$\phi$  = failure stress ratio =  $\frac{\text{average failure stress}}{\text{yield strength } s_{yc}}$

The quantity  $\phi$  represents the effectiveness of the plating after buckling, and it is expressed as

$$\phi = \frac{b_e}{b} \quad (37)$$

where  $b_e$  = effective width and  $b$  is the actual width.

There are a number of different representations of this  $\phi$  value for plates which depend upon the parameter  $\beta$  defined by

$$\beta = \frac{b}{t} \sqrt{\frac{s_{yc}}{E}} \quad (38)$$

where  $E$  = the modulus of elasticity of the material and  $t$  = plate thickness. A semi-empirical formula for the effective width was proposed by Faulkner [68] in the form

$$\frac{b_e}{b} = \frac{2}{\beta} - \frac{1}{\beta^2} \quad (39)$$

An illustration of some of the different expressions for the effective width ratio according to different formulations, as shown in [69], is given in Figure 13.

Ultimate Buckling Strength  
of Unstiffened Thin Plates

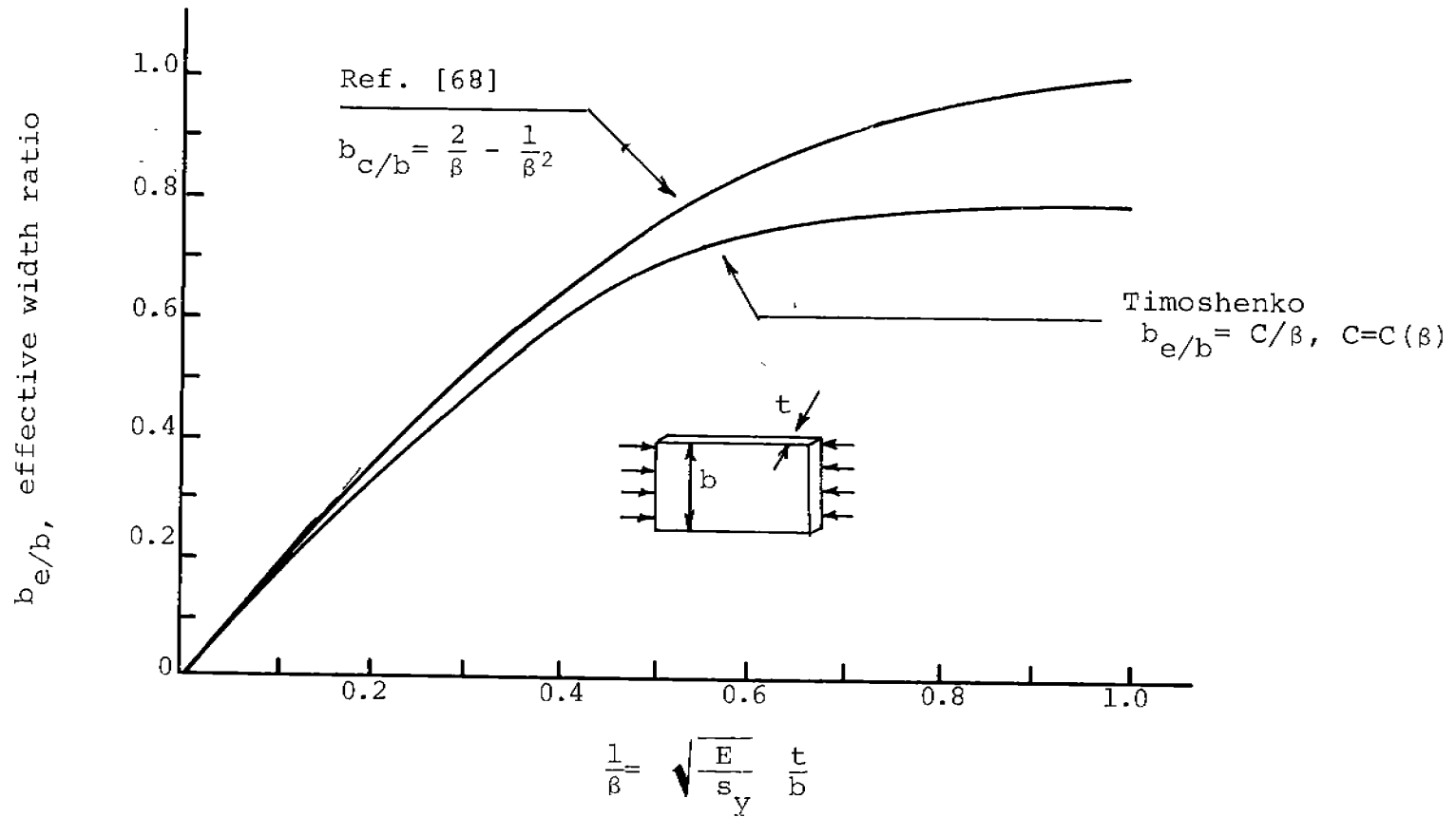


Fig. 13 Effective breadth of plates

The analysis of panel buckling considers the flexural buckling of longitudinal stiffeners together with the effective plating between transverse frames, which is treated like a column. The ultimate moment due to panel buckling failure, denoted as  $M_{bn}$ , is represented by

$$M_{bn} = Z_e s_{yc} \phi \quad (40)$$

where  $\phi$  is the average failure stress ratio taking into account plate effectiveness.

In the panel buckling analysis, the Euler critical stress is considered close to the failure stress if buckling occurs in the elastic range. For conditions where the critical stress exceeds the proportional limit stress of the material, the tangent modulus  $E_t$  must be used instead of  $E$  in determining that critical stress from the Euler formula. If data from a compression test diagram are not available, the quadratic parabola formulation of Bleich [70] may be used in the form

$$E_t = E \left( \frac{s_{yc} - s}{s_{yc} - s_p} \right) s_p \quad (41)$$

with  $s_p$  the proportional limit of the material.

The analysis of tripping, which results from coupled flexural and torsional buckling, is treated in an approximate manner in [69] using somewhat similar concepts. The expression for the ultimate bending moment due to stiffener tripping failure is similar to that of Eq. (40), with the major requirement being the determination of the proper value of the quantity  $\phi$ . However, in the practical case for ships, if adequate anti-tripping brackets are present then that failure mode will not be a factor determining the hull ultimate strength.

Overall grillage failure involves the buckling of the entire grillage, including both longitudinal and transverse stiffeners. The ultimate moment due to grillage buckling is represented by

$$M_{bg} = Z_e s_{yc} \phi \quad (42)$$

where  $\phi$  in this case is the ratio of the average failure stress to the yield strength  $s_{yc}$ . The determination of the value of  $\phi$  is the important element for analysis of grillage failure, just as in the case of all of the other

where  $b_e/b$  is the plate effectiveness considered previously and  $\zeta$  is the area ratio of stiffener to plate. The elastic buckling stress  $s_c$  for grillages under uniaxial compression is found from the expression given in [72]

$$s_c = k \frac{\pi^2 \sqrt{D_x D_y}}{h_x B^2} \quad (44)$$

where  $D_x$  and  $D_y$  are the grillage flexural rigidities in the  $x$ - $x$  and  $y$ - $y$  directions;  $B$  is the length of the loaded edge;  $h_x$  is the equivalent thickness of the plate and stiffeners which is found as the average cross-sectional area per unit width of effective plating and stiffeners;  $k$  is a constant that depends on the boundary conditions and is found in [73]. There is a limitation to the use of the expression for  $\phi$  in Eq. (43) since no allowance was made for nonlinear large deformations in its derivation, which only allows its use for heavily stiffened grillages.

In addition to the consideration of buckling of grillages and grillage components per se described above in terms of the elastic section modulus, another representation that considers the influence of buckling on the ultimate bending moment was also given by Caldwell [12]. In order to include the effects of buckling, a strength factor denoted by the quantity  $\phi$  is introduced into the analysis of [12], where the quantity  $\phi$  is the ratio of the average ultimate stress to the yield stress. While different values for this strength factor were considered in the derivation in [12], the assumption that this factor is the same for both the deck and the sides can be made. That simplification is based on the assumption that the sides and deck develop the same average ultimate compressive stress at collapse.

The expression for the ultimate plastic vertical bending moment with buckling included in this manner is given by

$$M_u = \left\{ A_D g \phi + 2A_S \left[ \frac{D}{2} - g + \frac{g^2}{D} \frac{(1+\phi)}{2} \right] + A_B (D-g) \right\} s_y \quad (45)$$

where

$$\frac{g}{D} = \frac{2A_S + A_B - A_D}{2A_S (1+\phi)} \quad (46)$$

with all of the geometric terms therein defined previously as for Eqs. (24) and (25). This expression is used in the

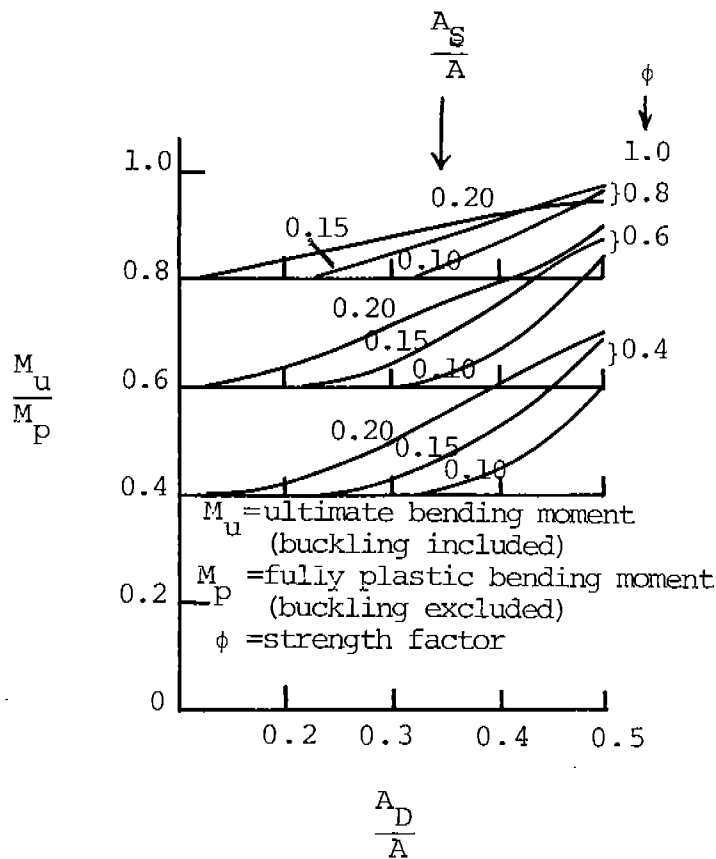


Fig. 14 Effect of buckling on ultimate longitudinal strength-single deck ship-sagging condition

which is taken from [12]. This figure shows the degree of reduction of the fully plastic moment as a result of buckling of the deck and side of the hull. The results in Figure 14 show that the ratio of this ultimate moment to the plastic moment can never be less than the value of the strength factor  $\phi$ , and in most cases the ratio will exceed the value of  $\phi$  by a significant degree.

How this representation relates to the other models of ship strength described in terms of the elastic section modulus and the various representations of the strength factor  $\phi$  in those cases for buckling, as described by the preceding models for grillage and component buckling, will determine which mechanism would be the possible cause of failure for any particular ship. Since there is no specified expression for the quantity  $\phi$  in this ultimate moment given by Eqs. (45) and (46), the value of  $\phi$  to be used with that representation would be the value of  $\phi$  from the particular buckling case (from grillage and component analysis) that results in the smallest  $\phi$  value.

## 6.1 Application to Representative Ships

In order to illustrate the nominal strength of ship hull structures, as well as establish the prospective governing mode of failure, calculations are made using the preceding expressions for 3 representative ships. These ships are the tanker UNIVERSE IRELAND, the bulk carrier FOTINI-L, and the containership SL-7 that have been considered previously in the evaluation of wave loads. Mid-ship section drawings for these vessels were used in order to determine the values of various parameters that are used in the different equations, making use of approximations involving average "lumped" values of areas, dimensions, etc. The general procedure followed is that in [69].

The tanker UNIVERSE IRELAND has the general dimensions  $L_{BP} = 1082.67$  ft.,  $B = 174.87$  ft. and  $D = 104.99$  ft. The areas of deck, bottom and side are given by  $A_D = 29.43$  ft.<sup>2</sup>,  $A_B = 36.96$  ft.<sup>2</sup> and  $A_S = 23.27$  ft.<sup>2</sup>. The areas of the ship section are broken down further in terms of average thickness of plating, number of stiffeners, thickness and depth of stiffener web, thickness and breadth of stiffener flange, etc., where these detailed element considerations are used in a later section for another type of analysis. An analysis of the case of buckling for typical unstiffened plate element in the deck (thickness = 0.035m., length = 5.35m., width = 0.88m) showed the critical longitudinal stress to be  $0.99s_y$ , and for a deck flat bar stiffener (0.4m x 0.035m) that critical stress was found to be  $0.997s_y$ .

Further analysis of buckling considered flexural buckling of a longitudinal flat bar stiffener whose section is shown in Figure 15. The calculated properties of

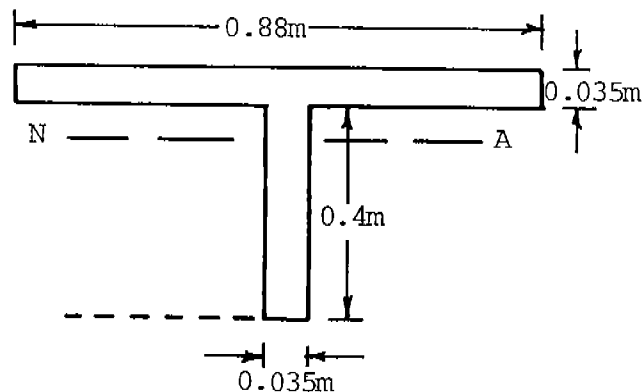


Fig. 15 Flat bar stiffener section, UNIVERSE IRELAND

the section  $I = 1548$  in.<sup>4</sup>,  $A = 69.4$  in.<sup>2</sup>, neutral axis (N.A.) at 13.76 in. from tip of web, with the stiffener

length of 5.35m. (210.58 in.). The analysis of buckling was based on column formulas. Using a plasticity reduction factor approach with the quadratic tangent modulus, etc. results in a critical stress of  $0.94s_y$ . This ship has no longitudinal deck girder, and consideration was then given to analysis of tripping, which was analyzed in the same manner as for the flexural buckling case. In the case of a flat bar stiffener whose pinned ends are prevented from twisting, the analysis extended to the inelastic range gave a critical tripping stress of  $0.959s_y$ .

For the investigation of overall grillage instability, the deck flat bar stiffener takes the place of a composite girder, for which it is assumed that the whole plating is effective. The expressions used to find the factor  $\phi$  for this case are Eqs. (43) and (44). The value of plate effective width used is the average between the values given by Faulkner and Timoshenko, as shown in Figure 13, leading to  $\phi = 0.913$ .

Using this value of  $\phi$  in the expression for ultimate strength given by the Caldwell analysis [12] that includes buckling in a plastic analysis gives a section modulus value of 651,042 in<sup>2</sup> - ft. given on the vessel plans. With a yield stress value  $s_y = 15.18$  tons/in<sup>2</sup> the moment initiating yield is found to be  $8.6 \times 10^6$  ft. - tons, and the governing case for failure according to the method of [69] for the UNIVERSE IRELAND is overall grillage instability with  $\phi=0.913$ , which results in the ultimate load of  $7.85 \times 10^6$  ft.-tons. This case is the governing mode despite the fact that all of the plating was considered to be effective in the derivation of the critical stress. The value given by the analysis of [12], when considering buckling, leads as expected to a higher strength value for the ship. With a design load from the ABS 1982 Rules given by  $5.66 \times 10^6$  ft.-tons, there is certainly an ample safety factor for this ship even when considering the possible critical failure mode above.

The same type of analysis was carried out for the FOTINI-L bulk carrier using similar type approximations to lump different areas, size of stiffeners and plates, etc. in order to allow an effective analysis of midship section properties for this vessel. This vessel has dimensions  $L_{BP} = 800$  ft.,  $B = 106$  ft.,  $D = 60$  ft., with component areas  $A_D = 17.73$  ft<sup>2</sup>,  $A_B = 25.69$  ft<sup>2</sup>, and  $A_S = 5.51$  ft<sup>2</sup>. This area breakdown was based upon the top longitudinal bulkhead being diffused with the side shell; the bottom of the top tanks being diffused with the deck; the bottom hopper longitudinal bulkhead diffused with the bottom; and the inner bottom diffused with the bottom. Representative dimensions for thickness, lengths, etc. were also established from the plans drawing information.

The analysis considered the determination of the fully plastic collapse moment, with and without buckling considered;

the moment initiating yield; buckling instability applied to elements of the hull (deck plate, deck girder web plate, deck flat bar stiffener analyzed via plate formulas); panel failure of longitudinal stiffening, considering flexural buckling and tripping applied to flat bar stiffeners and the longitudinal deck girder; and grillage failure modes (buckling of a sub-panel with 2 equidistant flat bar stiffeners and overall grillage in stability).

The results of this analysis, which followed the procedures in [69] similar to those applied to the UNIVERSE IRELAND showed that all of the hull elemental buckling modes have critical stress in the range of  $0.961s_y - 0.997s_y$ . The overall grillage instability resulted in a critical stress of  $0.944s_y$  (based upon using the average plate effectiveness value) so that this is the critical failure mode. With the midship elastic section modulus given as  $158,556 \text{ in}^2 \text{ - ft.}$  the ultimate strength moment is found to be  $2.27 \times 10^6 \text{ ft.-tons.}$  For this case, the moment initiating yield is  $2.41 \times 10^6 \text{ ft.-tons.}$

This type of analysis was also carried out for the SL-7 vessel, with dimensions  $L_{BP} = 880.5 \text{ ft.}$ ,  $B = 105.5 \text{ ft.}$ , and  $D = 64 \text{ ft.}$  The separate areas of the ship midsection were determined by diffusing the inner bottom with the bottom; the second deck was diffused with the deck; and the side of the box girder parallel to the side shell was diffused with the deck. For this ship, the various analyses of buckling of plate elements, panel failure including flexural and tripping modes, etc. all gave critical stresses just about equal to yield  $s_y$ . The critical failure mode of this ship was found to be due to overall grillage instability, based upon the use of average plate effectiveness, with the critical stress being  $0.948s_y$ . With the elastic section modulus given as  $169,593 \text{ in}^2 \text{ ft.}$ , the ultimate strength moment is then  $2.33 \times 10^6 \text{ ft.-tons}$  for this vessel.

In all of these ships, the analysis of grillage failure was based upon use of the value of the buckling stress  $s_c$  in Eq. (40) to be the inelastic buckling stress  $s_{ci}$ , which is related to the elastic buckling stress  $s_c$  in Eq. (44) by means of the relation

$$\frac{s_{ci}}{s_c} = \sqrt{\frac{E_t}{E}} \quad (47)$$

where  $E_t$  is the tangent modulus relation given by Eq. (41). This relation is necessary since the use of the elastic buckling stress is not appropriate for the low slenderness ratios of the plating for these ships. The UNIVERSE IRELAND has the largest value of the slenderness ratio  $\frac{b}{t}$  of these ships, viz.  $\frac{b}{t} = 25$ , for which the quantity  $\beta$  defined in Eq. (38) is less than 1.0 for mild steel, with the other ships being even smaller values. In this range, the plating strength is large, with the average stress almost being the yield stress (see Fig. 59 of [74]). Furthermore, the results of [14] for nearly perfect plates (small residual

stress and initial deformation) with this range of slenderness ratio show that failure would not occur until the average strain is well beyond yield strain. The range of values where  $\beta < 1$  is generally the region where the relation in Eq. (39) is limited and the plate effective width ratio is considered to be 1.0, based upon the data used to establish that relationship [68].

It would thus appear from these results that the critical failure mode for these ships is quite close to the yield condition, as indicated by the values of the strength factor  $\phi$  found in this type of analysis. The resulting consequences of this fact on the main contributing uncertainties in ship strength will be considered in the next section.

## 7.0 ANALYSIS OF UNCERTAINTY OF SHIP STRENGTH

The uncertainties associated with variation in material properties, dimensions of structural elements, corrosion, etc. are among the objective uncertainties that can be determined from an established representation of the ship strength. The strength  $S$  (or the ultimate bending moment) is represented as a function of the various parameters  $\alpha_i$  in the form

$$S = f(\alpha_1, \alpha_2, \dots, \alpha_n) \quad (48)$$

from which the mean and variance are determined. This function is expanded in a Taylor series about the mean values of the constituent  $\alpha_i$  terms, and only linear terms are retained within the context of this linear error theory. On this basis, the mean value  $\mu_S$  and the variance  $\delta_S^2$  are determined in terms of the means and variances of the individual parameters, as shown by

$$\mu_S = f(\bar{\alpha}_1, \bar{\alpha}_2, \dots, \bar{\alpha}_n) \quad (49)$$

$$\sigma_S^2 = \sum_{i=1}^n \left( \frac{\partial S}{\partial \alpha_i} \right)^2 \sigma_{\alpha_i}^2 \quad (50)$$

where  $\bar{\alpha}_i$  and  $\sigma_{\alpha_i}^2$  are the mean and variance of the variables  $\alpha_i$  that determine the ship strength, with the partial derivatives evaluated at the mean value  $\bar{\alpha}_i$ . The expression in Eq. (50) applies when the  $\alpha_i$  parameters are independent. The coefficients of variation (COV) are then expressed as

$$\delta_S^2 = \left( \frac{\sigma_S}{\mu_S} \right)^2 = \sum_{i=1}^n \left( \frac{\partial S}{\partial \alpha_i} \frac{\bar{\alpha}_i}{\mu_S} \right)^2 \delta_{\alpha_i}^2 \quad (51)$$

in terms of the coefficient of variation of the  $\alpha_i$ , denoted as  $\delta_{\alpha_i}$ .

The procedure described above is the basis for determining the COV values for the different possible modes of ship structural failure described previously. Illustrations of the application of this type of analysis to representative models of ship structural strength have been given in [10] and [23] to determine the objective uncertainties. An example that was treated in both [10] and [23] is discussed here, viz. the determination of the strength COV for the failure mode due to initial yield moment. With the strength model given by Eq. (32), which is repeated below as

$$S = Z_e s_y \quad (52)$$

where  $Z_e$  is the conventional elastic section modulus and  $s_y$  is the material tensile yield stress, the application of the procedure of Eqs. (48) - (51) leads to

$$\delta_S^2 = \delta_{Z_e}^2 + \delta_{S_y}^2 \quad (53)$$

The determination of the section modulus COV depends upon the mathematical model used for its representation. A simplified model for a symmetric section was used in [10], while a more detailed model was established in [23] in terms of the lengths and thicknesses of webs and flanges in different parts of the section structure (deck, bottom, side), number of stiffeners in different parts of the section, etc. A detailed examination of the representation used in [23] for the UNIVERSE IRELAND showed that the assumption was made in [23] that the deck and bottom areas were equal, which is not true in general, and neither are the dimensions of the stiffeners equal in those two regions. A more appropriate model for the elastic section modulus was given in the discussion by Evans of [12], with that expression given by

$$Z_e = A_D g + 2A_S \left( \frac{D^2}{3g} - D + g \right) + A_B \frac{(D-g)^2}{g} \quad (54)$$

where

$$\frac{g}{D} = \frac{A_S + A_B}{A_D + A_B + 2A_S} \quad (55)$$

which also reduces to the value given in [23] where  $A_B = A_D$ . Each of the areas is represented in terms of appropriate dimensions of plating and also for the webs and flanges of the stiffeners in the different regions, etc. The extent of detail used for these geometric quantities determines the algebraic complexity of the resulting expression for the COV of the elastic section modulus, but the basic principles are the same for any case.

When considering the cases corresponding to failure arising as a result of buckling, the model used to represent the strength is given in accordance with [60] by

$$S = Z_e s_{y_c} \phi \quad (56)$$

where  $s_{y_c}$  is the compressive yield stress of the material and  $\phi$  is the failure stress ratio or strength factor. It is this factor  $\phi$  which differs for each buckling failure mode, and it is, therefore, the most critical element to determine (together with its uncertainty) when considering these failure modes. The expression for the COV of the strength in these cases is then

$$\delta_S^2 = \delta_{Z_e}^2 + \delta_{s_{y_c}}^2 + \delta_{\phi}^2 \quad (57)$$

where  $\delta_{\phi}$  is the COV for the quantity  $\phi$ .

The COV values for elastic section modulus can be determined in terms of the variability in dimensions as discussed above, and the variability in the yield stress can be found from data on material properties. Since the quantity  $\phi$  reflects average conditions, and it functions as a factor reflecting distributed effects throughout an element or larger component of the ship structure (e.g. grillage), the mathematical representation is understood to be an approximation to a relatively complex effect. The various expressions for this factor  $\phi$  given previously in this report, in [10], [69], and other cited references are to be viewed in this manner. It can be expected, however, that for values of  $\phi$  in the range 0.90 - 1.0 the representations used would have greater validity since the departure from a pure yielding condition for the ultimate strength is not large for such cases. Thus, significant nonlinear deformations, plasticity effects, etc. would not be manifesting themselves and, hence, this simplified model would be expected to have greater validity. Since the range of  $\phi$  values for the 3 representative ships considered here have values in that range, these vessels are in that category.

From the point of view of failure due to buckling, these ships would not appear to have a significant dependence on the  $\phi$  value, with their ultimate strength being close to that associated with yield strength as would be expected by the low  $\beta$  values, results indicated in [74], etc. Since the  $\phi$  values are approximate average measures insofar as these values per se are concerned, there is then a question concerning the validity of their variability when determined using the approximate formulas that have been established for the various failure modes (as described above). This feature should be recognized as an inherent property of any approximate representation unless there is additional proof that the gradients, i.e. derivatives with respect to the pertinent parameters, are also valid representations.

The more recent simplified mathematical models used to represent the ship strength, from which uncertainties in the form of COV values are determined, are generally represented by the work in [10]. A close examination of [10] shows that some of the models are also represented in [69], while the original representation in [10] and [69] can really be traced back to results given in [71] and [75]. Those models were established on the basis of limited data, making use of representations involving the elastic modulus in the form of the tangent modulus representation, as well as other expressions appropriate in the elastic range. In addition, other expressions that represent the effect of residual stresses in an analytic formulation are also presented in [10] based

upon the same origin for such expressions, viz. the unpublished work of Faulkner in [71] and [75].

The data used for establishing these relationships were limited in their applicability, and the resulting analytic functions also exhibit rather unusual behavior. Particular examples are shown in [10] which involve numerical evaluation at a selected location along the stress-strain diagram in the representation of the tangent modulus using the parabolic model given in Eq. (41). The choice of the particular location at which this coefficient is found can result in large changes in values for the COV of the tangent modulus, which is dependent on the variability of the yield strength as well, according to the formulations in [10]. Furthermore, there is a "singularity" for the value  $\beta=0.5$ , resulting in extremely large magnitudes since the denominator rapidly approaches zero in some of the expressions given for the uncertainties of the various  $\phi$ -factors. This would provide an extremely large value generally for the COV of the  $\phi$ -factors, although for  $\beta$  values  $<1$  there is only a small degree of dependence of ship strength on buckling phenomena which are represented by the quantity  $\phi$ . In fact, for the SL-7 vessel, the numerical value of  $\beta$  for a typical plate panel is close to 0.5.

It would thus appear that the mathematical models given in [10], which have their origin in earlier work, may not be applicable to a large range of ships of practical interest when considering the class of merchant ships that has been examined herein. Most of the data probably arose in the course of analysis of lightly build ships such as naval warships, rather than the heavily built structural configurations represented by the merchant vessels that have been considered here. In view of this situation, it would appear that the use of simplified mathematical models such as those in [10] to represent the ship strength may have limited utility when considering the uncertainties associated with buckling phenomena as a possible cause of ultimate failure of the ship hull girder. At least this would appear to be the case with the use of the formulas used herein which provide values of  $\phi$  close to 1.0, thereby indicating only small effects due to buckling.

If further data were obtained which would allow establishment of a simplified analytical formulation that would be valid in intermediate ranges of  $\phi$  wherein buckling effects would be predominant, then the direct procedures of uncertainty analysis by means of truncated linear error theory would have a greater prospect of utility. However, in view of the lack of any simplified models (in explicit form) appropriate to a large range of ship structural configurations, another approach should be considered for possible implementation to determine objective uncertainties of realistic ship structures. A description of this proposed approach is given below.

## 7.1 Suggested Procedure for Calculating Objective Uncertainties

An advanced computational procedure for determining the ultimate strength of a ship hull from the point of view of compressive failure is given by the work of Smith [14]. The particular analysis is based upon a finite-element approach which also allows consideration of residual stresses and initial deformations. The method of analysis is a linearized incremental finite-element process wherein loads (or displacements) are applied incrementally, combined with iteration operations to achieve equilibrium convergence. The assumptions within the procedure are that the vertical curvature of the hull occurs incrementally, with corresponding incremental element strains calculated assuming that plane sections remain plane and that bending occurs about the instantaneous elastic neutral axis of the cross section. The element incremental stresses are derived from the incremental strains using the slopes of the stress-strain curves derived from the analysis applied to stiffened panels under both tensile and compressive loads. These element stresses are integrated over the cross-section in order to obtain bending moment increments, with the incremental curvatures and bending moments then summed to provide cumulative values. The moment-curvature relations are then used to evaluate the ultimate longitudinal strength of the hull.

Within the analysis in [14], special treatments are made. For cases where the stress in any fiber of an element exceeds the yield stress, the fiber is assumed to contribute no stiffness in the next incremental step, assuming that an elastic-perfectly plastic material stress-strain curve is present. The stiffness for the complete frame is modified in this manner before the next incremental solution step. Allowance is made for elastic unloading of yielding fibers so that the fiber is assumed to recover its elastic section properties in a following incremental step after elastic unloading of the yielded fiber in the preceding increment. The loss of stiffness due to local plate buckling is included when analyzing a cross section that includes such a plating element. The characteristics of such unstiffened plating are represented in the form of load-shortening curves, as shown in the curves of Figure 16 for square plates (which can also be used for rectangular plates as well), which have been derived from the theory of [14]. These curves also illustrate the effects of initial distortion and residual stresses.

The analytical method was applied in [14] to a representative midship section of a destroyer hull, with each stiffened panel treated as a beam-column made up

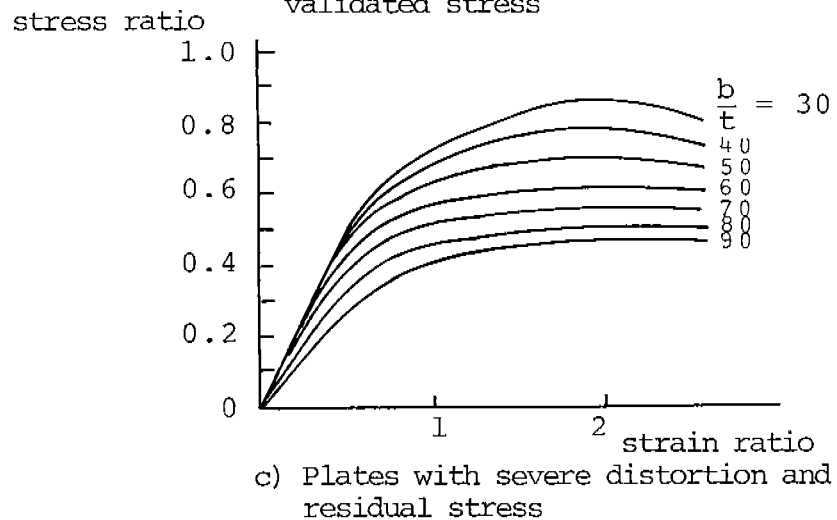
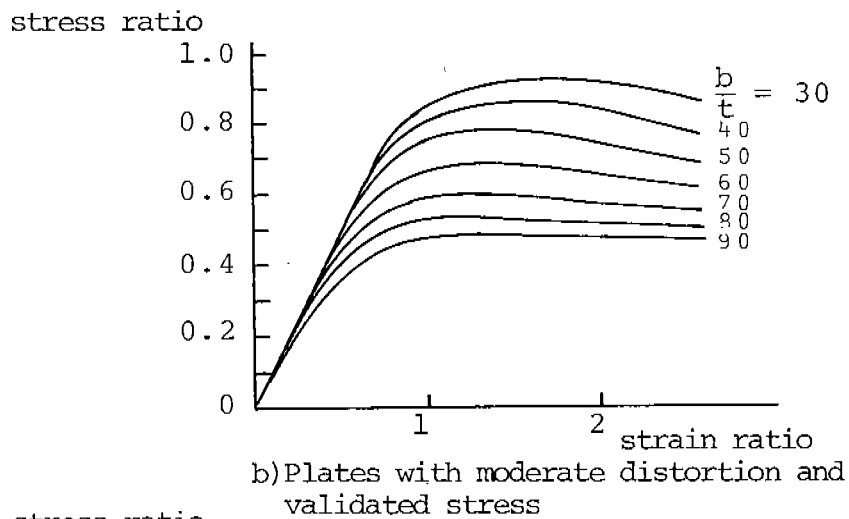
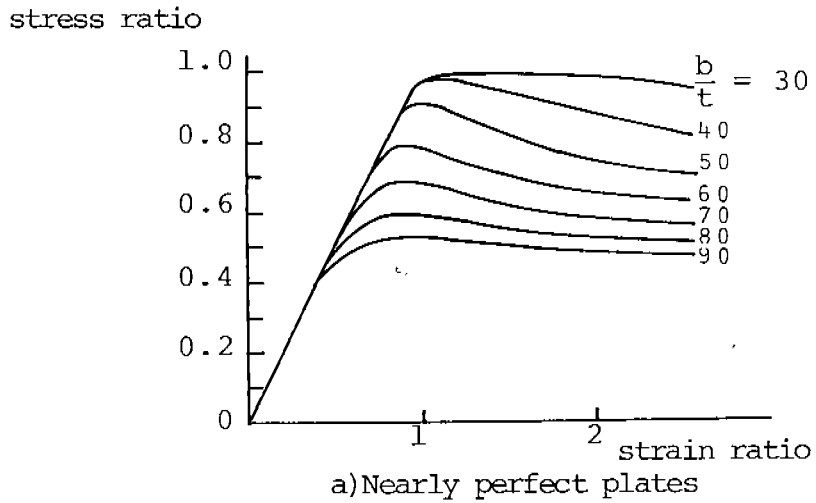


Fig. 16 Load-shortening curves for square plates under uniaxial compression

of a representative stiffener with an attached plating strip. The effects of adjacent frames was included, with calculated results for different cases representing variations in plate slenderness, column slenderness, and frame spacing found for each stiffened panel as a means of representing the changes in the stress-strain relationship. This procedure was then extended to the entire hull cross section to determine the ultimate strength (bending moment limit) for five different cases for the entire hull girder.

While the analysis in [14] was applied to static loads, an extension has been made in [76] to dynamic loads represented as impulses. In addition to that analysis, the basic theory of [14] was correlated with experimental data on welded steel box-girder models with satisfactory agreement exhibited.

In view of the utility of this theory, it would appear to represent a useful method for determining ship ultimate strength by calculation. However, the method in [14] also requires extensive computational effort, so that applying such a procedure to obtain results for a large set of parametric variations in ship section properties would not be practical. Other procedures that are somewhat similar in nature, although simplified in form, have been established by Billingsley [15] and Adamchak [77], with associated computer programs. The program by Adamchak, known as ULTSTR, can be used to estimate the collapse moment of a ship hull under longitudinal bending. A solution can be achieved in about 10 sec. computer time on a CDC 6000 Series digital computer when analyzing a representative naval ship section.

Since the ULTSTR program (or possibly also the program developed by Billingsley [15]) can provide values of the collapse moment or ultimate strength of a ship with small computational effort, it can be used effectively and efficiently to determine the changes in strength associated with variations in parameters characterizing the ship section. The particular procedure envisioned for use of such a program involves parametric changes in quantities such as the material yield strength, dimensions of the plate and stiffener elements, etc., with the ultimate strength determined in each case. The parametric variation results allow simple linear (or possibly higher order curve fit) determination of changes in ship strength associated with such changes in basic parameters. That information, according to the procedures shown by Eqs. (48)-(51), will allow determination of the COV values for the objective uncertainties of ship strength. This procedure, making use of advances in computational methods for more valid analysis of physical phenomena with reduced time and cost, is proposed in view of the limited experimental data available for determining the uncertainties associated with ship strength.

In addition to the direct use of a simplified program (e.g. ULTSTR) as described above for determining the ship strength as well as its variability, this computational procedure can also be applied to establish the range of validity of simplified analytic expressions for evaluating ship strength, e.g. as represented by the  $\phi$  factors described previously. Since the development of the expressions for  $\phi$  in the preceding section was based upon data obtained in investigations related to more lightly built ship structures such as naval warships, the results from the simplified finite-element procedure can be used to corroborate and/or correlate the analytical models for that range of structural configuration. Other possible simplified analytical models that have applicability to some of the intermediate range conditions between heavily built merchant ships and warships can possibly be structured on the basis of the results determined from the use of the computer program described above. Thus, a combined analytical and computational procedure can be used as a means of establishing more valid analytical representations of a simpler nature, so that it will then be possible for designers that do not have access and/or experience with such a computer program to estimate ship strength and its variability by use of simplified analytical expressions. How well this possible use of the program will function in actual cases cannot be forecast, but it appears to be a useful procedure that could provide a useful adjunct method of determining ultimate strength for an important class of ships.

## 7.2 Data for Determining Objective Uncertainties

The preceding analysis, as well as the results of many other studies of ship strength uncertainties, indicates that the major contribution toward the objective uncertainties (which can be calculated from mathematical formulas or other numerical analyses) is primarily dependent upon the variability in material properties and basic dimensions of structural elements. With regard to material properties, the most significant parameters are the variability of the yield strength and the modulus of elasticity. Data for yield strength variability are presented in [10], [23], and [24] as examples together with some information also on the elastic modulus. The results of all of these references can be summarized by the information below for the COV values of these quantities, with the value range given by:

<u>QUANTITY</u>	<u>COVE RANGE (%)</u>
Yield strength $s_y$	6 - 8
Modulus of elasticity E	1 - 2

In addition to the use of ordinary steel used for ship construction, it is also possible for some applications to

make use of new materials. Particular examples are high-strength steels, low-temperature alloys, materials with extraordinary high toughness, etc., which might be applied to special types of vessels. For such cases, the numerical values of variability of the material properties (yield strength and modulus of elasticity) must be determined from special tests on the basic materials. The COV range is then determined from the test data, and that tabulated information can then be used in studies of probabilistic design for specific cases using such materials. No particular values of such material variability measures are provided here.

A review of the published data for variability of dimensions shows that the variation in the beam and depth of conventional ship overall dimensions has a COV that is less than 0.2%. Thus, this variability can generally be considered as negligible for use in determining strength uncertainties. The major dimensional variations that influence strength uncertainty are variations in length and breadth of plate and stiffener elements (web and flange) as well as the thickness of the various elements. Information for determining the COV values for uncertainties in such breadth and length dimensions for plates and stiffeners is presented in [23], where the primary source of data is the Japanese Shipbuilding Quality Standards. The uncertainty in thickness is the more significant variable affecting uncertainty, with values available when neglecting the corrosion allowance (treated separately below). The general plate thickness COV can range up to 4% for use in uncertainty analysis, with the value decreasing with increase in the actual plate thickness. Values listed in [24] range from a COV = 3.6% for 0.25-in.-thick plates down to a COV of 0.7% for a 2-in.-thick plate.

When considering plate thickness, some allowance should be made for the effects of corrosion, which is a measure of the general reduction of thickness for the material, where this variability is actually a function of time. A method of treatment of the effects of corrosion which does not consider the time variability is given in [10], where the thickness of the material is represented in the form

$$t = t_o - t_c \quad (58)$$

where  $t_o$  is the initial thickness and  $t_c$  is the corrosion allowance. According to the procedures<sup>c</sup> for determining the COV by means of the relationships in Eqs. (48)-(51), the thickness COV is represented by

$$\delta_t^2 = \delta_{t_o}^2 + \left(\frac{t_c}{t}\right)^2 \delta_{t_c}^2 \quad (59)$$

where

$\delta_{t_0}$  = COV of plate thickness due to production tolerances

$\delta_{t_c}$  = COV of corrosion

Although the corrosion rate will vary in accordance to which strength member is considered and also depending upon the location in the ship, an approximate approach can be used to establish a single value for the corrosion allowance for the entire vessel. The data shown in [10] are taken from other data sources as well, where average rates of corrosion of structural steel for representative ship regions are presented in the form of mils per year. A more recent source of data is given in [31], which summarizes the mean corrosion rate for different types of ships, covering a total of 519 ships analyzed in Japan. The average corrosion rate is given as 0.10mm per year, and the average value of the standard deviation is given as 0.08. This information can then lead to a value of the COV  $\delta_{t_c} = 0.8$  from these data. Other information obtained from [31] shows that the general magnitude of the ratio  $(t_c/t)$  can be interpreted as having a value of 0.10 (as mentioned in [10]), which can then be correlated with the information for reduction in strength for ships as shown in Figure 17 (obtained from [31]). This variation can be considered applicable to larger ships, as shown in Figure 17, with an even larger reduction of strength represented by a larger ratio of  $(t_c/t)$  than 0.10 for smaller vessels. On the basis of the above value for the COV due to thickness, variability can then be expressed by

$$\delta_t^2 = \delta_{t_0}^2 + (.08)^2 \quad (60)$$

where the COV for the thickness variability  $\delta_{t_0}$  lies anywhere between 0.7% and 4%, depending upon initial thickness.

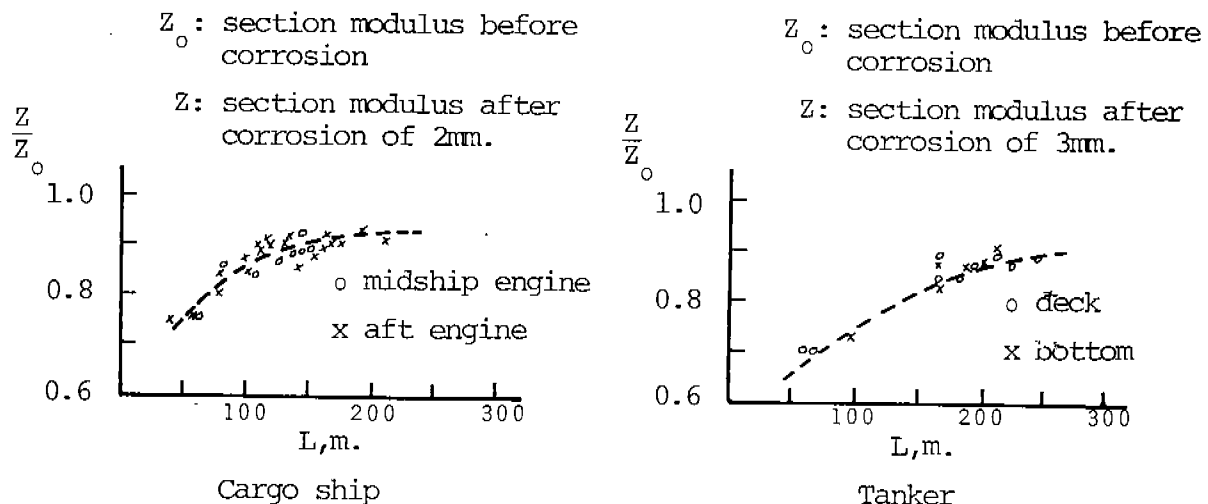


Fig. 17 Reduction of section modulus due to corrosion

## 8.0 SUBJECTIVE UNCERTAINTIES IN SHIP STRENGTH

As mentioned previously, the various uncertainties that affect ship strength are categorized into those that are denoted as objective and those that are subjective. The objective errors are those that can be measured in principle, and that arise from variability in the basic dimensions as well as the material and fabrication properties of the structure. The effects of objective errors are usually assessed by the use of truncated linear error theory applied to representative mathematical models, as illustrated in the previous section. The largest component contributing to the total objective uncertainty frequently arises from the uncertainties of yield strength.

The subjective uncertainties are associated with the lack of perfect knowledge, which is generally attributed to uncertain boundary and loading conditions. In addition, the literature also considers the effect of small shape imperfections to be a subjective uncertainty. However, these small shape imperfections can be treated objectively in accordance with more recent developments, as shown in Figure 16 and described in [14], with adequate knowledge of the measured range of such imperfections. In many cases, it has proven impossible to either measure or account for these boundary and loading factors in a satisfactory manner in mathematical strength formulations for design use, or to control the imperfection factors sufficiently in the manufacturing stage. Since the occurrence of such effects is essentially random, that is the basis for analysis of these effects in regard to determining the total uncertainty for ship strength. Often the amount of data is also inadequate to allow proper assessment of such effects. Obtaining additional data would not necessarily reduce the magnitude of these uncertainties, although the confidence levels associated with the values would thereby reduce and thus improve the basic estimates. In addition, a better and more complete mathematical description of all of the above phenomena would certainly reduce the uncertainty. Since the scatter in the various results for strength is regarded as unexplained and subjective, estimating the value of these subjective uncertainties requires a good degree of professional judgment and experience.

It is possible to use some available test data which allow estimating the COV values for such uncertainties that can then be used in reliability studies for ship structural design. The use of the data for subjective uncertainties in determining the total random uncertainty in strength is applied by means of the square root of the sum of the squares of the subjective and objective uncertainties, as shown by the relation

$$\Omega = \sqrt{\delta^2 + \Delta^2} \quad (61)$$

where  $\delta$  is the objective COV,  $\Delta$  is the subjective COV, and  $\Omega$  is the COV of the total uncertainty. This result is obtained on the basis that the two types of uncertainty are independent random variables that are uncorrelated. A general description of these procedures is given in many references sources, e.g. [9], and [10], etc. One of the important considerations for use of published values is to recognize that lightly framed structures generally have higher COV values for subjective uncertainties as compared to more heavily built structures.

Previous discussions about uncertainties in ship structures have considered the possibility of using advanced finite-element and finite-difference analyses that can accurately model many of the difficult nonlinear factors characterizing ship structural strength. The effects of different types of imperfections and distortions as well as weld-induced residual stresses also play a significant role in failure of structural elements. Some of these factors can be included in the advanced computer analyses that are capable of handling nonlinear geometrical and material behavior for a wide range of structural geometries. The results of such analyses using these numerical programs can then be correlated with fabrication and test information (whenever possible) so that adequate validation can be established. This increased effectiveness of mathematical modeling can then be used as a means of assessing the influence of the different types of subjective uncertainties due to initial distortions and residual stresses, thereby possibly reducing their degree of subjectivity and allowing a more objective determination of uncertainty.

Among the significant contributors to the subjective uncertainties are imperfections such as those due to initial deformations and residual stresses caused by welding and cold forming. Both of these types of imperfections influence the strength and stiffness of stiffened panels that are used in ship structures. The magnitude of out-of-plane distortions has been found to be proportional to  $\beta^2$ , where  $\beta$  is the plate slenderness parameter. These distortions, relative to the thickness of plating, range typically from  $0.05 \beta^2$  to  $0.15 \beta^2$ , with values up to  $0.4 \beta^2$  found in heavily welded plating. Measurements of weld-induced residual stresses range from  $0.1 - 0.25s_y$ , and in some cases they have been found to reach as high as  $0.5s_y$ .

The effect of initial deformation generally reduces the compressive strength of a plate. It also changes the form of failure from a sudden event, which is followed by a sharp drop in load, to a more gradual process with less severe post-collapse load reduction. The weld-induced residual stresses also generally cause a reduction in compressive strength. In addition, the residual stress also results in pre-collapse loss of plate stiffness

caused by premature yielding. A number of different references support all of these findings, with a general summary of the effects of these imperfections given in [78].

Each of the two imperfections considered here, viz. initial deformations and residual stresses, cause a loss in strength in stiffened plating of ships. However, the effects of each one of these imperfections which occur in isolation are not directly additive, i.e., the influence of initial distortion is reduced in the presence of residual stress, and that of residual stress is reduced in the presence of initial distortion. In addition, residual stress effects appear to be less severe in practice than what is predicted, possibly as a result of "shake-out" resulting from the actual fabrication procedures as well as the cyclic type of loading that is experienced in sea service.

There are various rules that have been established regarding design tolerances for ships by different classification societies. However, these rules do not specify tolerances for flat stiffened panels. There are some rules and procedures that have been established for offshore structures that deal with design tolerances for such panels, and in addition there are specifications for tolerances such as the Japanese Shipbuilding Quality Standard as well as the British Standard for steel box-girder bridges. As far as the use of such information is concerned for application in the present study, the most suitable summary of the state of the art regarding these imperfections is given by a quote from the conclusions of [78], viz. "The treatment of imperfection effects and tolerances in present design rules for ships and offshore structures is generally incomplete and inconsistent and clearly has not yet been established on a sound statistical basis."

One of the influences on the strength model representation is the effect of workmanship and the extent of deviation from tolerances during the construction phase. Associated with such aspects of workmanship is the extent of prescribed inspection and the standards of acceptance of ship construction features, which are usually considered by the ship classification society surveyor present during the construction activity. The particular quality control standards for workmanship (also applied to inspection and acceptance) include consideration of the departure from tolerance level values of geometrical variables, imperfections, alignment, unfairness of plating, etc.

A comparison was made by an ISSC Committee of existing ship production tolerances and quality standards, in different countries, and the results reported in [79]. It was found that among the 15 production items considered, the various tolerance levels were approximately the same in different national standards for items that were determined from theoretical guidelines such as fillet weld gap, butt and overlapping weld gap. However, items determined from

experience or fabrication practice, such as plate unfairness are not consistent in their values from country to country, as well as between shipyards in the same country.

The acceptance of any ship structure for purposes of classification is the responsibility of the local classification society surveyor in the shipyard, as mentioned previously. The level of tolerance acceptability should be based upon certain criteria regarding strength alteration and/or contribution toward a significant change in the estimated failure probability. Such assessments lie beyond the general capability of a local shipyard surveyor, but some efforts by particular ship classification societies are being directed towards establishing acceptable ship construction tolerance levels by means of reliability analysis, as described below.

While there is no definite established procedure to determine the effects of variability in imperfections of ship structures (e.g. due to tolerances, workmanship, quality control, etc.), some attempts have been made to assess this influence in the context of reliability analysis. A particular approach is that in [80], which represents a method considered by a ship classification society to apply a reliability analysis as a means of assisting in the appraisal of quality control standards. The specific application in [80] only considered a plate panel, with concern directed toward the structural capability (with a fixed load input) as a function of changes in material properties, geometry and distortions (represented by different tolerance levels, which is the major item of interest here).

It is necessary in this analysis to have knowledge of the probability distribution of the variabilities of these different items in order to carry out such an analysis. The method of determining the structural strength by analytical means must also be sufficiently accurate, with limited computational complexity, cost, etc. Furthermore, the results of such an analysis must also correlate well with service organizations having sufficient information to allow such a comparison and point to areas where greater control of tolerances and other imperfections would have the greatest benefit. The basic methodology of [80] can be applied to help determine permissible tolerances, after further extension of the approach to more complex structural arrangements. The use of simplified structural models such as that in [77], which has been discussed previously for use in assessing other aspects of uncertainty, would be a possible tool that could be applied in that type of analysis.

In view of the above status of considering imperfections, the question arises as to how to treat this problem in the context of the present study. Any statistical

collection of data on initial distortions will deal with plating of as-built ships. These properties will change significantly due to the events associated with docking, berthing, cargo loading, etc. which are part of the actual operational scenario of a ship in service. As mentioned above, the effects of residual stress also reduce as a consequence of shake-out associated with operational use. The only feasible procedure at this time to account for these effects would appear to be to include them within the entire characterization of subjective uncertainties that are estimated for ship strength associated with different failure modes.

An approach to estimate the subjective uncertainty associated with initial distortions and residual stresses was made by Ang [81], who used the results obtained for the load shortening curves of plates (shown in Figure 16) found in [14]. In that case, the range of values for the buckling stress, relative to the calculated strength for a near-perfect plate, was from 0.75 - 1.0, with a mean value of 0.92 (corresponding to a bias value) and an associated dispersive COV of 0.064.

Other errors considered in [81] included an assessment of the influence of different panel boundary conditions as well as the assumed effect of certain regions of the section that could resist buckling (known as "hard corners" in [14]). The work of Smith [14] was used, for the five cases assumed for the illustrative calculations of a destroyer midship section, to relate the theoretical strength factors in [81] in order to establish the mean value and COV for the calculated ship collapse strength due to interframe flexural buckling. Different values were found for the two different frame spacings considered in [14], with COV values of 0.06 and 0.12 for the two spacings (the larger COV value for the larger spacing).

The above results were obtained in [81] by the analysis of a limited set of theoretical results presented in [14], with relatively gross estimation procedures applied to the end results of the calculation in [14]. While such estimates are useful, they only represent analysis of a limited set of calculated results that exhibit the variability associated with different degrees of imperfections, boundary condition and physical assumption changes, etc. for a single type of structure, viz. naval vessels which are generally lightly framed ship structures. Other sources of information about subjective uncertainties are found from available experimental data, where generally the scatter (reflected in COV values) is greater for unstiffened structures than for stiffened structures.

Considering the case of longitudinally stiffened plates, the suggested COV value for strut strength is about 6-7% based upon the data in [9] and [82]. For tripping strength,

there are insufficient data available, but the COV is expected to be somewhat larger, of the order of 8-9%. In the case of grillage strength, the subjective COV value, as indicated by the data in [26] and the values given in [9], is in the range of 8-10%. All of these values are appropriate to lightly framed structures, having been established and applied to problems of naval warships primarily. For the case of more sturdy ships such as tankers, the COV values are expected to be about up to 2% less. This same point of view is present in the earlier work such as [9], but only the larger values appropriate to the lighter built ships have been quoted in subsequent published literature (e.g. as in [23]).

Another suggested approach for determining subjective uncertainties is via use of calculated results, similar to the analysis in [81] but using a larger set of calculated results. This approach would make use of advanced numerical computer programs such as the ULTSTR program [77] or others that evolve from approaches similar to [14] (but simplified to allow rapid calculation ability) in order to assess the effects of initial imperfections (distortions and residual stresses) as well as assumptions as to boundary conditions, behavior of ends and corners, etc. The variability in the results for the ship collapse strength due to changes in these initial and boundary conditions will reflect the subjective uncertainties as determined by the computer analyses, just as the objective uncertainties are found from the slopes of the variation of strength with changes in material properties and dimensions (described in the preceding section). Thus, future progress in determining a more rational set of values for both subjective and objective uncertainties will depend upon the use of computationally efficient advanced numerical codes that are now becoming available for analysis of ship sections in a more complete manner than previous models.

## 9.0 SPECIAL CASES - LOADS AND STRENGTH

Among the various effects that influence ship structural failure, considering both loads and strength characteristics, are special situations of a more unusual nature than the various elements previously discussed. In the case of loads, these special cases include collision and grounding, where the loads are difficult to estimate and the occurrence is relatively rare. As a general rule, for use in a reliability-type analysis, the loads due to collision and grounding are not considered in a general "global" analysis but they are usually treated in a deterministic fashion.

The emphasis in considering collision and grounding is initially on load estimation, from which some means of protection via structural design of critical regions of the ship can be established (see [83] for a literature survey of protection or resistance against such loads). Such effects are considered to be important for particular vessels such as nuclear powered ships (due to possible radioactive contamination that may result) as well as tankers, LNG ships, and chemical carriers with hazardous and/or polluting cargoes. In addition, a number of other situations involving bridges, offshore oil storage facilities, supply ships and offshore platforms, etc. require some consideration of possible collision effects.

The structural arrangements considered for different ships as a means of collision protection involve modifications such as additional decks to absorb the energy during a collision. Other type energy-absorption methods have been considered, including honeycomb structures. In addition, some ideas concerning purely resistant structures (which are sufficiently strong to resist the collision impact without much energy absorption) have been proposed, as well as hybrid schemes for ship structures that combine the features of absorption (for minor collisions) and resistance (for major collisions).

For the case of grounding, ships are designed with double bottoms to withstand flooding in the event of an accidental grounding. The concern with pollution due to various types of hazardous cargo has also influenced the need for double bottom designs. Such a design requires consideration of its influence on the midship section structural arrangement. However, much less work has been devoted to the problem of estimating the local structural damage of grounded ships, as compared to the case of collisions.

While estimates of the occurrence of collisions and groundings of ships have been made on a probabilistic basis, including available statistical data, the magnitude of structural damage that results has not been quantified in the same manner for use in a reliability analysis. Thus, no

direct application toward assessment of uncertainty measures can be made for either loads or strength variability when considering these accidental events.

Among the features of structural examination that influence ship strength (and reliability) are the frequency of surveys by classification societies and the maintenance schedule. These factors refer to actions when the ship is in operating service. The ordinary practice of classification societies involves a time interval of 4 years between special surveys. This type of survey can usually detect any changes in ship structure due to directly observed damage (e.g. crack, deformation or corrosion wastage), which should be repaired. In addition to repairs made following periodic surveys, repairs following mechanical damage associated with operation, fatigue cracks and fracture-induced cracks, etc. require different degrees of responsiveness in providing repair and/or replacement of affected structural members.

According to the results shown in [31], the cumulative probability of a damage occurrence is about 20% for the 4 year period between surveys. The type of damage considered here includes small effects such as cracks and dents which do not necessarily lead to ultimate failure. Only the number of damages over a group of ships is considered in such an analysis, without any consideration of the degree of importance of the damage, its location and/or extent, etc. All of the information obtained as a result of ship surveys, the accumulation of damage statistics and related analysis by classification societies, etc. has been fed back (via classification society rules and recommendations) into the design of ships in order to overcome some of the problems and/or damage discovered over a period of time. However, no specific quantitative identification of the effect of such surveys and/or maintenance schedules on uncertainties for use in a reliability analysis via probabilistic methods has been established.

The treatment used in probabilistic design and reliability analysis considers time-dependent loads to be treated as static values corresponding to extreme conditions. The only concept involving time-dependent effects considered here has been that due to corrosion, and that is treated in a special manner that also reduces it to an effective stationary value. However, other physical effects may introduce consideration of time variation, such as the possible dynamic enhancement of yield strength as a function of the speed of loading (such as occurs in slamming).

That particular problem of yield stress variation has been considered in the analysis in [76]. Since the strain rates associated with whipping in the cases illustrated in [76] were too low, there would not be any expectation of any significant increase in yield strength for the cases of

frigates analyzed in [76]. The only conditions where such an effect would be meaningful would be at the higher modes of vibration of short ships, which is not a problem of interest here. The important effect which acts to limit the deformation of a ship structure during impulsive loading due to slamming is the inertia of the structure, which can be accounted for in any analysis.

Another type of error or uncertainty arises due to blunders or gross errors. These are defined as a major or fundamental mistake of some aspect of planning, design, analysis, construction, inspection, or in use or maintenance of a structure. This type of error arises due to some degree of negligence, or as a result of circumstances leading to a mode of behavior for which the structure was not originally designed. In some cases, errors arise in the calculation of design loads or the load-carrying capacity, or because of weaknesses introduced during construction, which make up the primary type of gross errors. The other type of errors leading to failure occur mainly due to a lack of knowledge, including basic ignorance within the engineering profession due to the present state of the art and knowledge in a particular field.

Many of these gross errors arise from human errors, and they also play an important part as the cause of many accidents. A particular example in the area of ship operation will include improper cargo loading of a ship, operation in heavy weather at inappropriate speeds, headings, etc., which can lead to failure due to exceeding prudent operational conditions.

A gross error or blunder should not be considered as part of the extreme value in the "tail" of the probability distribution that models a particular random variable, but it is a discrete event that radically alters the failure probability by changing the models that are applicable to describe the different phenomena. As a result, such errors cannot be treated in a formal manner within the present context of probabilistic design, and no numerical representation of uncertainty can be assigned for use in that type of analysis.

## 10.0 APPLICATION TO RELIABILITY EVALUATION

The results obtained in the preceding sections provide information on uncertainties in both ship loads and structural strength. This information can be applied in different ways to assess the reliability (or probability of failure) of a ship during its operation. With the uncertainties expressed in the form of COV values, together with procedures to establish mean values of loading and strength, the approach based on the safety index concept (defined in Eq. (5)) is the most direct way of using the present information.

Another related method of analysis involves the use of partial safety factors in terms of characteristic values as described in [17] and [10], which also makes use of the COV values together with chosen values of factors that are selected on the basis of an assumed probability level for an assumed type of distribution (for both load and strength). The more advanced method of reliability analysis is the complete probabilistic approach which requires full knowledge of the probability characteristics of both the loads and the strength, including all parameter values associated with those probability functions. This procedure is illustrated briefly in Eqs. (1)-(4).

While the more advanced full probabilistic approach cannot be applied using the information in the present report, since complete probability information is not available, some limited application of probabilistic analysis can be made with particular aspects of the information contained herein as a means of illustration of the basic procedure. That specialized application is for the case of combined wave-induced and slam bending moments, which was analyzed in an earlier section considering the combination of such loads (as described in Eqs. (25)-(29) and illustrated in Figure 11). The probability of failure when considering such a load combination, together with simplifying assumptions about the still-water bending moment and the ship structural strength, is found by the procedures described below.

In order to illustrate this particular special case, we assume, for simplicity, that the resisting bending moment  $S$  and the still-water bending moment  $L_s(t) = L_s$  are deterministic. This is considered to be a reasonable assumption only for the purposes of illustration in the present example. By defining  $M_m = S - L_s$ , the probability of failure of the ship will be obtained as the probability that  $M_m$  will be exceeded by  $Z(t)$  at least once in a specified period of ship operation (say, in one voyage).

Estimating the number of wave encounters,  $n_j$ , in the  $j$ -th sea state (assume a specific ship speed for that sea state), one can evaluate the probability  $R_j$  that the ship will survive the sea state as

$$R_j = [p_j P_j\{M_m > Z_m\} + (1-p_j)P_j\{M_m > X_m\}]^{n_j} \quad (62)$$

In Eq. (62),  $p_j$  is the probability of a significant slam per wave encounter (which is found from the work of Ochi [81], and  $P_j\{M_m > Z_m\}$  is the probability that the peak bending moment under the combined action of the wave and a slam will be less than the resisting bending moment (and hence no failure will occur), while  $P_j\{M_m > X_m\}$  is the same probability under the wave action alone. All these probabilities are assumed to be dependent upon the sea state and, hence, their expressions carry the subscript  $j$ . The probabilities  $P_j\{M_m > Z_m\}$  and  $P_j\{M_m > X_m\}$  may depend on the sea state since the parameters  $\alpha$  and  $\sigma$  respectively in Eqs. (27) and (28) may take different values ( $\alpha_j$  and  $\sigma_j$ ) depending on the sea state.

The probability of a ship surviving a voyage is then given by

$$R = \prod_{j=1}^N R_j \quad (63)$$

where  $N$  is the total number of sea states the ship is expected to encounter during the voyage.

To utilize Eq. (63) one must first estimate the following quantities:

$n_j$  = number of wave encounters in the  $j$ -th sea state

$p_j$  = probability of a significant slam per wave encounter in the  $j$ -th sea state

$\alpha_j$  = parameter value of the exponential distribution function used for the maximum slam-induced bending moment

$\sigma_j$  = rms value of the wave-induced bending moment in the  $j$ -th sea state

$M_m = S - L_s$

$S$  = resisting bending moment

$L$  = still-water bending moment

Also, use the following equations for  $P_j\{M_m > Z_m\}$  and  $P_j\{M_m > X_m\}$ :

$$P_j\{M_m > Z_m\} = 1 - F_{Z_m}\{M_m; \alpha_j, \sigma_j\} \quad (64)$$

$$P_j\{M_m > X_m\} = 1 - F_{X_m}\{M_m; \sigma_j\} \quad (65)$$

In Eqs. (64) and (65),  $F_Z \{M_m; \alpha_j, \sigma_j\}$  is obtained from Eq. (29) by replacing  $z$ ,  $\alpha$  and  $\sigma_m$  with  $M_m$ ,  $\alpha_j$  and  $\sigma_j$ , while  $F_{X_m} \{M_m; \sigma_j\}$  is modified similarly using the Rayleigh relation.

$$F_{X_m}(x) = 1 - e^{-x^2/2\sigma^2} \quad (66)$$

The probability of failure  $P_f$  is then obtained as

$$P_f = 1 - R \quad (67)$$

Since  $R$  is known to be very close to unity, a numerical scheme would have to be devised to evaluate  $P_f$  directly so that one can retain at least the first two significant figures accurately in the process of numerical evaluation.

The above analysis represents only an idealized example of the use of some of the information given in the present report in order to estimate failure probability. However, it is a special case and is subject to the assumptions concerning the variability of ship strength. More detailed analyses would be required when considering strength variability in a complete manner, as well as a more complete representation of the total load system acting on the vessel. Such analyses will evolve as more information on both loads and strength become available so that the full probabilistic approach to structural analysis and design can be readily used for ship hull structures.

## 11.0 DESIGN LOAD ESTIMATION

As a result of the methods described herein, it is possible to provide a procedure for design load estimation using the probabilistic approach. The procedure involves consideration of the uncertainties in ship strength also, since both loads and strength are related when considering safety. The concept of the safety index  $\beta_f$ , as well as the determination of partial safety factors, involves uncertainties of both load and strength and, hence, features of both effects enter into the design load estimation as shown below.

The first element to be determined is the mean value of the extreme load (bending moment). For still-water loads, a constant deterministic value corresponding to either full load or ballast conditions can be selected based on calculations using information about cargo loading, as discussed in Section 4.1. Alternatively, if sufficient information is available from analysis of operational data (as given in Tables 1 and 2 or similar information from an adequate data base of still-water loads), that value can be used. An estimate of thermal load can also be made, as described previously in Section 4.2.

The evaluation of the wave load mean value represents the primary load acting on a ship. A nominal mean value is found by use of the long-term probability method (as described in [34]) or by use of the extreme value method [35]. Each of the methods actually provides the modal value of the maximum load, which is sufficiently close to the mean value (about 3% different, as indicated in [17]). Since the values obtained from both approaches are close to each other, and also close to the nominal load value obtained from classification society rules (as shown in [46]), the use of either method can be considered for determining the mean wave load.

The mean value of a total load, when considering only static loads and wave loads, is found as the sum of the respective mean values. When considering cases involving combined wave loads and vibratory loads, such as those due to springing or slamming, a different procedure has to be used. In the case of combined springing and wave loads, the rms value of the combined load is found from Eq.(23) and the discussion following that equation in Section 5.3. The mean value of the extreme combined load for springing and wave loads is a multiple of the rms value, with the multiplying factor given in [67] in terms of the spectral width parameter  $\epsilon$ , the ratio of the average periods of the two constituent loads, and the relative magnitude of the separate component rms values.

For the case of combined wave and slam loads, the mean value of the combined load is obtained from Eq.(30). The quantities in Eq.(30) represent the mean value of the extreme wave and

and slam loads found separately. The mean slam load extreme value is found from the formula  $M_{slam} = 0.00038\rho gL^3B$ , which is the value corresponding to  $10^{-8}$  probability in [60]. This value is one-half that in [60] since the data in [60] are for peak-to-peak values, as described in Section 5.4.

When considering any case wherein there is a combined effect of a static load, a wave load, and a vibratory-type load, the mean value for the total load is obtained by adding the mean static load value to the particular combined wave and vibratory load. This procedure is considered adequate within the present state of the art for determining the mean value of any combined load due to various causes. The influence of any type of vibratory load is only applicable to special cases wherein such vibratory loads manifest themselves, and, hence, they are only considered for special classes of ships (e.g. Great Lakes bulk carriers for springing; slender cargo ships, container ships and naval frigates for slamming, etc.)

The measure of uncertainty for the total load, which in general is made up of static, wave-induced and dynamic vibratory loads (either springing or slamming), is represented by the total load COV, denoted as  $COV_t$ . The COV of the total load is given by the relation

$$COV_t = \left[ (COV_s)^2 \mu_{L_s}^2 + (COV_w)^2 \mu_{L_w}^2 + (COV_d)^2 \mu_{L_d}^2 \right]^{1/2} / \mu_{L_t} \quad (68)$$

where  $\mu_{L_s}$ ,  $\mu_{L_w}$  and  $\mu_{L_d}$  are the mean values of the static load, wave load and dynamic load, respectively, with similar definitions for the corresponding subscripted COV quantities. This can be simplified further if the approach wherein the static (still-water) load is taken as a constant value is used, so that the first term in the above relation is deleted (however the static load is considered when determining the total mean load magnitude). With the magnitude of the constituent elements in Eq.(68) given in the preceding sections of this report (or calculated for any specific case desired), the uncertainty in the form of  $COV_t$  for the total load is then known.

A particular reference value used in probabilistic analysis is known as the characteristic value. This characteristic value of any variable, having a specific probability of not being exceeded, is expressed as

$$x_k = \bar{x} + k\sigma_x = \bar{x}(1+kCOV_x) \quad (69)$$

where  $\bar{x}$  is the mean value of the basic variable,  $\sigma_x$  is its standard deviation, and  $k$  is a multiplier dependent on the probability distribution to achieve a particular probability ( $k=1.645$  for  $p=5\%$  with a normal distribution). The characteristic value is then just an augmented value beyond that of the

mean, in terms of a particular multiple of the COV for that quantity.

In some studies involving structural safety, the characteristic value is sometimes used as a design load value when combined with particular partial safety factors (e.g. see [10] and [17]). A more realistic estimate of the design load value can be obtained as a measure of the value of load most likely to cause failure, as determined for a particular structure using the concept of the limit state. The limit state is a condition beyond which the structure becomes unfit for its purpose, e.g. the ultimate collapse state of failure. The design value is found in terms of the safety index  $\beta_f$  by use of the relation

$$L^* = \mu_{L_t} (1 - \alpha_L \beta_f \text{COV}_t) \quad (70)$$

where the quantity  $\alpha_L$  is a load sensitivity parameter found from the definition of the limit state equation (see [85]). With the limit state relation given by

$$M = S - L \quad (71)$$

where S is strength and L is load (total values are understood here), the value of  $\alpha_L$  is found to be

$$\begin{aligned} \alpha_L &= \frac{-\sigma_L}{[\sigma_S^2 + \sigma_L^2]^{1/2}} \\ &= \frac{-\text{COV}_L}{[(\text{COV}_S)^2 \theta^2 + (\text{COV}_L)^2]^{1/2}} \end{aligned} \quad (72)$$

where

$$\theta = \frac{\mu_S}{\mu_L} \quad (73)$$

is the central safety factor (ratio of mean values of strength and load). The term in the parenthesis in Eq.(70) is referred to as the central partial safety factor for load, which is a factor multiplying the mean load in order to determine the design load.

Other types of partial safety factors have also appeared in the literature pertaining to ship structural safety (e.g. [17], [86]), such as the ratio of the characteristic strength to characteristic load,  $\gamma_o = S_k/L_k$  which is referred to as the overall partial safety factor in [86]. The quantity  $\gamma_o$  is related to the safety index  $\beta_f$  in terms of the central safety factor  $\theta$ , which then also requires knowledge of the COV values of both strength and load. Another type of partial safety factor is the ratio of the design load value to the characteristic load, which is often used when a particular characteristic value (representing a specified fractile probability such as 5%, for example) is selected as a reference value in some structural codes.

With the design load value defined according to Eqs.(70)-(73), it is seen that this design load is related to the safety index  $\beta_f$  and also the total COV values for both load and strength. This interrelationship, or coupling, requires some estimate of mean and COV values for ship strength in order to establish a design load estimate by the use of the present probabilistic design method. Since  $\beta_f$  is related to the probability of failure by means of Eq.(6), for an assumed normal distribution, this allows a design load estimate related to assumed levels of reliability. With most merchant ships having  $\beta_f$  values in the range of 4.0-6.0, corresponding to failure probabilities  $P_f$  in the range of  $10^{-5}$  to  $10^{-9}$ , selected parametric exercises using Eqs. (70)-(73) with a range of COV values, etc. will allow determination of the dependence of the central partial safety factor for design load estimation on the safety index and failure probability.

## 12.0 CONCLUSIONS AND RECOMMENDATIONS

As a result of this study, a number of conclusions have been found, together with recommendations for further work to enlarge upon the findings and/or procedure discussed in the report. A listing of some of the conclusions associated with the present analysis is given below.

### 12.1 Conclusions

1. A more firm value of the COV for wave loads due to statistical variability of the wave spectra (for a given significant height range) has been illustrated, with ranges found for different types of ships (COV range from 10-20% in larger sea states).
2. An estimate of the error of theoretical calculation capability for determining bending moment response operators was found, based on comparison of theory with model test data for 4-5 different ships. This error was estimated to be a COV of 10%.
3. The statistical variability associated with an estimate of the extreme value of bending moment, based upon properties of the extreme value probability functions was also determined. The COV value is found as a function of the number of cycles of operation in specified sea states, and ranges between 5-10% for most practical cases of interest.
4. An interpretation of the distribution of the long-term bending moment variability due to the basic probability characteristic for that quantity (i.e. Poisson distribution) was also provided.
5. The influence of ship form, such as the distinguishing effects of flare compared to wall-sidedness, is shown to result in unsymmetrical sagging and hogging loads. This nonlinear effect is shown by existing data to result in sagging extreme loads being about 20% larger than hogging for vessels such as container ships, where this effect is associated with the wave-induced loads without considering any influence of vibratory responses.
6. The overall COV for wave-induced loads, based upon consideration of wave spectral variability, limits of hydrodynamic theory, and the statistical variability of extreme values is found to be about 20%.

7. Analysis of springing loads per se resulted in a COV Value estimated to be about 29% based on sensitivity to spectral variability (in the high-frequency range), limits of theoretical calculation capability, and the effects of extreme value variability.
8. Whipping loads due to slamming are estimated based on analysis of measured full-scale data, with a nondimensional coefficient found to be applicable to container ships, cargo ships and naval vessels. The amplitudes of whipping loads are approximated by an exponential distribution, and an estimate of the COV of such loads was also determined from the available (limited) data.
9. Combinations of loads are considered, with still-water loads initially recommended as a large constant (but not absolutely known) representative value that is to be added to the wave load corresponding to that operating condition, i.e. whether fully loaded or in ballast. Thermal loads are also treated as a selected constant value so that the sum of still-water and thermal loads is a static reference level for the large time-varying loads. If sufficient information on statistical properties of still-water loads becomes available, a procedure for combining such data with the wave load data is provided to enable evaluation of the COV for the load combination.
10. The combination of wave-induced and springing loads is analyzed as well as combined vertical and lateral wave bending moments. The COV of combined vertical and lateral wave bending moments is about 22%, while that for combined wave and springing loads can range between 22-29% depending on which mode is predominant in the measured total load.
11. A method for combining the magnitudes of extreme wave loads and whipping loads due to slamming is shown, together with an approximate representation of the cumulative probability for their sum. The COV value for the sum of wave and whipping loads is estimated to be in the range of 25-30%.
12. The analysis of ultimate strength for representative large modern merchant ships (tanker, bulk carrier and containership) showed only small prospect of any type of buckling failure, with failure close to yield conditions. This is due to the influence of the small slenderness parameter value for such heavily built vessels.

13. Expressions for the failure strength factor introduced into ship strength bending moment models are based on approximations and data primarily valid for a limited class of vessels, viz. lightly framed naval vessels. There is questionable validity of some of the simplified analytical models when used to determine measures of uncertainty since the necessary partial derivation gradients used in determining objective COV values have not been verified adequately, especially when considering their application to heavier built ship structures.
14. Subjective uncertainty COV values for different types of failure of longitudinally stiffened panels are estimated based on limited experimental data and analysis of theoretical results. Values appropriate to naval vessels are given with a recommended range of values to be used for tankers and other heavily built ship structures.
15. Proposed procedures are described for applying recently developed advanced numerical computer programs to determine both objective and subjective uncertainty values for various types of ships, changes in material properties and dimensions, variations in initial imperfections, boundary condition assumptions, etc.
16. A recommended procedure for estimating design loads is presented which depends upon mean values and COV values of both the load and strength. The design load is also related to the safety index (and hence to failure probability), thereby allowing direct use of uncertainty measures in establishing design load estimates. Various partial safety factors are identified and defined in terms of the design load and the characteristic load (and strength) values.

## 12.2 Recommendations

Among the recommendations established as a result of this study are the following:

1. Further data analysis should be made for more ships and/or more actual spectral wave records to establish the sensitivity of COV values due to wave spectral variability and hydrodynamic theory prediction capability.
2. Additional theoretical development to allow adequate prediction of springing loads should be continued, together with validation with experimental data (model and full scale). The influence of nonlinearity in the input excitation forces should be expanded in detail in order to determine if present methods of response analysis are adequate for that type of load.

3. Further data should be obtained to characterize whipping loads, using either full-scale data or by use of analysis of theoretical models exercised via computer simulation. There are insufficient data available for both sources, and more extensive validation relative to available data is necessary for any computer model before employing it to generate whipping loads.
4. More detailed computational experiments should be carried out to determine the degree of validity of using a steady constant value of still-water bending moment in the analysis of failure (initially with the safety index method) when combining still-water and wave-induced loads. The forthcoming availability of more data on still-water loads and their variability, together with additional analysis of predicted wave loads for different ship loading conditions, will allow such a determination as well as the results of using the combined COV value with adequate still-water load statistics.
5. The use of computer simulation models of slam and whipping loads, together with wave-induced loads represented in proper time phase relative to the disturbing incident waves, will allow empirical development of relationships between wave-induced and whipping loads. Such relationships will provide data that can be used to establish probability characteristics, extreme values, and variability measures for the combined wave and whipping loads of specialized ships that are vulnerable to such effects.
6. The use of newly developed efficient numerical computer programs that can allow evaluation of effects of changes in various features of a ship section should be applied to determine objective uncertainties of ship strength. These programs should be exercised over a range of parametric variations in material properties, dimensions of elements, etc. for different types of ships in order to determine values of such objective uncertainties in a fast and reliable manner. Possible procedures to allow validation of simplified mathematical models for the strength factors representing different types of buckling failure should also be sought as a means of extending such simple models to conditions never treated previously.

7. Similar exercising of the numerical programs to determine subjective uncertainties should also be carried out by varying the degree of initial imperfections, boundary conditions, behavior of special regions of the ship section, variations in frame spacing, etc. The accumulation of a large data base representing the effects of such changes by using a valid computational tool will provide better estimates of this type of uncertainty.

### 13.0 ACKNOWLEDGMENTS

The authors wish to acknowledge the efforts of the technical personnel who provided significant assistance to us during the course of this work. Prof. E. V. Lewis was an early contributor who provided inspiration and initial guidance during the proposal stage for this project and also during the course of the work in all phases. Prof. M. Shinozuka provided consultant services in the area of load combinations, and was especially helpful when the problem of combined wave-induced and slam loads was being analyzed. The work of Prof. T. A. Acharides was provided in the capacity of a consultant on this project.

#### 14.0 REFERENCES

1. St. Denis, M., and Pierson, W.J., "On the Motions of ships in Confused Seas," Trans. SNAME, 1953.
2. Freudenthal, A.M., "Safety of Structures", Trans. A.S.C.E., Vol. 112, 1947.
3. Freudenthal, A.M., "Probabilistic Approach to Economic Design of Maritime Structures," XXII Int. Navigation Cong., Paris, 1969.
4. Abrahamsen, E., Nordenstrom, N. and Roren, E.M.Q., "Design and Reliability of Ship Structures," Spring Meeting, SNAME, 1970.
5. Lewis, E.V., "Ship Structural Design for Extreme Loads," Schiffstechnik, 1976.
6. Nordenstrøm, N., "Probability of Failure for Weibull Load and Normal Strength," Rpt. No. 69-28-5, Det Norske Veritas, March 1970.
7. Mansour, A., "Probabilistic Design Concepts in Ship Structural Safety and Reliability," Trans, SNAME, 1972.
8. Mansour, A., "Approximate Probabilistic Method of Calculating Ship Longitudinal Strength," J. of Ship Research, 1974.
9. Mansour, A. and Faulkner, D., "On Applying the Statistical Approach to Extreme Sea Loads and Ship Hull Strength," Trans. RINA, 1973.
10. Stiansen, S.G., Mansour, A., Jan, H.Y. and Thayamballi, A., "Reliability Methods in Ship Structures," Trans. RINA, 1979.
11. Nibbering, J.J.W., "Permissible Stresses and Their Limitations," Ship Structure Comm. Rpt. SSC-206, 1970.
12. Caldwell, J.B., "Ultimate Longitudinal Strength," Trans. RINA, 1965.
13. Vasta, J., "Lessons Learned from Full-Scale Structural Tests," Trans. SNAME, 1958.
14. Smith, C.S., "Influence of Local Compressive Failure on Ultimate Strength of a Ship's Hull," PRADS-Int. Conf. on Practical Design in Shipbuilding, Tokyo, 1977.
15. Billingsley, D.W., "Hull Girder Response to Extreme Bending Moments," Spring Meeting/STAR Symp., SNAME, 1980.

16. Ang, A.H-S., and Ellingwood, B., "Critical Analysis of Reliability Principles Relative to Design," Proc. 1st Int. Conf. Appl. of Statistics and Probability to Soil and Structural Engineering, Hong Kong Univ. Press, 1971.
17. Faulkner, D. and Sadden, J.A., "Toward a Unified Approach to Ship Structural Safety," Trans. RINA, 1978.
18. Cartwright, D.E. and Longuet-Higgins, M.S., "The Statistical Distribution of the Maxima of a Random Function," Proc. Roy. Soc. of London, Ser. A, Vol. 237, 1956.
19. Abkowitz, M.A., Vassilopoulos, L.A. and Sellars, IV, F.H., "Recent Developments in Seakeeping Research and its Application to Design," Trans. SNAME, Vol. 74, 1966.
20. Lewis, E.V., et al, "Load Criteria For Ship Structural Design," Ship Structure Comm. Rpt. SSC-240, 1973.
21. Jasper, N., "Temperature-Induced Stresses in Beams and Ships," ASNE Journal, August 1956.
22. Dalzell, J.F., Maniar, N.M. and Hsu, M.W., "Examination of Service and Stress Data of Three Ships for Development of Hull Girder Load Criteria," Ship Structure Comm. Rpt. SSC-287, 1979.
23. Daidola, J.C. and Basar, N.S., "Probabilistic Structural Analysis of Ship Hull Longitudinal Strength," Ship Structure Comm. Rpt. SSC-301, 1981.
24. Baker, M.J., "Variations in the Strength of Structural Materials and their Effect on Structural Safety," Imperial College, London, 1970.
25. Lewis, E.V., Discussion of Committee V.1 Report, ISSC 1979, in Proceedings of the 7th ISSC, Vol. 2.
26. Smith, C.S., "Compressive Strength of Welded Steel Ship Grillages," Trans. RINA, 1975.
27. Ivanov, L., and Madjarov, H., "The Statistical Estimation of SWBM (Still Water Bending Moment) for Cargo Ships," Shipping World and Shipbuilder, 1975.
28. Soding, H., "The Prediction of Still-water Wave Bending Moments in Containerships," Schiffstechnik 1979.

29. Little, R.S., Lewis, E.V. and Bailey, F.C., "A Statistical Study of Wave-Induced Bending Moments on Large Oceangoing Tanker and Bulk Carriers," Trans. SNAME, 1971.
30. Akita, Y., Research Comm. No. 200-5, "Allowable Stress of Ship Structural Member," Rpt. No. 93, Japan Shipbuilding Research Association, August 1980.
31. Akita, Y., "Lessons Learned From Failure and Damage of Ships," Joint Session I, 8th International Ship Structures Cong., 1982.
32. Kaplan, P. and Raff, A.L., "Evaluation and Verification of Computer Calculations of Wave-Induced Ship Structural Loads," Ship Structure Comm. Rpt. SSC-229, 1972.
33. Salvesen, N., Tuck, E.O. and Faltinsen, O., "Ship Motions and Sea Loads," Trans. SNAME, 1970.
34. Lewis, E.V., "Predicting Long-Term Distribution of Wave-Induced Bending Moment on Ship Hulls," SNAME, Spring Meeting, 1967.
35. Ochi, M.K., "Wave Statistics for the Design of Ships and Ocean Structures," Trans. SNAME, 1978.
36. Hoffman, D. and Miles, M., "Analysis of a Stratified Sample of Ocean Wave Records at Station 'India'," SNAME Tech. and Res. Bull. No. 1-35, May 1976.
37. Hoffman, D., "Wave Data Application for Ship Response Predictions," Webb Inst. of Naval Architecture, Oct. 1975.
38. Ochi, M.K. and Hubble, E.N., "On Six-Parameter Wave Spectra," Proc. 15th Coastal Engineers Conf., ASCE, 1976.
39. Raff, A.I., "Program SCORES - Ship Structural Response in Waves," Ship Structure Comm. Rpt. SSC-230, 1972.
40. Wahab, R. and Vink, J.H., "Wave Induced Motions and Loads on Ships in Oblique Waves," Netherlands TNO Rpt. No. 193 S, May 1979.
41. Kaplan, P., Sargent, T.P. and Silbert, M., "A Correlation Study of SL-7 Containership Loads and Motions - Model Tests and Computer Simulation," Ship Structure Comm. Rpt., SSC-271, 1977.

42. Kaplan, P., Sargent, T.P. and Cilmi, J., "Theoretical Estimates of Wave Loads on the SL-7 Container Ship in Regular and Irregular Seas," Ship Structure Comm. Rpt. No. SSC-246, 1974.
43. Clarke, J. D., "Measurement of Hull Stresses in Two Frigates During a Severe Weather Trial," Trans. RINA, 1981.
44. Jensen, J.J. and Pedersen, P.T., "Wave-Induced Bending Moments in Ships-a Quadratic Theory," Trans. RINA, Vol. 121, 1979.
45. Jensen, J.J. and Pedersen, P.T., "Bending Moments and Shear Forces in Ships Sailing in Irregular Waves," Journal of Ship Research, December 1981.
46. Liu, D., Chen, H. and Lee, F., "Application of Loading Predictions to Ship Structure Design: A Comparative Analysis of Methods," Proc. SSC-SNAME, Extreme Loads Response Symp., Arlington, Va., October 1981.
47. Karst, O., "Statistical Techniques," Appendix A to Ship Structure Comm. Rpt. SSC-196, 1969.
48. Goodman, R.A., "Wave Excited Main Hull Vibration in Large Tankers and Bulk Carriers," Trans. RINA, April 1970.
49. van Gunsteren, F.F., "Springing, Wave Induced Ship Vibrations," Int. Shipbuilding Prog., Vol. 17, No. 195, November 1970.
50. Kaplan, P. and Sargent, T.P., "Further Studies of Computer Simulation of Slamming and Other Wave-Induced Vibratory Structural Loadings on Ships in Waves," Ship Structure Comm. Rpt. SSC-231, 1972.
51. Hoffman, D. and Van Hooff, R., "Experimental and Theoretical Evaluation of Springing on a Great Lakes Bulk Carrier," Int. Shipbuilding Prog., June 1976.
52. Achtarides, T.A., "Wave Excited Two-Node Vertical Resonant Vibration (Springing) of Flexible Ships," Proc. Mar. Tech. Soc. Ocean Energy Conf., New Orleans, La., October 1979.
53. Troesch, A.W., "Ship Springing-An Experimental and Theoretical Study," Dept. of Naval Arch. and Marine Eng., Univ. of Michigan, Ann Arbor, Rpt. No. 219, May 1980.

54. Skjoldal, S.O. and Faltinsen, O.M., "A Linear Theory of Springing," J. of Ship Research, Vol. 24, No. 2, June 1980.
55. Stiansen, S.G., Mansour, A. and Chen, Y.N., "Dynamic Response of Large Great Lakes Bulk Carriers to Wave-Excited Loads," Trans. SNAME, 1977.
56. Ochi, M.K., and Motter, L.E., "Prediction of Slamming Characteristics and Hull Responses for Ship Design," Trans. SNAME, 1973.
57. Belik, O., Bishop, R.E.D. and Price, W.G., "On the Slamming Response of Ships to Regular Head Waves," Trans. RINA, Vol. 122, 1980.
58. Meyerhoff, W.K. and Schacter, G., "An Approach for the Determination of Hull Girder Loads in Seaway Including Hydrodynamic Impacts," Ocean Engineering, Vol. 7, 1980.
59. Yamamoto, Y., Fujino, M., Fukasawa, T. and Ohtsubo, H., "Slamming and Whipping of Ships Among Rough Seas," Proc. Euromech Coll. 122, ATMA, 1979.
60. Aertssen, G., "An Estimate of Whipping Vibration Stress Based on Slamming Data of Four Ships," Int. Shipbuilding Prog., February 1979.
61. Clarke, J.D., "Measurement of Hull Stresses in Two Frigates During a Severe Weather Trial," The Naval Architect, March 1982.
62. Shinozuka, M., et al, "Probability Based Load Criteria for the Design of Nuclear Structures: A Critical Review of the State-of-the-Art," BNL Rpt. NUREG/CR-1979, BNL-NUREG-5136.
63. Anzia, T., Bryant, L.M. and Pedersen, F.B., "Comparison of a Limit State Design Code With API RP 2A" OTC 4191, Proc. Offshore Tech. Conf., Houston, Texas, May 1982.
64. Dalzell, J.T., "Application of Multiple Input Spectrum Theory," Int. Shipbuilding Prog., No. 236, 1974.
65. Mansour, A.E., "Combining Extreme Environmental Loads for Reliability-Based Designs," Proc. SSC-SNAME Extreme Loads Response Symp., Arlington, Va., October 1981.
66. Lewis, E.V. and Zubaly, R.B., "Predicting Hull Bending Moments for Design," Proc. SSC-SNAME Extreme Loads Response Symp., Arlington, Va., October 1981.

67. Gran, S., "Statistical Description of Wave Induced Vibratory Stresses in Ships," U.S. Coast Guard Report CG-M-2-81, December 1980.
68. Faulkner, D., "A Review of Effective Plating for Use in the Analysis of Stiffened Plating in Bending and Compression," J. of Ship Research, March 1975.
69. Mansour, A.E. and Thayamballi, A., "Ultimate Strength of a Ship's Hull Girder Plastic and Buckling Modes," Ship Structure Comm. Rpt. SSC-299, June 1980.
70. Bleich, F., Buckling Strength of Metal Structures, McGraw-Hill Book Co., New York, 1952.
71. Faulkner, D., "The Overall Compression Buckling of Partially Constrained Ship Grillages," M.I.T. Rpt. 1973.
72. Mansour, A., "Ship Bottom Structure Under Uniform Lateral and Inplane Loads," Schiff and Hafen, Heft 5, 1967.
73. Mansour, A.E., "Gross Panel Strength Under Combined Loading," Ship Structure Comm. Rpt. SSC-270, 1977.
74. MacNaught, D.F., "Strength of Ships," Chapter IV of Principles of Naval Architecture, J.P. Comstock, Editor, SNAME, 1967.
75. Faulkner, D., "Compression Strength and Chance," Defense Fellowship Thesis, MIT, 1971.
76. Dow, R.S., et al, "Evaluation of Ultimate Ship Hull Strength," Proc. SSC-SNAME Extreme Loads Response Symp., Arlington, Va., 1981.
77. Adamchak, J.C., "ULSTR: A Program for Estimating the Collapse Moment of a Ship's Hull Under Longitudinal Bending," David W. Taylor Naval Ship Res. and Dev. Ctr. Rpt. 82/076, October 1982.
78. Smith, C.S., "Imperfection Effects and Design Tolerances in Ships and Offshore Structures," Inst. of Engrs. & Shipbuilders in Scotland, Paper No. 1434, Feb. 1981.
79. "Fabrication and Service Factors," Rpt. of Comm. III. 3, 8th Int. Ship Structures Cong., 1982.
80. Goodman, R.A. and Mowatt, G.A., "Assessment of Imperfections in Ship Structural Design," Proc. Conf. of Influence of Residual Stresses and Distortions on Performance of Steel Struct., Inst. of Mech. Eng. London, October 1976.

81. Ang, A. H-S., "Probability Bases for Ship Structural Analysis and Design," Class Notes for U.S. Coast Guard, June 1979.
82. Faulkner, D., "Compression Tests on Welded Eccentrically Stiffened Plate Panels," Proc. Int'l Symp. on Steel Plated Structures, Imperial College, London, 1976.
83. Jones, N., "A Literature Survey on the Collision and Grounding Protection of Ships," Ship Structure Comm. Rpt., SSC-283, 1979.
84. Ochi, M.K., "Prediction of Occurrence and Severity of Ship Slamming at Sea," Proc. 5th Symp. on Naval Hydrodynamics, Bergen, Norway, Sept. 1964.
85. Construction Industry Research and Information Assoc., "Rationalization of Safety and Servicability Factors in Structural Codes," Rpt. 63, July 1977.
86. Faulkner, D., "Semi-Probabilistic Approach to the Design of Marine Structures," Proc. SSC-SNAME Extreme Loads Response Symp., Arlington, Va., 1981.

1" Head = 6 Pcs

Committee on Marine Structures  
Marine Board  
National Academy of Sciences - National Research Council

The Committee on Marine Structures has technical cognizance of the Interagency Ship Structure Committee's research program.

- Mr. A. D. Haff, Chairman, Annapolis, MD
- Prof. A. H.-S. Ang, University of Illinois, Champaign, IL
- Dr. K. A. Blenkarn, Amoco Production Company, Tulsa, OK
- Mrs. Margaret Ochi, Gainesville, PA
- Mr. D. Price, National Oceanic and Atmospheric Administration, Rockville, MD
- Mr. D. A. Sarno, ARMO Inc., Middletown, OH
- Mr. J. E. Steele, Naval Architect, Quakertown, PA
- Mr. R. W. Rumke, Executive Secretary, Committee on Marine Structures

LOADS ADVISORY GROUP

The Loads Advisory Group prepared the project prospectus.

- Mr. J. E. Steele, Chairman, Quakertown, PA
- Prof. R. G. Davis, Texas A&M University, Galveston, TX
- Mr. J. P. Fischer, American Steamship Company, Buffalo, NY
- Mr. P. W. Marshall, Shell Oil Co., Houston, TX
- Prof. Robert Plunkett, Univ. of Minnesota, Minneapolis, MN
- Mr. C. B. Walburn, Bethlehem Steel Corp., Sparrows Point, MD

PROJECT ADVISORY COMMITTEE

The Project Advisory Committee provided the liaison technical guidance, and reviewed the project with the investigator.

SR-1280

- Mr. P. W. Marshall, Chairman, Shell Oil Company, Houston, TX
- Prof. A. H.-S. Ang, University of Illinois, Urbana, IL
- Dr. J. E. Goldberg, National Science Foundation, Washington, DC
- Dr. H. E. Sheets, Analysis & Technology, Inc., North Stonington, CN

486-329

Cover 3

7 Pcs Back

4 1/2 Pica Head

SHIP STRUCTURE COMMITTEE PUBLICATIONS

- SSC-316      Ship Structure Committee Long-Range Research Plan: Guidelines for Program Development by E.M. MacCutcheon, O.H. Oakley and R.D. Stout, 1983, AD-A140275
- SSC-317      Determination of Strain Rates in Ship Hull Structures: A Feasibility Study by J. G. Giannotti and K. A. Stambaugh, 1984
- SSC-318      Fatigue Characterization of Fabricated Ship Details for Design by W. H. Munse, T. W. Wilbur, M. L. Tellalian, K. Nicoll and K. Wilson, 1983, AD-A140338
- SSC-319      Development of A Plan to Obtain In-Service Still-Water Bending Moment Information for Statistical Characterization by J. W. Boylston and K. A. Stambaugh, 1984
- SSC-320      A Study of Extreme Waves and Their Effects on Ship Structures by W. H. Buckley, 1983, AD-A140317
- SSC-321      Survey of Experience Using Reinforced Concrete in Floating Marine Structures by O.H. Burnside and D.J. Pomeroy, 1984
- SSC-322      Analysis and Assessment of Major Uncertainties Associated With Ship Hull Ultimate Failure by P. Kaplan, M. Benatar, J. Bentson and T.A. Achtarides, 1984
- SSC-323      Updating of Fillet Weld Strength Parameters for Commercial Shipbuilding by R.P. Krumpfen, Jr., and C.R. Jordan, 1984
- SSC-324      Analytical Techniques for Predicting Grounded Ship Response by J.D. Porricelli and J.H. Boyd, 1984
- SSC-325      Correlation of Theoretical and Measured Hydrodynamic Pressures for the SL-7 Containership and the Great Lakes Bulk Carrier S. J. Cort by H.H. Chen, Y.S. Shin & I.S. Aulakh, 1984
- SSC-326      Long-Term Corrosion Fatigue of Welded Marine Steels by O.H. Burnside, S.J. Hudak, E. Oelkers, K. Chan, and R.J. Dexter, 1984
- None          Ship Structure Committee Publications - A Special Bibliography, AD-A140339

6 Picas Outside

486-329

Cover 4

*[Faint handwritten scribbles]*